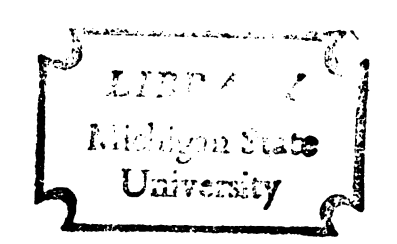
ELECTROMAGNETIC RADIATION FROM AUTOMOTIVE IGNITION CIRCUITS

Thesis for the Degree of MSEE

MICHIGAN STATE UNIVERSITY

THOMAS LEE SCHALLHORN

1976



ABSTRACT

ELECTROMAGNETIC RADIATION FROM AUTOMOTIVE IGNITION CIRCUITS

Ву

Thomas Lee Schallhorn

Radio frequency interference (RFI) has been studied nearly (75) years, as documented by a review of the literature. This thesis addresses a specific RFI problem: modeling the automotive ignition circuit to predict the radiated electric field.

The selected ignition circuit model uses lumped elements for the resistance, capacitance, and inductance in the secondary of the ignition circuit. The spark plug and distributor gaps are shown as capacitances which are shunted when the gaps break down, and the coil is represented by its effective capacitance.

Analysis begins with an initially charged circuit, and predicts the current and voltage waveforms as a function of time for a single spark plug firing. Examples of the theoretical waveforms obtained from computer solutions are shown to be in general agreement with observed behavior.

The transform of the theoretical ignition circuit current was obtained to show frequency information. While these equations are somewhat complicated, it is demonstrated that the separation, Δf , between recurring maxima observed in frequency domain is

$$\Delta f \approx \frac{1}{t_1} \tag{4.43b}$$

where \mathbf{t}_1 is the time in seconds between the distributor and spark plug gap breakdowns, and $\Delta \mathbf{f}$ is the separation between maxima in Hertz.

General agreement between the theoretical amplitude density of the transform of the ignition circuit current and the observed current density is also demonstrated using computer solutions.

Using the theoretical current amplitude density in a circular loop antenna model, the electric field is predicted. The field strength is shown to be significantly reduced in frequency domain by the addition of resistance to the circuit, and examples demonstrate reasonable agreement with known behavior.

Finally, the maximum field strength is predicted as a function of time. The peak value of the electric field is given simply as

$$\frac{\int_{0}^{\infty} \omega_{0} I_{0}}{r} \quad \text{for} \quad t \approx \frac{r}{c}$$
 (5.25)

where

 η = characteristic impedance of free space (=120 π ohms)

 $\omega_{_{\rm O}}$ = cutoff frequency of current in frequency domain, radians/ second

I = low-frequency amplitude of current in frequency domain,
amperes per radian/second

r = distance from the antenna in meters

c = speed of light in free space (=3 \times 10⁸ meters/second)

ELECTROMAGNETIC RADIATION FROM AUTOMOTIVE IGNITION CIRCUITS

Ву

Thomas Lee Schallhorn

A THESIS

Submitted to
Michigan State University
in partial fulfillment of the requirements
for the degree of

MASTER OF SCIENCE

Department of Electrical Engineering and Systems Science

ACKNOWLEDGMENTS

I am especially grateful to Dr. K. M. Chen, Professor of Electrical Engineering at Michigan State University, for his guidance and patient assistance in the preparation of this thesis.

I am indebted to my wife, Lynn, for her understanding and support, and also thank Cindy Beard for her careful typing of the final manuscript.

TABLE OF CONTENTS

Chapte	r						Page
I.	INTRODUCTION	•	•	•	•	•	1
	Background						1
	Statement of Problem			•	•		2
	General Procedure	•	•	•	•	•	2
II.	REVIEW OF LITERATURE	•		•		•	3
	Ignition Circuit Operation						3
	Typical Ignition Circuit Values						6
	Electric Field Measurements						9
	RFI Measurement Standards						11
	Some Early Ignition Circuit Models						14
	Transmission line approach						14
	Treatment of RFI as an impulse						16
	Lumped element approach						17
	Recently Published Research	•	•	•	•	•	19
	system						19
	Experimentation with new suppression		-	-	-	-	
	techniques						19
	Alternative characterizations of	•	•	•	•	•	17
	ignition noise						20
	RF current distribution on car bodies						22
III.	SPARK PLUG CURRENT AS A FUNCTION OF TIME	•	•	•		•	23
	Ignition Circuit Model						23
	Circuit Equations Before Spark Plug Fires						25
	Circuit Equations After Spark Plug Fires						31
	Numerical Examples						34
	Results using Newell's values	_		_			34
	Effect of changing R						35
							37
	Effect of changing $E_2 \dots \dots$	•	•	•	•	•	37
	Effect of changing C $_{ m dg}$ and E $_{ m 1}$	•	•	•	•	•	37
IV.	FREQUENCY SPECTRUM OF SPARK PLUG CURRENT	•	•		•	•	40
	Derivation of Amplitude Density Equations				_		40
	Amplitude Density-Spark Plug Gap Only						41
	Amplitude Density-Distributor and Spark	•	•	•	•	-	•
	Plug Gaps						42
	Check of Equations						42
	Significance of Time Between Gap Breakdowns	•	•	•	•	•	51

Chapte	r		Page
ΙV.	Numerica	al Examples	55
	Resul	lts of using Newell's values	55
	Effec	et of changing R	55
	Effec	et of changing E $_2$	57
	Effec	et of changing $c_{ ext{dg}}^{ ext{ and } E_1 \dots \dots$	57
V.	ELECTRIC FI	IELD FROM CIRCULAR LOOP ANTENNA MODEL	58
	Predicte	ed Field Strength in Frequency Domain	58
		al Examples - Frequency Domain	
	Resul	lts using Newell's values	61
	Effec	et of changing R	63
	Effec	et of changing E $_2$	63
		et of changing ${\tt C}_{ extsf{dg}}^{ extsf{2}}$ and ${\tt E}_{ extsf{1}}$	
	Predicte	ed Field Strength in Time Domain	65
		od #1	
		od #2	
	Numerica	al Examples - Time Domain	70
	Discussi	ion and Recommendations	71
VI.	CONCLUSIONS	5	74
	LIST OF REF	FERENCES	. 76
	APPENDICES		
	Α	Program IGNITI	. 79
	В	Program IGNITII	
	С	Program ADP	
	D	Program EMAX	
	F	Program FNTRES	90

LIST OF TABLES

Table		Page
1	Nominal Ignition Circuit Values	7
2	Significant Features of Two RFI Measurement Standards	12

LIST OF FIGURES

Figure		Page
1	Typical Ignition System	4
2	Typical Voltage Patterns During One Spark Plug Firing	8
3	Published Measurements of Electric Field Strength	10
4	Comparison of Measurements with SAE J551a Limits	15
5	Newell's Current and Electric Field Spectra	18
6	Results of Recent Studies of Spark Plug Current and RFI	21
7	Proposed Ignition Circuit Model	24
8	Theoretical Waveforms Using Newell's Values	35
9	Theoretical Current Waveforms	36
10	Theoretical Waveforms for Constant Initial Distributor Gap Charge	39
11	Theoretical Amplitude Densities of Ignition Circuit Current	53
12	Theoretical Amplitude Densities of Ignition Circuit Current	56
13	Coordinate System for Circular Loop Antenna	60
14	Theoretical Field Strength Limit in Frequency Domain	62
15	Theoretical Field Strength Limit in Frequency Domain	64

Figure		Page
16	Theoretical Field Strength Limit in Time Domain	71
17	Theoretical Phase Angle of Transform of Current Using Newell's Values	73

CHAPTER I

INTRODUCTION

Background

In 1902, observers detected radio frequency interference (RFI) originating from automotive ignition systems [1]. By 1930, when automobile manufacturers first installed radios at the factory, the search was on for an effective means of RFI suppression [2].

Now, the widespread increases in television and FM services, and the more recent popularity of Land Base Mobile Communication systems, demand more effective management of the radio frequency spectrum [2,3].

Research in the problem of interference has been concentrated in two complementary areas: 1) quantification of RFI and its effects, and 2) development of a theoretical model consistent with observations.

Experimentation has resulted in the inclusion of resistance spark plugs, a widened distributor gap, and distributed resistance spark plug wires on most American automobiles to reduce RFI [4]. Other ignition circuit modifications have shown promising results in recent tests [5].

In developing models, researchers had to decide whether or not a lumped element model could validly be assumed. Some writers in the subject area favored the lumped element treatment, and they manipulated their circuit formulations to obtain favorable results [6, 7, 8].

Other authors attempted uniform transmission line models to achieve greater accuracy [9, 10]. However, as recently as 1969, solutions for

current in the ignition circuit required so much computation that these models are generally not employed in analysis.

While the lumped element model lends itself to an analytical solution, the state of the art models employ simplifying assumptions which in some cases are not strictly correct. In particular, one model which yielded favorable results assumed complete independence of the effects of the distributor and spark plug gap breakdowns. Since these gaps break down sequentially, the model can be improved by including this fact.

Statement of Problem

The problem is to develop a lumped element ignition circuit model which includes the sequential nature of the distributor and spark plug gap breakdowns.

General Procedure

Solution of this problem required several steps. First, available research on RFI reduction and ignition circuit modeling was studied.

This included a review of the characteristics of typical ignition circuits.

Second, the desired modification was incorporated into a lumped element ignition circuit model, and the circuit equations were written and solved using LaPlace transform techniques.

In the next step, the amplitude density of the LaPlace transform of the spark plug current was obtained and compared with published results.

Finally, using a circular loop antenna model, limits on the magnitude of the electric field strength were predicted.

CHAPTER II

REVIEW OF LITERATURE

This chapter summarizes past approaches to the problem of managing radio frequency interference (RFI) from automotive ignition circuits.

First, ignition circuit operation is described, and typical component values and circuit measurements are presented. Next, published results of electric field strength measurements are given, followed by a review of the development of RFI measurement standards.

Some early attempts at modeling the ignition circuit are discussed, and a condensation of recently published research concludes the chapter.

Ignition Circuit Operation

The ignition circuit serves a dual purpose: first, it provides a spark with sufficient potential to ignite the gases in the combustion chamber, and second, it provides that spark at the proper instant. A step-up transformer (commonly called the coil) develops the required voltage; meanwhile, the opening and closing of a contact breaker times the spark.

Figure 1 shows a typical battery-powered ignition system. The primary circuit consists of the battery, primary coil winding, and associated low voltage devices and wiring, while the secondary coil winding, rotor, spark plugs, and high voltage wiring comprise the secondary circuit.

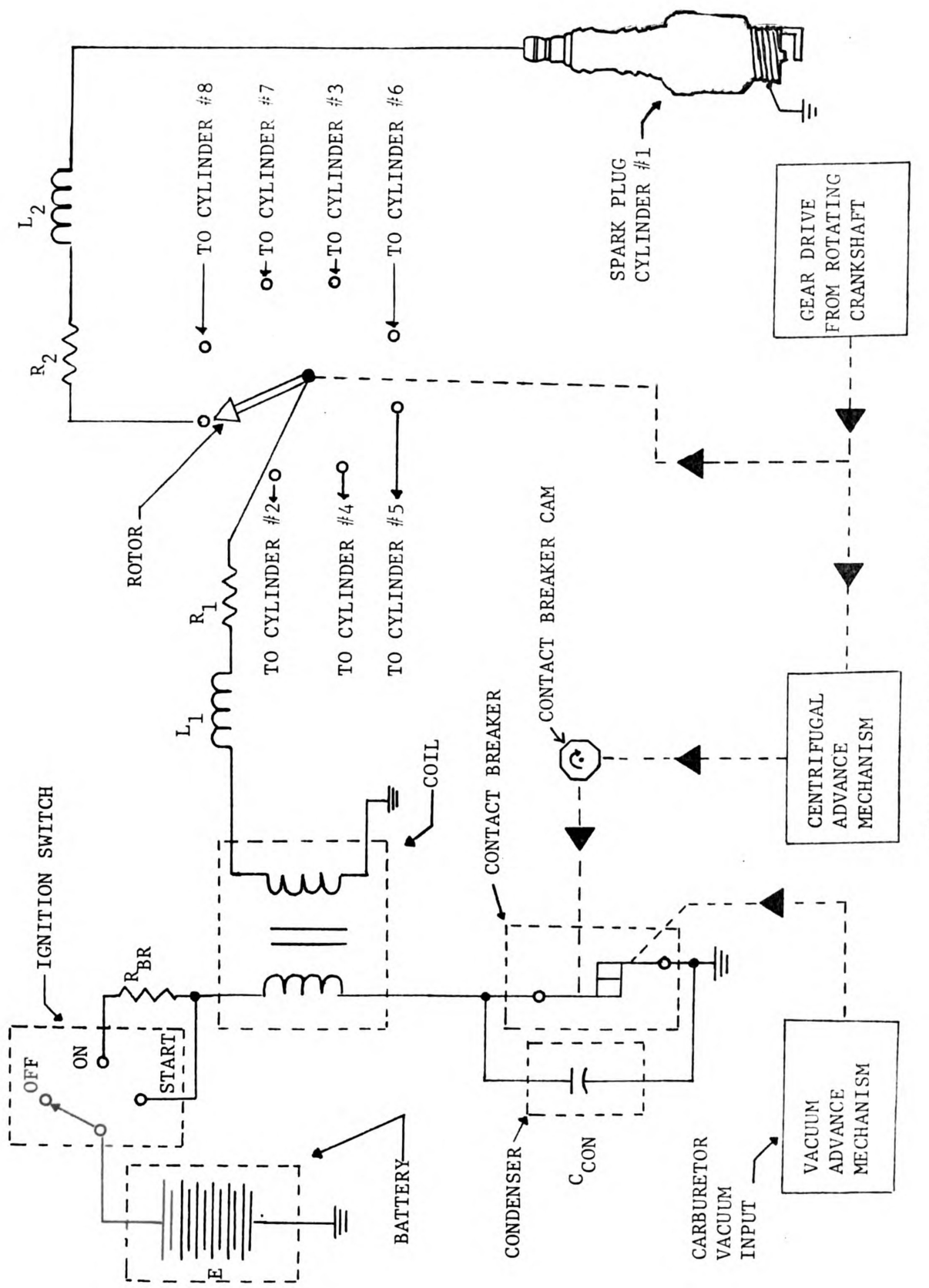


Figure 1 - Typical Ignition System

Mechanically, the crankshaft simultaneously rotates the rotor and the contact breaker cam, so the electrical activity in the primary occurs at the proper time to fire the desired spark plug.

The spark plug firing sequence is as follows:

- 1. To start the engine, the start position of the ignition switch bypasses the ballast resistor, $R_{\rm BR}$, and compensates for reduced battery voltage during starting. With the engine running, inclusion of the ballast resistor limits the maximum current, and keeps the current constant for varying engine speeds when the contact breaker opens [11].
- 2. With the contact breaker closed, the battery voltage and the ballast resistance determine the steady state value which the primary current approaches.
- 3. As the rotor aligns with a spark plug terminal, the contact breaker opens. This abruptly interrupts the steady state current, causing a voltage to appear on the coil. The condenser, shown as C_{CON} in Figure 1, reduces the effects of bounce in the operation of the contact breaker. Also, the condenser assures an adequately rapid change in current necessary to attain the desired voltages.
- 4. With the opening of the contact breaker, the coil secondary voltage rises until the breakdown potential across the distributor gap is reached.
- 5. For normal operation, the flux in the coil continues to collapse after the distributor gap breakdown; thus, the secondary potential still rises until the spark plug voltage is sufficient to fire the spark plug.
- 6. As the gases in the cylinder ionize, the potential required for conduction in the gap drops to about half of the breakdown potential.

- 7. With the contact breaker still open, the coil voltage drops until the voltages at the gaps become insufficient to maintain conduction. The energy in the secondary then dissipates through resistance in the circuit.
- 8. While the rotor advances, the contact breaker closes. The voltage induced by this closure attenuates before the contact breaker opens again.
 - 9. Steps 2 through 8 repeat for the next spark plug.

Typical Ignition Circuit Values

Similarities in the performance of different ignition circuit designs allow the indication of typical values, as shown in Table 1.

First, the times associated with the spark plug firing cycle are of interest. The camshaft, which operates the rotor and contact breaker, rotates once for every two revolutions of the crankshaft. Since the rotor passes each spark plug terminal once in each revolution, four spark plug firings occur during each crankshaft revolution for an eight cylinder car.

Table 1 shows the cycle times associated with different engine speeds. A dwell of 30° is used, where dwell refers to the length of time in degrees of camshaft rotation that the contact breaker is closed.

Next, specification of the operating conditions of an ignition system is desired. Based on a wide range of sources, the remainder of Table 1 gives nominal values for discrete components and for selected circuit parameters.

A final area of interest is the time variation of the currents and voltages in the ignition system. Figure 2 on page 8 shows some of the more important waveforms documented in the literature.

Table 1. Nominal Ignition Circuit Values

Cycle Times for 8-cylinder Engines

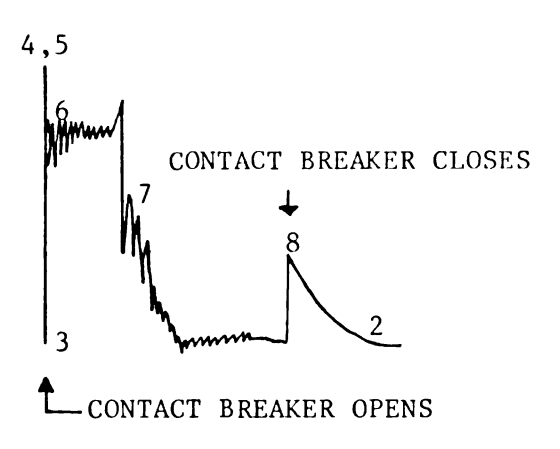
Engine Speed (RPM)	Time Between Spark Plug Firings (Seconds)	Time Contact Breaker Open (Seconds)	Time Contact Breaker Closed (Seconds)
500	0.030	0.0100	0.0200
1,000	0.015	0.0050	0.0100
1,500	0.010	0.0033	0.0067
3,000	0.005	0.0017	0.0033

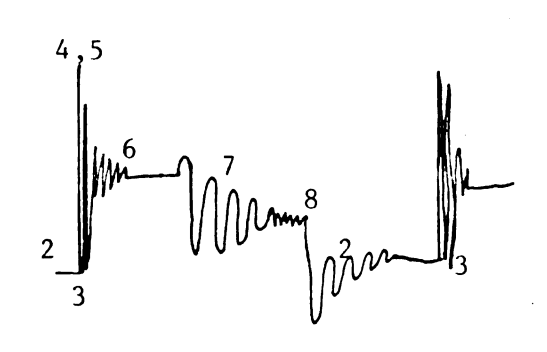
Primary Circuit Values

Condenser capacitance	.18 to .30 microfarads [12, 13]
Current	4 amperes, maximum [14]
Ballast resistor	135 ohm-8 cyl, 180 ohm-6 cyl.[15]
Contact breaker gap	0.019 inches [16]

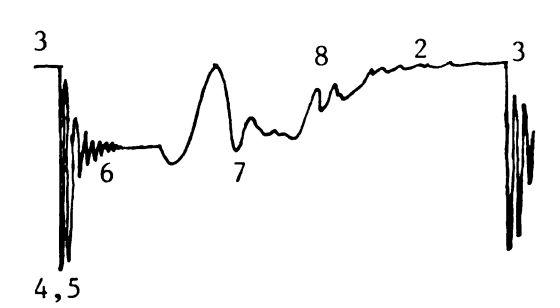
Secondary Circuit Values

Distributor gap	0.031 inches (GM before 1969) [4] 0.094 inches (GM after 1969) [4]		
Distributor gap breakdown	3,000 volts (before 1969) [9] 10,000 volts (GM after 1969) [5]		
Spark plug gap	0.030 to 0.035 inches		
Spark plug gap breakdown voltage	3,000 to 25,000 volts (depending on operating conditions)[9,14,17]		
Time between distributor gap and spark plug gap breakdowns	10 to 20 microseconds [5]		
High voltage resistance cable	4,500 to 5,000 ohms/foot [3,5]		
Total resistance added for RFI suppression	5,000 to 25,000 ohms [18, 19]		
Coil capacitance	50 picofarads [9]		





- (a) Rectified Primary Coil Voltage [20]
- (b) Spark Plug Voltage [21].



NOTE: Numbers in figures correspond with description on pages 5 and 6.

(c) Secondary Coil Voltage [22]

Figure 2 - Typical Voltage Patterns During One Spark Plug Firing

Figure 2(a) shows the primary coil voltage for one spark plug firing cycle as it appears on a commercially available cathode ray tube ignition analyzer, and Figure 2(b) and 2(c) show the secondary spark plug and coil voltages, respectively.

The patterns in Figure 2 give only a general indication of the actual circuit behavior. They indicate when in the cycle oscillations can be expected, without accurately showing the frequency of oscillation. Similarly, the relative magnitudes only approximate the expected behavior.

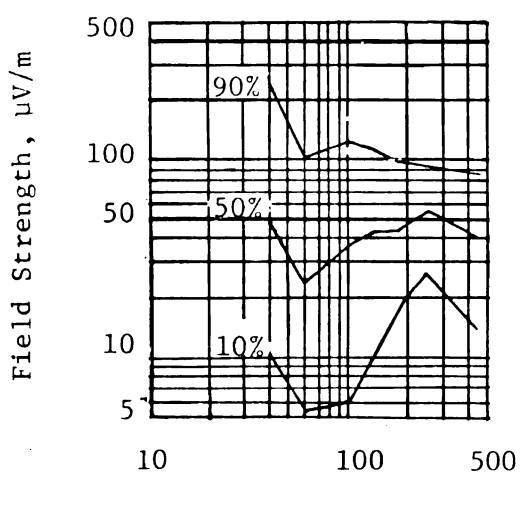
Electric Field Measurements

Without the benefit of modern receivers and computers, the obtaining and processing of data on the electric field strength of RFI requires a prodigious effort. As a result, the literature contains a limited number of reports on these data.

The earliest published results come from two sources: the work of R. W. George [23], and the results of B. G. Pressey and G. E. Ashwell [24].

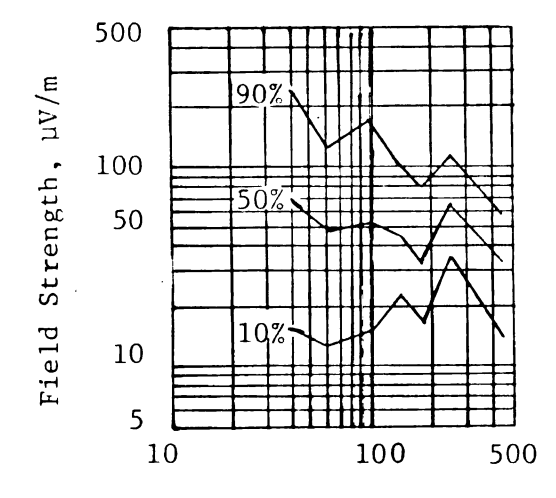
George, working in the late 1930's, made peak electric field strength measurements between 40 and 450 MHz. He calibrated the output from knowledge of the aerial and receiver, and he treated his results statistically. These results are shown in Figures 3(a) and 3(b).

Pressey and Ashwell made measurements for a four-cylinder and a six-cylinder Vauxhall. Their results for the six-cylinder, shown in Figure 3(c), represent measurements taken thirty feet from the center of the car on the distributor side. Measurements made at three other locations around the car indicated no definite radiation pattern.



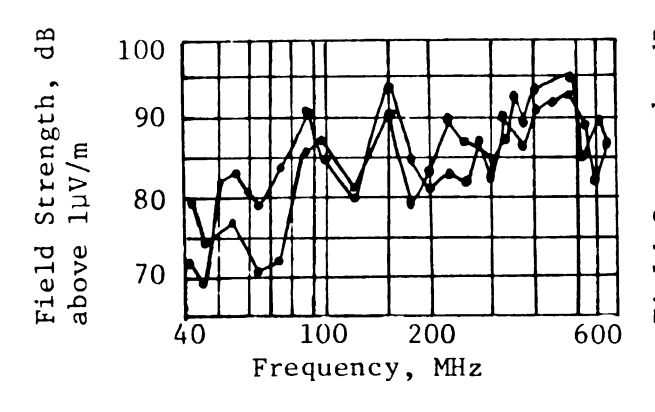
Frequency, MHz

(a) George-Results for Horizontal Polarization [23].



Frequency, MHz

(b) George - Results for Vertical Polarization [23].



Frequency, MHz

600

- (c) Pressey and Ashwell Results
 for 4-cylinder Vauxhall [24]
- (d) Pressey and Ashwell Results
 for single cylinder [24]

NOTES:

- 1. Figure 3(a) bandwidth is 10 kHz, distance is 100 feet.
- 2. Figure 3(b) bandwidth is 10 kHz, distance is 100 feet.
- 3. Figure 3(c) bandwidth is 2.5 MHz, distance is 30 feet.
- 4. Figure 3(d) bandwidth is 2.5 MHz, distance is 60 feet.

Figure 3 - Published Measurements of Electric Field Strength

Pressey and Ashwell also investigated the measurable electric field for a single cylinder magneto and sparking plug. Figure 3(d) shows measurements made in the horizontal plane at a distance of sixty feet.

More recently, F. Bauer published the results of electric field measurements made in June, 1965, on twenty vehicles [3]. The field strength was found to increase with the compression ratio and the number of cylinders, but no correlation was found between interference and engine displacement.

RFI Measurement Standards

The diverse methods of quantizing radio frequency interference require adoption of a standard. At present, the two most prominent standards are: 1) SAE J551b, a standard of the Society of Automotive Engineers used primarily in the United States [25], and 2) CISPR Recommendation 18/2, an international standard defined by the Comite International Special des Perturbation Radioelectrique and which has been adopted by several European countries [26]. Table 2 lists significant features of these procedures.

Both standards observe the EM radiation in the frequency domain to avoid the complications of frequency dependence and limited bandwidth from devices which measure in time domain [27]. The Fourier transform describes the frequency occupancy of a signal from the definition

$$F(s) = \int_{-\infty}^{\infty} f(t) e^{-st} dt$$
 (2.1)

Approximating equation (2.1) by a finite series.

Table 2. Significant Features of Two RFI Measurement Standards

-	CISPR 18/2 [26] (1970)	SAE J551b [25] (1973)	
Antenna Distance	33 Feet	33 Feet	
Antenna Height	10 Feet	10 Feet	
Antenna Type	Dipole	Dipole or Broadband	
Measuring Instrument Distance from Vehicle			
Scan Between Check Frequencies	No	Yes	
Characteristic Maximum reading from horizontal and vertical surements taken on both right and left side.			
Statistical Technique	vehicles conform		
Test Site	Ellipse - 20 meters 100 foot radius by 17.3 meters		
Units for Readings	μV/m, 120 kHz band- width	dB above $1\mu V/m$ per kHz bandwidth	
Limits	$40-75 \text{ MHz} = 50 \mu\text{V/m}$	Curve passing through	
	rising linearly to 120 μV/m at 250 MHz	20-75 MHz	l 2dB
	For comparison with	100 MHz	l4dB
SAE standard, con- vert above limit to		150 MHz	l6dB
	dB, add 20 dB to get limit for peak measurements, then	200 MHz	L8dB
	subtract 41.6 dB from peak limit to	250 MHz	20dB
	get dB above 1µV/ m/kHz bandwidth.	300 MHz	21dB
m/kHz bandwidth. Result is: 40-75 MHz = 12.4 dB ris-		350 MHz	22dB
	ing linearly to 20.0 dB at 250 MHz.	400-1,000 MHz	23dB
	20.0 db at 230 mmz.	Subtract 20 dB for quas	si-

$$F(s) \approx \lim_{\Delta t \to 0} \Sigma \quad f[t_1 + n(\Delta t)]e^{-s[t_1 + n(\Delta t)]}(\Delta t)$$

$$= \int_{0}^{\infty} \int_{0}^{\infty} e^{-s[t_1 + n(\Delta t)]} (\Delta t)$$

$$= \int_{0}^{\infty} \int_{0}^{\infty} e^{-s[t_1 + n(\Delta t)]} (\Delta t)$$
(2.2)

where Δt = length of subinterval of time used in obtaining product for summation

 $n(\Delta t)$ = length of time signal is observed

 t_1 = time when observation begins

s = complex frequency

For physical measurements, the bandwidth is roughly inversely proportional to the shortest detectable length of time, Δt . Thus,

$$F(s) \approx \left(\frac{1}{BW}\right) \sum_{n=0}^{n} f[t_1 + (\frac{n}{BW})]e^{-s[t_1 + (\frac{n}{BW})]}$$
(2.3)

In making RFI measurements, the receiver samples the signal for a time, $n(\Delta t)$, while scanning a range of values of frequency, s. The output voltage represents the amplitude of the Fourier transform of the input signal multiplied by the bandwidth.

Comparison of the receiver output with the SAE J551b standard uses the relationship contained in that standard:

$$F = 20 \log_{10} (R \times H \times B)$$
 (2.4)

where F = field intensity in dB above 1 $\mu V/m/kHz$ bandwidth

 $R = instrument reading in \mu V$

- H = antenna and transmission line factor. This factor relates a receiver's output in μV to the field intensity in $\mu V/m$ at the antenna, and accounts for line losses.
- B = bandwidth factor, 1 kHz/bandwidth of measuring set in kHz.

The utility of the limits defined in the standards depends in part on the attainability of these limits. Selected results from two researchers show that the limits are, indeed, reasonable.

In comparing the test results of RFI from single vehicles versus a matrix of (21) vehicles, Doty [2] plotted the greatest upper bound from these tests against the SAE standard (see Figure 4(a) and 4(b). The results justify the SAE procedure of using the maximum of the vertically and horizontally polarized readings, since neither polarization dominates over the frequency range of the specification.

Bauer's results [3] also show the attainability of the SAE standard. As shown in Figure 4(c), the substitution of resistance high voltage cable for steel secondary ignition cable suppressed the RFI to within the SAE limit.

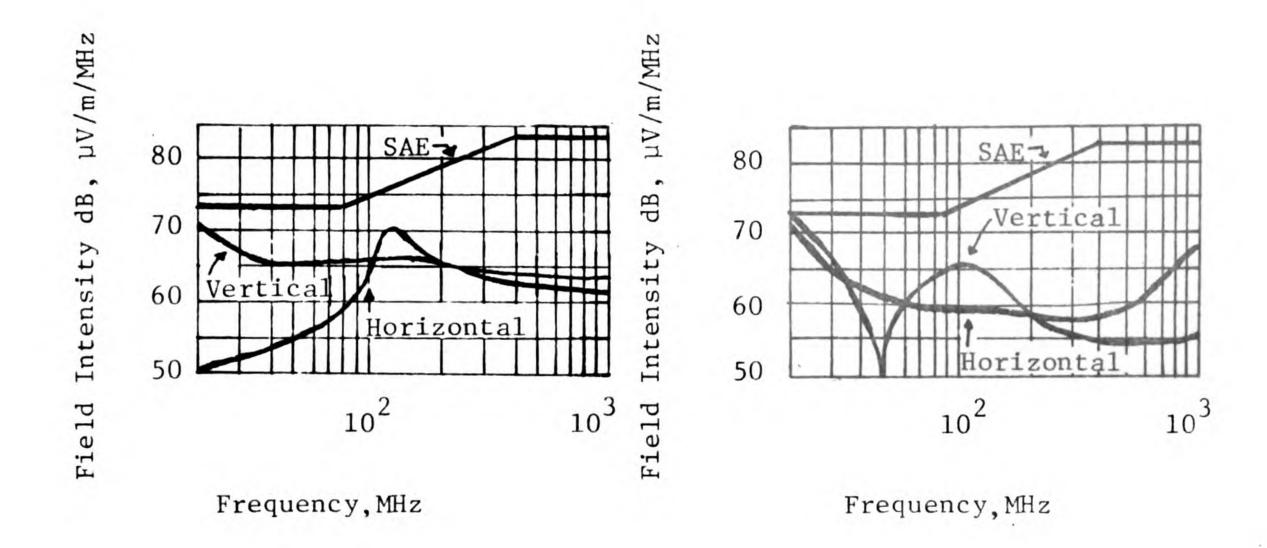
Some Early Ignition Circuit Models

The task of modeling the interference from ignition systems attracted the interest of several researchers in the 1940's and 1950's. Summaries of three unique approaches follow:

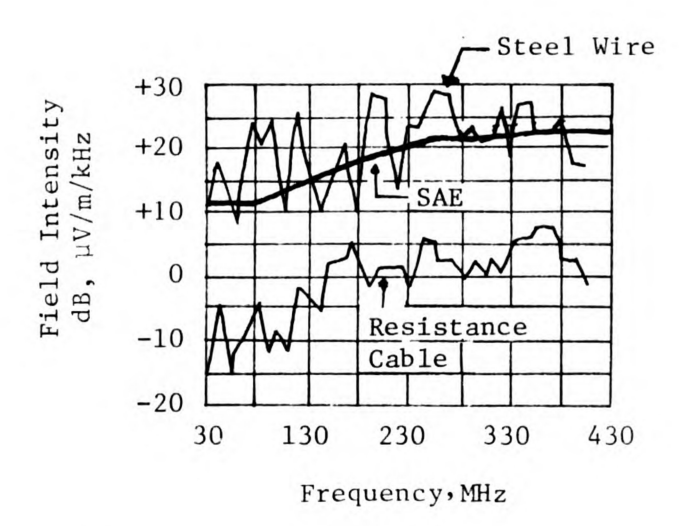
<u>Transmission line approach</u>. Nethercot [9] modeled the ignition system as a uniform transmission line terminated by the spark plug at one end and the secondary of the coil at the other.

Ignoring the distributor gap, Nethercot postulated that the break-down of the spark plug gap initiates a traveling current pulse which is repeatedly reflected at the coil and at the spark plug. Using the reflection coefficient for a uniform line terminated by a capacitor, he predicted the current in the spark plug gap.

The addition of resistance for RFI suppression had been experimentally established by the time of his article. To demonstrate agreement



- (a) Upper bounds of RFI from single vehicles [2].
- (b) Upper bounds of RFI from 21-vehicle matrices [2].



(c) Suppression from changing ignition wires [3].

Figure 4 - Comparison of Measurements with the SAE J551a Limits

between this fact and his theory, Nethercot made two observations:

1) a resistor inserted by the spark plug reduces the initial magnitude of the current pulse and 2) a resistor placed near the coil alters the reflection coefficient to reduce the radiation intensity.

Nethercot did not make any quantitative estimates of the radiated field strength in his theory.

Treatment of RFI as an impulse. Eaglesfield [6] viewed the radiated interference as a very short pulse which excites the impulse response of a receiver. Replacing the spark plug by a switch, he predicted the magnitude of the current surge due to the spark plug firing.

Then, viewing the cables as a magnetic dipole loop antenna, Eagles-field used equations for sinusoidally varying sources to deduce the magnitude of the electric field pulse. Multiplying this expression by the receiver bandwidth, Eaglesfield predicted an equivalent electric field strength for comparison with experimental measurements as

equivalent electric field =
$$\frac{\mu \text{ AVB}}{4\pi \text{ cLR}}$$
 microvolts/meter (2.5)

where μ = permeability of free space (= $4\pi \times 10^{-7}$ henry/meter)

c = velocity of light in free space (= 3×10^8 meters/second)

A = area of magnetic dipole loop, m²

V = breakdown voltage of spark plug, volts

L = inductance of ignition leads, henries

R = distance from magnetic dipole loop, m

B = receiver bandwidth, Hz

In a subsequent article [7], Eaglesfield extended his treatment to allow an arbitrary impedance in the ignition cables, and he defined a suppression ratio to describe its effect.

Finally, Eaglesfield considered the effects of a uniform line. He concluded that the use of lumped elements is reasonable, and he demonstrated agreement of this theory with published results.

Lumped element approach. Newell [3] suggested modeling the ignition secondary as an RLC circuit with switches replacing the distributor and spark plug gaps. Assuming that the spark plug current flows uniformly through the secondary, he used simple circuit theory to solve for the current after the gap breakdowns.

From the known solution of a step voltage applied to a series RLC circuit, Newell assumed the ignition current to be of the form:

$$i = \frac{E}{Lg} e^{-at} \sin(gt)$$
(2.6)

where
$$\omega_0^2 = \frac{1}{LC}$$
, $a = \frac{R}{2L}$, and $g = v\omega_0^2 - a^2$

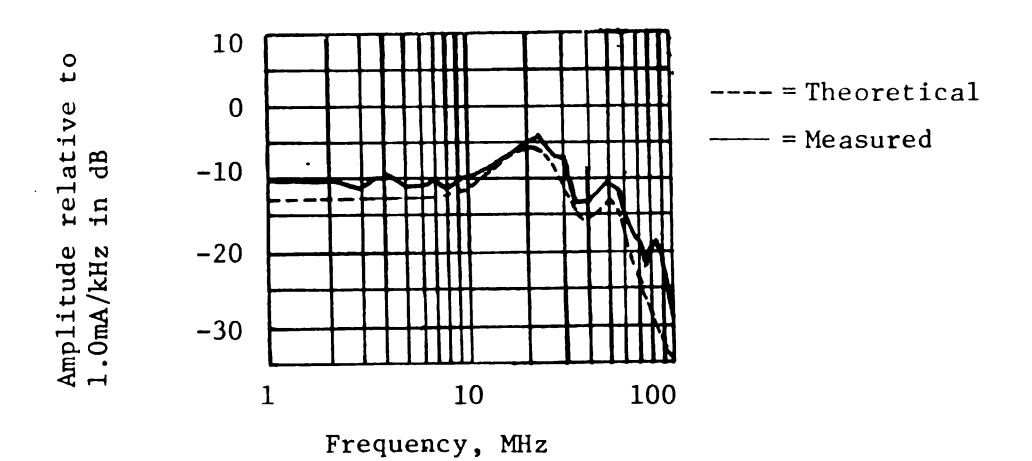
He then claimed that the peak amplitude of the current measured by a receiver would be

I(peak) =
$$\frac{2EB}{L\sqrt{(\omega^2 - \omega_0^2)^2 + 4\omega^2 a^2}}$$
 (2.7)

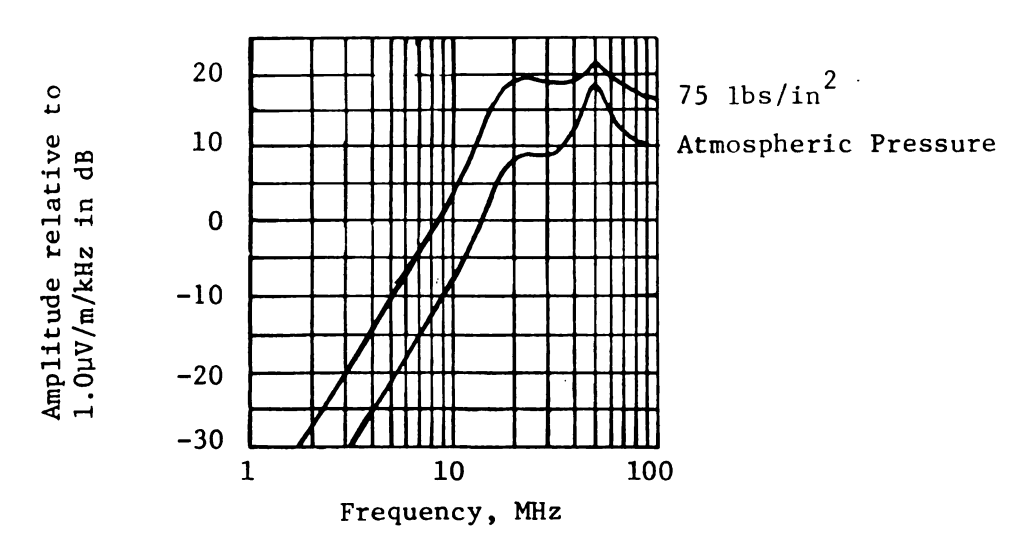
where B = receiver pandwidth

Next, Newell assumed that, for a narrow band receiver, the peak current would be the sum of the amplitude contributions from each gap breakdown.

To test his theory, Newell constructed a dummy engine block with variable air pressure in the cylinders. Combustible mixtures were not used, and a comparison of the theoretical and measured results is shown in Figure 5(a).



(a) Current spectrum for distributor and plugs at atmospheric pressure [8].



(b) Theoretical radiated field strength [8].

Values for Theoretical Results:

E (Each Gap) = 2,500 volts
$$L = 1.4 \times 10^{-6}$$
 Henries R = 90 ohms (selected to provide best fit) C when distributor gap breaks down = 7.35 x 10^{-12} Farads C when spark plug gap breaks down = 40.0 x 10^{-12} Farads

 $A = 0.037 \text{ m}^2$ D = 30.48 m

Figure 5 - Newell's Current and Electric Field Spectra

Finally, Newell regarded the ignition system as a loop antenna carrying a uniform current, where the field strength due to a single spectral component of angular frequency, ω , is:

$$E = \frac{\eta A I \omega^2}{4\pi c^2 D}$$
 (2.8)

where E = field strength, volts/meter

 η = intrinsic impedance of free space (120 π ohms)

A = area of loop, m²

D = distance from loop, m

I = amplitude of spectral component

Substituting his expression for the peak amplitude of the current in equation (2.8), Newell obtained an expression for the peak field strength for a receiver. Figure 5 (b) shows his theoretical result when the cylinder pressure is atmospheric (spark plug breakdown voltage = 2,500 volts), and when the cylinder pressure is 75 lb/in^2 gauge (spark plug breakdown voltage = 9,000 volts).

Recently Published Research

Continued crowding of the radio spectrum has maintained interest in RFI from automobiles. Some recent investigations are summarized below:

State variable model of ignition system. McLaughlin [10] developed the state equations for a uniform transmission line model of the ignition system. However, excessive computations were required to solve these equations for the time interval between point opening and spark plug gap breakdown, and no results were given.

Experimentation with new suppression techniques. In 1969, General Motors began installing its Radio Frequency Interference Suppression,

(RFIS), package on automobiles to meet the limits of the SAE standard. The package involved three modifications [4]: 1) the use of distributed resistance ignition cables, 2) an increase of the distributor gap from 0.031 inches to 0.094 inches, and 3) the use of specially designed resistor type spark plugs.

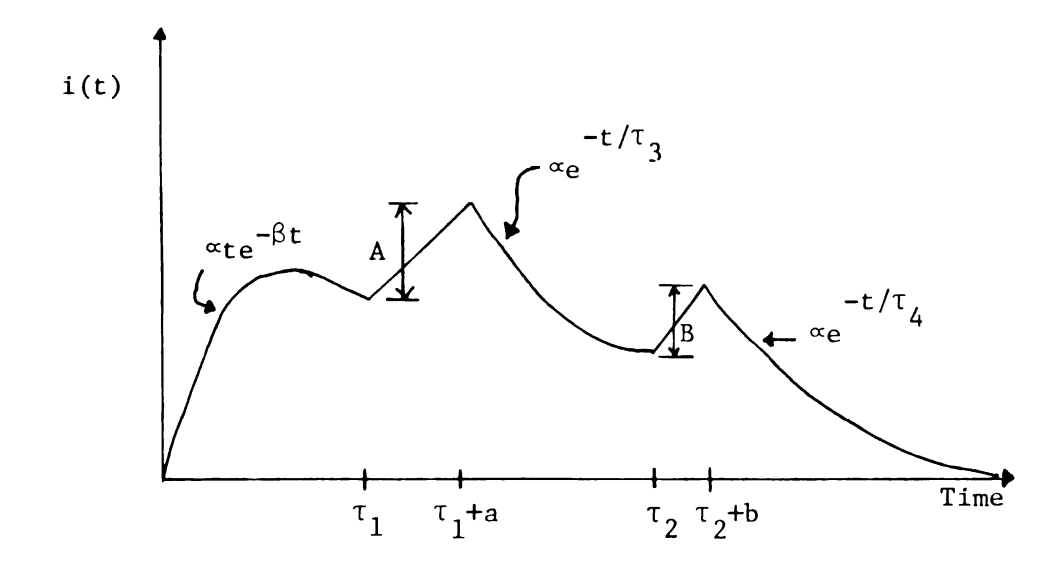
Hsu and Schlick [28] made measurements on a simulated ignition system with a variable distributor gap, and observed the form of the spark plug current to be similar to that shown in Figure 6(a). From the Fourier transform of the current equation, they demonstrated reduced interference for increases in the distributor gap (which appear as decreases in the time, τ_1).

Burgett et. al. [19] investigated the effects of different spark plug designs on RFI, and measured the interference for different spark plug gaps as shown in Figure 6(b). Noting the influence of the gap on the interference spectrum, they recommended further study without drawing a specific conclusion on their data.

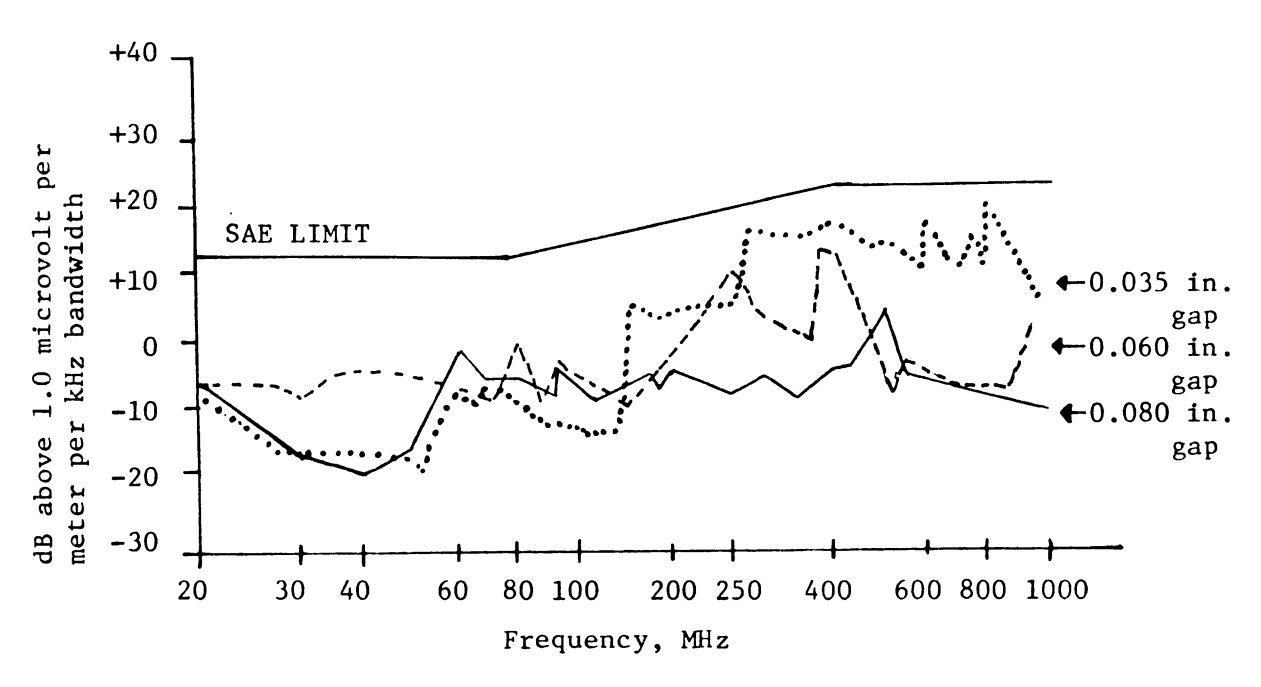
At Stanford Research Institute, Shepherd et. al. [5] demonstrated significant suppression improvement of two different vehicles already equipped with the General Motors RFIS package. Their technique involved low-pass filtering to restrict the radiation associated with the gap breakdowns and contact breaker operation.

Alternative characterizations of ignition noise. Alternative methods of representation are continually being sought to accurately depict ignition noise. Research at General Motors has concentrated on pulse height distributions 1 which, for identically equipped vehicles, were approximately found to be Weibull distributions [29].

PHDs plot the number of detected pulses against their peak amplitude.



(a) Hsu's approximation of spark plug current waveform [28].



(b) Interference for different spark plug gaps [19].

Figure 6 - Results of recent studies of spark plug current and RFI.

Shepherd [30] investigated amplitude probability distributions, (APDs), and found these distributions to be part Rayleigh and part Weibuli.

RF current distribution on car bodies. Minozuma [31] observed several aspects of automobile radio noise, including a unique study: the measurement of radio frequency currents on the surface of a car.

Using a sliding current probe, Minozuma made measurements along a vertical line just behind both front doors of a small van, and at constant heights around the body. He observed resonance patterns in the horizontal directions, and a 3/4 wave-length antenna current distribution in the vertical direction at 220 MHz for the unsuppressed vehicle. With the application of suppression techniques, some resonance was still observed, but the amplitude of the current was noticeably reduced away from the neighborhood of the engine.

CHAPTER III

SPARK PLUG CURRENT AS A FUNCTION OF TIME

This chapter presents a model for predicting current and voltage waveforms in an ignition circuit. First, the assumptions are stated.

Next, solutions of the circuit equations are obtained for two time periods: between the distributor and spark plug gap breakdowns, and after the spark plug gap breakdown.

Finally, numerical examples compare the theory with published results.

Ignition Circuit Model

A circuit model provides a simplified means for understanding an observed physical event and for anticipating future behavior. In doing this, a model should be analyzable, and it should accurately portray the modeled event.

Using distributed elements and transmission line theory undoubtedly results in an accurate model of the ignition system. However, as shown in the previous chapter, the complexity of such a model generally precludes a researcher from performing a complete analysis. The objective of the following research, then, is to enhance the accuracy of a state of the art, lumped element ignition circuit model.

Figure 7 shows the proposed model based on the following assumptions:

1. Whether the system employs a conventional contact breaker or an electronic switch, the purpose of the primary circuit is the same: to

interrupt the primary current and cause the coil secondary voltage to rise. Therefore, details of the primary circuit are not given.

- 2. As shown in Figure 2 on page 8, the secondary circuit reaches a steady state just prior to the opening of the contact breaker. With negligible current in the secondary, the voltage builds rapidly at the coil, and the distributor gap immediately breaks down. These events are represented by an instantaneous charging of a coil capacitance, $\mathbf{C}_{\mathbf{C}}$, while the secondary current is zero immediately before the distributor gap breaks down.
- 3. The high voltage secondary ignition cables are assumed to be resistive and inductive only. The components \mathbf{R}_1 and \mathbf{L}_1 represent the coil-to-distributor cable, while \mathbf{R}_2 and \mathbf{L}_2 represent a spark plug cable.
- 4. When not broken down, the distributor and spark plug gaps are essentially capacitive, as shown by C_{dg} and C_{sg} , respectively.
- 5. The gaps are assumed to be either open circuits or short circuits, with zero transition time from one state to the other.

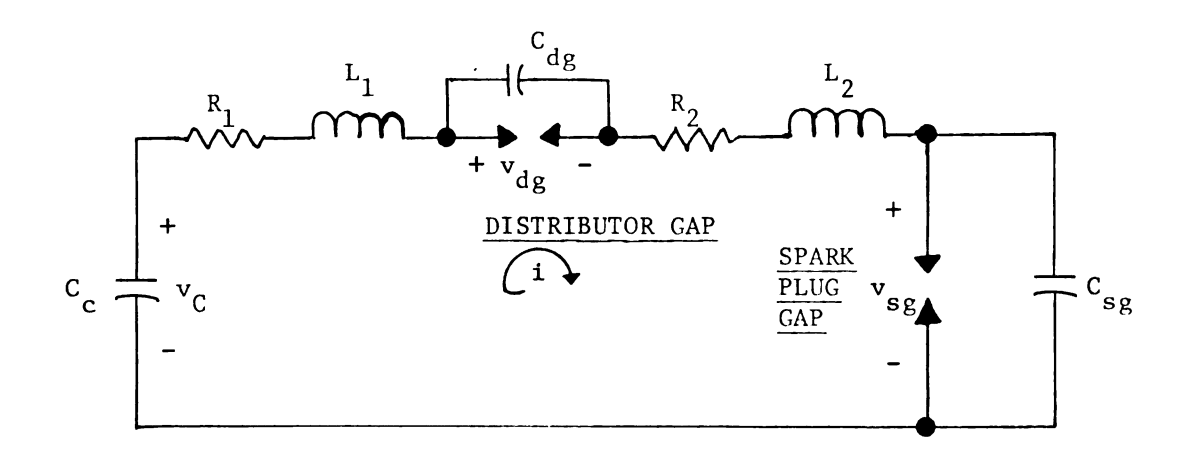


Figure 7 - Proposed Ignition Circuit Model

Circuit Equations Before Spark Plug Fires

Analysis of the ignition circuit model shown in Figure 7 entails the solution of differential equations for the time variation of all pertinent voltages and current. First, the solution for the voltage, $v_{\rm C}$, is sought following breakdown of the distributor gap, but before the spark plug gap breaks down.

Using Kirchoff's voltage law,

$$v_C(t) = R_1 i(t) + L_1 \frac{di(t)}{dt} + v_{dg}(t) + R_2 i(t) + L_2 \frac{di(t)}{dt} + v_{sg}(t)$$
 (3.1)

At any given time, the current through the capacitors is given by:

$$i(t) = -C_c \frac{dv_C(t)}{dt} = +C_{sg} \frac{dv_{sg}(t)}{dt}$$
 (3.2)

where the change in sign results from the requirement of conservation of charge.

Also, equation (3.2) may be differentiated, since the voltages are continuous; that is, the voltages across the capacitors do not change instantaneously due to finite current inputs [32]. Then, equation (3.1) becomes (using $R = R_1 + R_2$ and $L = L_1 + L_2$):

$$v_{c}(t) = -R C_{c} \frac{dv_{c}(t)}{dt} - L C_{c} \frac{d^{2}v_{c}(t)}{dt^{2}} + v_{dg}(t) + v_{sg}(t)$$
 (3.3)

Also, integrating equation (3.2),

$$\int_{0}^{t} \left(\frac{dv_{C}(t)}{dt} \right) dt = -\frac{c_{sg}}{c_{c}} \int_{0}^{t} \left(\frac{dv_{sg}(t)}{dt} \right) dt$$
 (3.4)

from which

$$v_{C}(t) - v_{C}(0) = -\frac{c_{sg}}{c_{c}} \left[v_{sg}(t) - v_{sg}(0) \right]$$
 (3.5)

The initial conditions required in equation (3.5) come from evaluating equation (3.1) at t=0. By assuming that the current in the ignition circuit has attenuated to zero just before the distributor gap breaks down, and further, if the time rate of change of the current is assumed to be zero at t=0, then equation (3.1) becomes:

$$v_{C}(0) = v_{dg}(0) + v_{sg}(0)$$
 (3.6)

Totally discharged capacitors which charge at the same rate build their voltages inversely to the ratio of their capacitances, so

$$\frac{v_{dg}(0)}{v_{sg}(0)} = \frac{c_{sg}}{c_{dg}}$$
(3.7)

The distributor gap is assumed to break down instantaneously once it has an arbitrary voltage, \mathbf{E}_1 , across it, so

$$v_{dg}(0) = E_1$$
 (3.8)

Substituting equations (3.7) and 3.8) into equation (3.6),

$$v_{C}(0) = E_{1} \left(1 + \frac{C_{dg}}{C_{sg}} \right)$$
(3.9)

Substituting equations (3.7, (3.8), and (3.9)) into equation (3.5) and solving for the spark plug voltage,

$$v_{gg}(t) = -\frac{C_c}{C_{gg}} \left[v_C(t) - E_1 \left(\frac{C_c C_{gg} + C_c C_{dg} + C_{gg} C_{dg}}{C_c C_{gg}} \right) \right]$$
 (3.10)

Finally, defining

$$\frac{1}{C_{X}} = \frac{1}{C_{c}} + \frac{1}{C_{dg}} + \frac{1}{C_{sg}} = \frac{C_{c} C_{sg} + C_{c} C_{dg} + C_{sg} C_{dg}}{C_{c} C_{dg} C_{sg}}$$
(3.11)

and combining equations (3.3), (3.10), and (3.11),

$$\left(1 + \frac{c_{c}}{c_{sg}}\right) v_{c}(t) = -R c_{c} \frac{dv_{c}(t)}{dt} - L c_{c} \frac{d^{2}v_{c}(t)}{dt^{2}} + v_{dg}(t) +$$

$$\frac{E_1 \quad C \quad C_{dg}}{C_{sg} C_X} \tag{3.12}$$

The differential equation given above may be solved by either of two methods: 1) the homogeneous/particular method of solution, or 2) the LaPlace transform method. Both methods were used to insure accurate results, but only the LaPlace transform solution follows.

Using the definition of the one-sided LaPlace transform to transform each term in equation (3.12), the first term is:

$$\mathcal{Q} \left\{ v_{dg}(t) \right\} = \int_{0}^{\infty} v_{dg}(t) e^{-st} dt = \int_{0}^{0^{+}} v_{dg}(t) e^{-st} dt + \int_{0^{+}}^{\infty} v_{dg}(t) e^{-st} dt$$
(3.13)

In the interval $[0^+ < t < \infty]$, $v_{\rm dg}(t)$ equals zero from the assumption that the distributor gap remains broken down for positive time.

For the interval $[0^- < t < 0^+]$, $v_{\rm dg}(t)$ is well-behaved, changing value from E_1 to zero. In the limit that the distributor gap voltage changes instantaneously (as has been assumed), the LaPlace transform of $v_{\rm dg}(t)$ becomes identically zero.

The LaPlace transform of the constant term is obtained from the definition as:

$$\mathcal{L} \left\{ \frac{E_1^C_c^C_{dg}}{C_{sg}^C_x} \right\} = \int_0^\infty \frac{E_1^C_c^C_{dg}}{C_{sg}^C_x} e^{-st} dt = \left(\frac{1}{s}\right) \left(\frac{E_1^C_c^C_{dg}}{C_{sg}^C_x}\right) \tag{3.14}$$

Transformation of the remaining terms in equation (3.12), combined with the preceding results, gives the equation

$$\left(1 + \frac{C_{c}}{C_{sg}}\right) v_{c}(s) = -RC \left[s v_{c}(s) - v_{c}(0)\right] - LC_{c}\left[s^{2} v_{c}(s) - s v_{c}(0)\right] - \frac{dv_{c}(0)}{dt} + \frac{1}{s} \left[E_{1}\left(\frac{C_{c}C_{dg}}{C_{sg}C_{x}}\right)\right]$$
(3.15)

Using equation (3.9) and its derivative for the initial conditions and rearranging, equation (3.15) becomes

$$V_{c}(s) = \frac{R C_{c} E_{1} \left(1 + \frac{C_{dg}}{C_{sg}}\right) + sLC_{c} E_{1} \left(1 + \frac{C_{dg}}{C_{sg}}\right) + \frac{E_{1}}{s} \left(\frac{C_{c} C_{dg}}{C_{sg} C_{x}}\right)}{s^{2} LC_{c} + s RC_{c} + \left(1 + \frac{C_{c}}{C_{sg}}\right)}$$
(3.16)

Equation (3.16) may be written as the partial fraction expansion:

$$V_c(s) = \frac{K_1}{s} + \frac{K_2}{s - s_1} + \frac{K_3}{s - s_2}$$
 (3.17a)

where

$$X = \left(\frac{R}{L}\right)^2 - \left(\frac{4}{LC_c}\right) \left(1 + \frac{C_c}{C_{sg}}\right)$$
 (3.17b)

$$s_1 = -\frac{R}{2L} + \frac{1}{2}\sqrt{X}$$
 (3.17c) $s_2 = -\frac{R}{2L} - \frac{1}{2}\sqrt{X}$ (3.17d)

$$K_{1} = \frac{E_{1}C_{c}C_{dg}}{C_{x}(C_{sg} + C_{c})}$$
 (3.17e)

$$K_{2} = \frac{\left(s_{1} + \frac{R}{L}\right)E_{1}}{\left(s_{1} - s_{2}\right)} + E_{1}\left(\frac{C_{dg}}{C_{sg}}\right)\left[\frac{s_{1}^{2} + s_{1}\left(\frac{R}{L}\right) + \frac{1}{LC_{x}}}{s_{1}\left(s_{1} - s_{2}\right)}\right]$$
(3.17f)

$$K_{3} = \frac{\left(s_{2} + \frac{R}{L}\right) E_{1}}{\left(s_{2} - s_{1}\right)} + E_{1} \left(\frac{c_{dg}}{c_{sg}}\right) \frac{\left[s_{2}^{2} + s_{2}\left(\frac{R}{L}\right) + \frac{1}{Lc_{x}}\right]}{s_{2}(s_{2} - s_{1})}$$
(3.17g)

Equation (3.17a) shows simple poles at s = 0, $s = s_1$, and $s = s_2$. The inverse transform is then easily calculated using the residue theorem [33]:

$$v_C(t) = \sum_{i=1}^{3} \left\{ \text{Residue of } [V_c(s)e^{st}] \text{ at the } i^{th} \text{ simple pole} \right\} (3.18)$$

where the residue of a function at the isolated singular point, s_0 , is given by

Residue (s =
$$s_0$$
) = $\lim_{s \to s_0} [(s - s_0)V_c(s)]$ (3.19)

After some simplification and rearrangement, the solution for the coil voltage is:

$$v_{c}(t) = \frac{E_{1}^{C_{c}}C_{dg}}{C_{x}(C_{c} + C_{sg})} + \frac{E_{1}}{2\sqrt{X}} \left(\frac{R}{L}\right) \left(\frac{C_{sg}}{C_{sg} + C_{c}}\right) \left(e^{s_{1}t} - e^{s_{2}t}\right) + \frac{E_{1}}{2} \left(\frac{C_{sg}}{C_{sg} + C_{c}}\right) \left(e^{s_{1}t} + e^{s_{2}t}\right)$$

$$(3.20)$$

The current in the secondary of the ignition circuit is obtained using equation (3.2). Performing the indicated differentiation and simplifying,

$$i(t) = \frac{E}{L\sqrt{X}} e^{-\frac{R}{2L}t\left(e^{\frac{1}{2}\sqrt{X}t} - e^{-\frac{1}{2}\sqrt{X}t}\right)} \quad \text{for} \quad \left(\frac{R}{L}\right)^2 > \frac{4}{LC_c}\left(1 + \frac{C_c}{C_{sg}}\right) \quad (3.21)$$

When the radical term is imaginary, equation (3.21) may be rewritten as:

$$i(t) = \frac{\frac{-\frac{R}{2L}}{e} t}{\frac{2E_1 e}{L\sqrt{|X|}}} \sin \left[\frac{1}{2}\sqrt{|X|} t\right] \qquad \text{for } \left(\frac{R}{L}\right)^2 < \frac{4}{LC_c} \left(1 + \frac{C_c}{C_{sg}}\right) \quad (3.22)$$

To emphasize the form of the solution given in equations (3.21) and (3.22), define

$$a = \frac{R}{2L}$$
 $\omega_0^2 = \frac{1}{LC_c}$ $f^2 = \left(1 + \frac{C_c}{C_{sg}}\right)$ (3.23)

$$g_1 = \sqrt{a^2 - (f\omega_0)^2}$$
 $g_2 = \sqrt{(f\omega_0)^2 - a^2}$ (3.23)

Then

$$i(t) = \frac{E_1}{2Lg_1} e^{-at} (e^{g_1^t} - e^{-g_1^t}) \qquad for (\frac{R}{L})^2 > \frac{4}{LC_c} (1 + \frac{C_c}{C_{sg}})$$
 (3.24a)

$$i(t) = \frac{E_1}{Lg_2} e^{-at} \sin(g_2 t) \qquad \text{for } \left(\frac{R}{L}\right)^2 < \frac{4}{LC_c} \left(1 + \frac{C_c}{C_{sg}}\right) \qquad (3.24b)$$

The current excited in the secondary of the ignition circuit by the closing of the distributor gap behaves either exponentially or as an exponentially decaying sinusoid. Note that the form of equation (3.24b) agrees with the solution assumed by Newell in equation (2.6).

Circuit Equations After Spark Plug Fires

The next step in the analysis determines the form of the ignition circuit current after the spark plug gap breaks down. The circuit shown in Figure 7 still applies, except that the distributor gap is now assumed to be perfectly conducting.

Kirchoff's voltage law now yields:

$$v_C(t) = R i(t) + L \frac{di(t)}{dt} + v_{sg}(t)$$
 (3.25)

Combining the above with equation (3.2),

$$v_{C}(t) = -R C_{c} \frac{dv_{C}(t)}{dt} - L C_{c} \frac{d^{2}v_{C}(t)}{dt^{2}} + v_{sg}(t)$$
 (3.26)

Using the LaPlace transform method of solution, the transformed equation is:

$$V_{C}(s) = -R C_{c} \left[sV_{C}(s) - v_{C}(0) \right] - L C_{c} \left[s^{2}V_{C}(s) - sv_{C}(0) - \frac{dv_{C}(0)}{dt} \right]$$
(3.27)

Using an approach similar to the solution of equation (3.13), the transform of \mathbf{v}_{sg} (t) is identically zero for an instantaneous spark plug firing.

In equation (3.27), the time scale is shifted so that t=0 when the spark plug gap breaks down. This breakdown occurs at a time $t=t_1$ after the distributor gap has broken down, and coincides with the build-up of a specified voltage, E_2 , across the spark plug gap.

The initial conditions for equation (3.27) are determined by combining equations (3.20), (3.21), and (3.25) to get:

$$v_{sg}(t) = \left(\frac{E_{1}C_{c}}{C_{sg} + C_{c}}\right) \left\{\frac{C_{dg}}{C_{x}} - \frac{e^{-\frac{R}{2L}t}}{2} \left[\left(\frac{R}{L\sqrt{X}} + 1\right) e^{\frac{l_{2}\sqrt{X}t}} - \left(\frac{R}{L\sqrt{X}} - 1\right)\right] e^{-\frac{l_{2}\sqrt{X}t}}$$

$$e^{-\frac{l_{2}\sqrt{X}t}}$$
(3.28)

which is the expression for the spark plug voltage after the distributor gap breaks down (t=0) and before the spark plug gap breaks down (t= t_1).

The spark plug gap breaks down when the spark plug voltage equals a specified voltage, $\rm E_2$. By setting equation (3.28) equal to $\rm E_2$, the value of $\rm t_1$ may be determined. Then, the values of $\rm v_C(t)$ and $\rm dv_C(t)/dt$ when the spark plug fires are determined from equations (3.2), (3.20), and (3.21) as follows:

$$v_{c}(t_{1}) = \frac{E_{1}^{C_{c}C_{dg}}}{C_{x}(C_{sg} + C_{c})} + \frac{E_{1}^{R}(e^{s_{1}^{t_{1}}} - e^{s_{2}^{t_{1}}})C_{sg}}{2L\sqrt{X}(C_{sg} + C_{c})} + \frac{E_{1}^{C_{sg}}(e^{s_{1}^{t_{1}}} + e^{s_{2}^{t_{1}}})}{2(C_{sg} + C_{c})}$$
(3.29)

$$\frac{dv_{c}(t_{1})}{dt} = \frac{-i(t_{1})}{C_{c}} = \frac{-E_{1}e^{-\frac{R}{2L}} t_{1}(e^{\frac{1}{2}\sqrt{X}} t_{1} - e^{-\frac{1}{2}\sqrt{X}} t_{1})}{LC_{c}\sqrt{X}}$$
(3.30)

The values determined in equations (3.29) and (3.30) above are directly substitutable into equation (3.27) as the initial conditions $v_{\rm C}(0)$ and $dv_{\rm C}(0)/dt$. Combining terms and rewriting,

$$V_{c}(s) = \frac{s v_{c}(t_{1}) + \left[\frac{R v_{c}(t_{1})}{L} + \frac{dv_{c}(t_{1})}{dt}\right]}{s^{2} + s(\frac{R}{L}) + \frac{1}{LC_{c}}}$$
(3.31)

Using the residue theorem to obtain the inverse transform, the voltage across the capacitor, $\mathbf{C}_{\mathbf{c}}$, after the distributor and spark plug gaps have both broken down is

$$v_{c}(t) = \frac{e^{\frac{s}{3}t}}{2\sqrt{Y}} \left[\left(\frac{R}{L} + \sqrt{Y} \right) v_{c}(t_{1}) + 2 \frac{dv_{c}(t_{1})}{dt} \right]$$

$$-\frac{e^{\frac{s}{4}t}}{2\sqrt{Y}} \left[\left(\frac{R}{L} - \sqrt{Y} \right) v_{c}(t_{1}) + 2 \frac{dv_{c}(t_{1})}{dt} \right]$$
 (3.32a)

where $Y = \left(\frac{R}{L}\right)^2 - \frac{4}{LC_c}$ (3.32b)

$$s_3 = -\frac{R}{2L} + \frac{1}{2}\sqrt{Y}$$
 (3.32c) $s_4 = -\frac{R}{2L} - \frac{1}{2}\sqrt{Y}$ (3.32d)

Time, t, in equation (3.32a) is measured from the instant the spark plug breaks down, and the values of $v_{\rm C}(t_1)$ and $dv_{\rm C}(t_1)/dt$ are given in equations (3.29) and (3.30).

Again, using equation (3.2) and simplifying,

$$i(t) = \left[v_{c}(t_{1}) + \frac{RC_{c}}{2} \left(\frac{dv_{c}(t_{1})}{dt}\right)\right] \left[\frac{e^{\frac{1}{2}\sqrt{Y}}t}{L\sqrt{Y}}\right] \left[e^{\frac{1}{2}\sqrt{Y}}t - e^{-\frac{1}{2}\sqrt{Y}}t\right]$$

$$-\left(\frac{C_{c}}{2}\right) \left(\frac{dv_{c}(t_{1})}{dt}\right) e^{-\frac{R}{2L}t} \left[e^{\frac{1}{2}\sqrt{Y}}t + e^{-\frac{1}{2}\sqrt{Y}}t\right]$$
for $\left(\frac{R}{L}\right)^{2} > \frac{4}{LC_{c}}$ (3.33)

Finally, if the radical term in equation (3.33) is imaginary,

$$i(t) = \left[2 v_c(t_1) + RC_c \left(\frac{dv_c(t_1)}{dt} \right) \right] \left[\frac{e^{-\frac{R}{2L}t}}{L\sqrt{|Y|}} \right] \sin\left(\frac{1}{2} \sqrt{|Y|} t \right)$$

$$- C_{c} \left(\frac{dv_{c}(t_{1})}{dt} \right) e^{-\frac{R}{2L}t} \cos \left(\frac{1}{2} \sqrt{|Y|} t \right) \qquad \text{for } \left(\frac{R}{L} \right)^{2} < \frac{4}{LC}$$
 (3.34)

Numerical Examples

This section presents the results obtained by substituting selected component values into the equations from the preceding sections.

A computer program (see Appendix A) was written to solve equations (3.10), (3.20), (3.21), and (3.22) for the current and voltage waveforms prior to the firing of the spark plug. The output of this program facilitates determination of the parameter, t_1 , for a given spark plug gap breakdown voltage.

Another computer program (see Appendix B) was written to solve equation (3.32), (3.33), and (3.34) given the value of t_1 , and the plots which follow utilize the outputs of both programs.

Results using Newell's values. Figure 8 shows the predicted behavior of the voltage and current for component values originally used by Newell [8]. While Newell used his values to obtain good results in the frequency

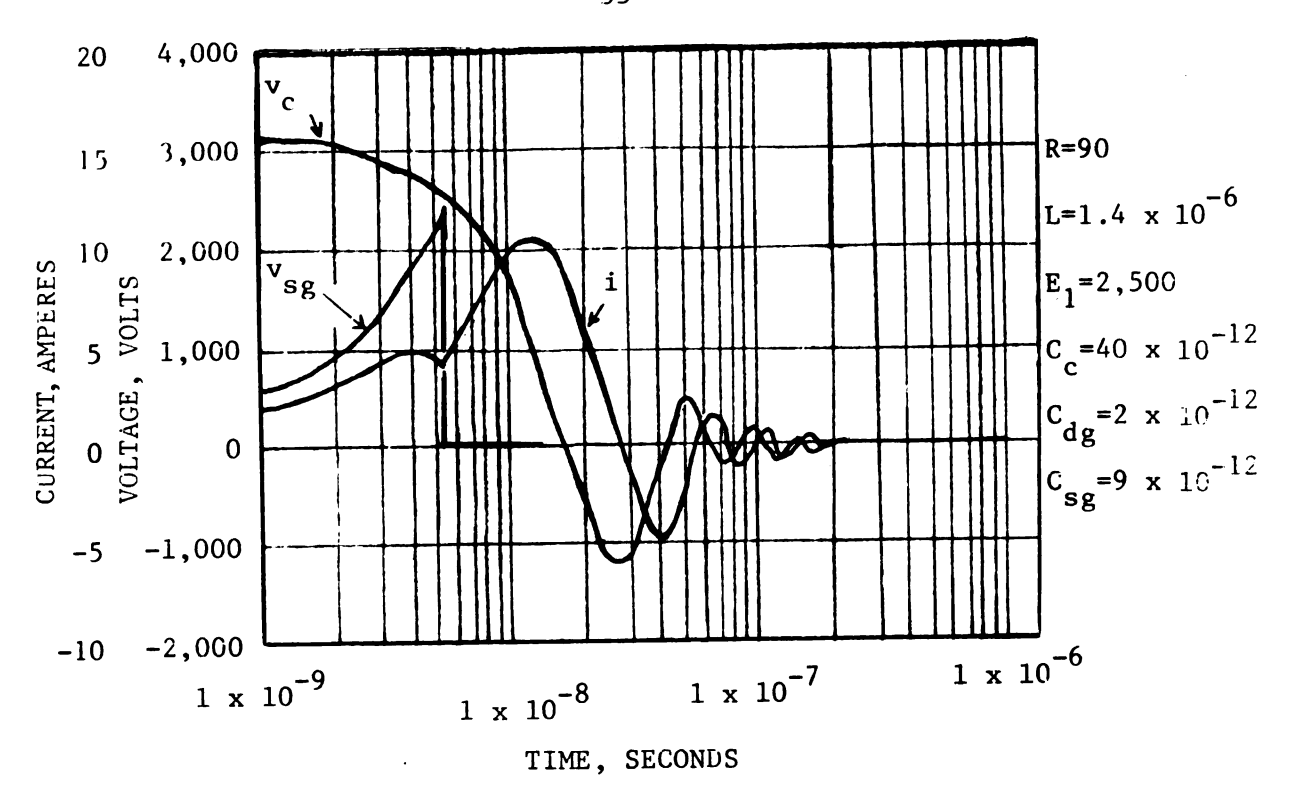


Figure 8 - Theoretical Waveforms Using Newell's Values

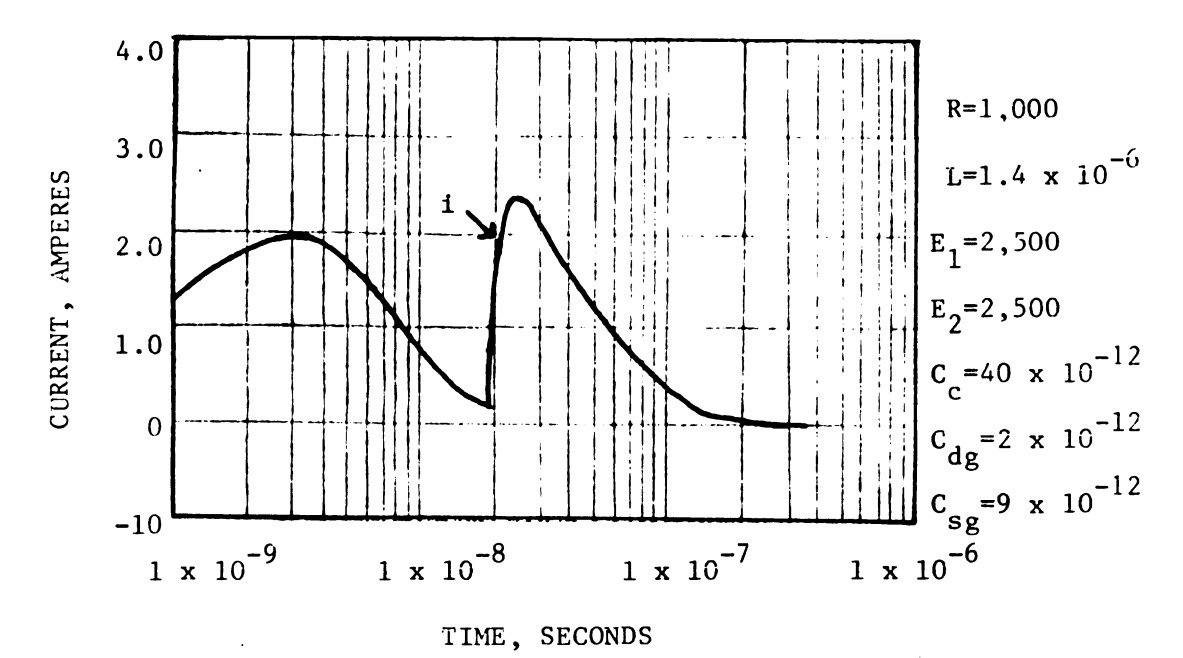
domain (see Figure 5(a) on page 18), he gave no consideration to the time behavior of the circuit.

Serious objection may be raised to the time between gap breakdowns, t_1 , of 5 x 10^{-9} seconds. This is nearly a thousand times faster than the value for modern ignition systems indicated in Table 1 on page 7.

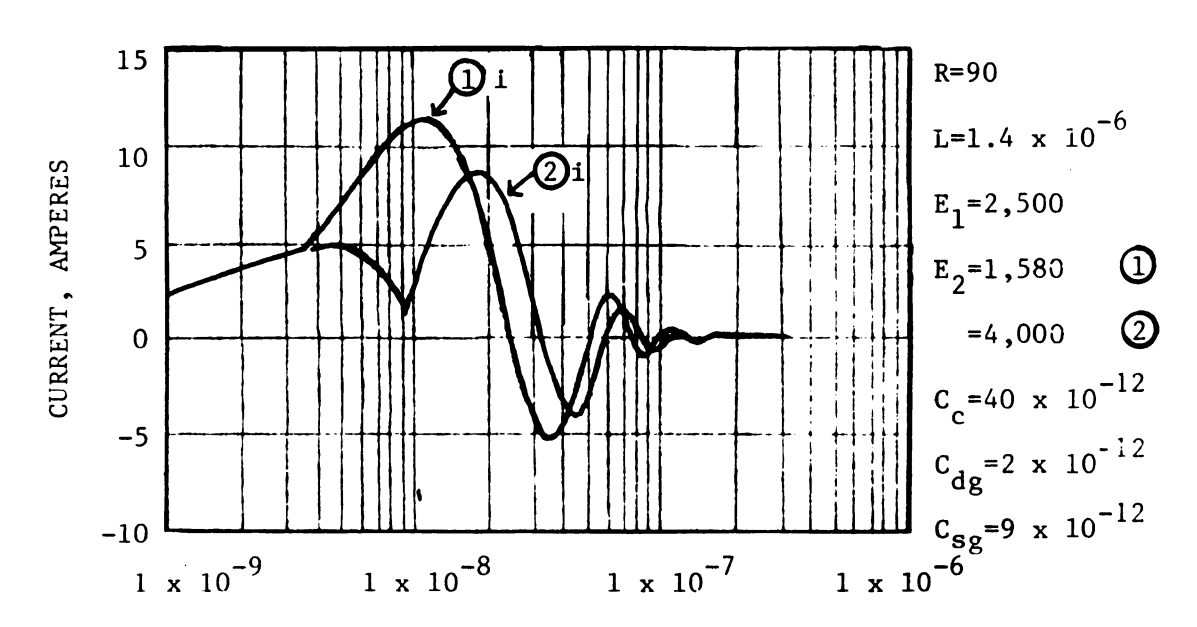
rurther, Newell used his equations with a spark plug gap breakdown voltage of 9,000 volts to compare his theory with data from a pressurized cylinder [8]. However, the maximum value of the spark plug voltage using Newell's values is under 4,100 volts.

The remaining examples demonstrate the changes in behavior attainable using different component values.

Effect of changing R. Increasing the resistance, R, slows the rate of oscillation in circuits below resonance, and increases the time constants of the exponential terms above resonance. Figure 9(a) shows the current for a circuit above resonance.



(a) Current for a Circuit above Resonance



(b) Effect of Change in Spark Plug Gap Breakdown Voltage

Figure 9 - Theoretical Current Waveforms

With higher values of resistance, the spark plug voltage takes longer to reach the same value, so t increases. Also, the amplitude of the current is reduced, with a corresponding reduction in the radio frequency interference associated with the circuit operation. However, for excessive values of resistance, so much energy dissipates through the resistance that the spark plug can not fire.

Effect of changing E_2 . Reducing the estimated spark plug gap breakdown voltage, E_2 , directly snortens the time between gap breakdowns. Also, the peak amplitude of the current is affected, as shown in Figure 9(b).

Effect of changing $C_{\rm dg}$ and $E_{\rm l}$. Capacitance describes the ratio of the magnitude of charge on either of two plates to the potential difference between the plates, or

$$C = \frac{Q}{V} \tag{3.35}$$

For two parallel plates, each with area, A, and separated by distance, d, equation (3.35) reduces to [34]:

$$C = \frac{\varepsilon A}{d}$$
 (3.36)

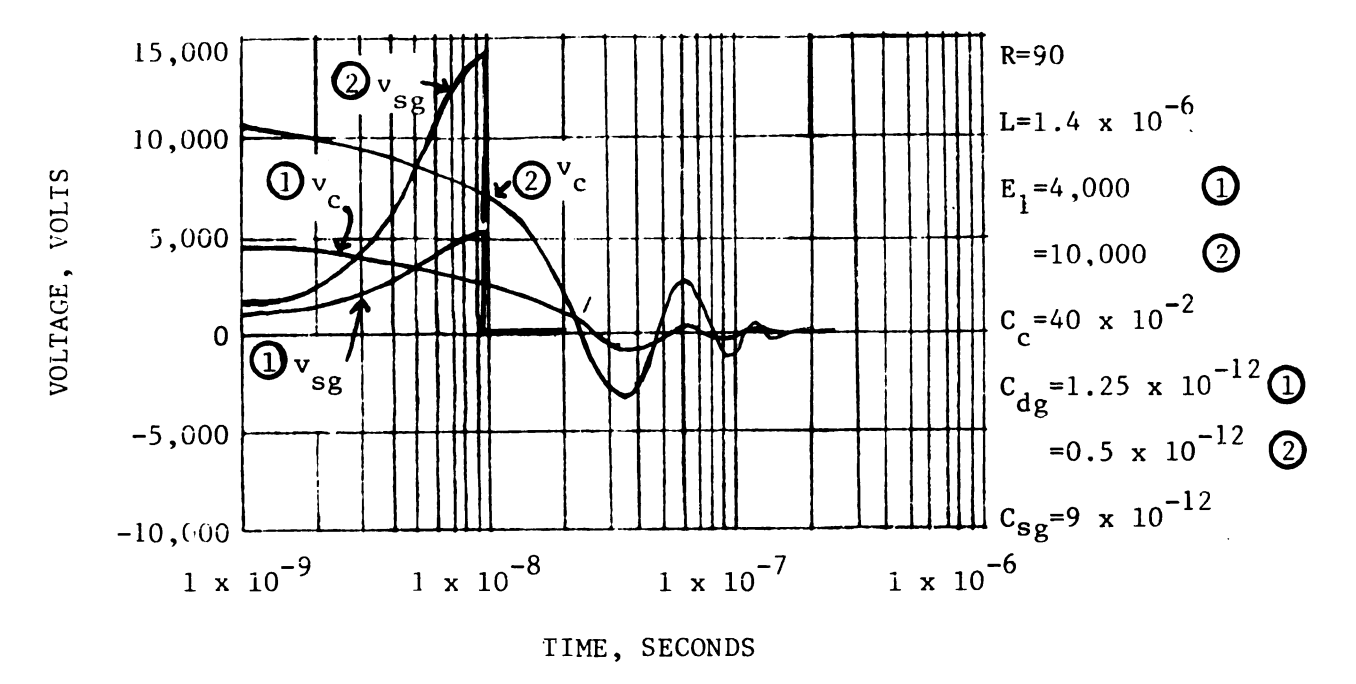
where ϵ , is the permittivity of the medium between the plates.

By analogy to the parallel plates, increasing the distributor gap should reduce the distributor gap capacitance. Further, if the initial charge on the distributor gap is the same both before and after the gap is changed, then the value of the distributor gap breakdown voltage should increase. This agrees with the observations listed in Table 1 on page 7 for General Motors' change of the distributor gap width in 1969.

Figure 10 shows the effect on the voltage and current waveforms for simultaneous changes in the distributor gap capacitance and breakdown voltage using the constant charge assumption. Whereas Newell's original values resulted in a restricted range of values for spark plug firing voltage, Figure 10(a) shows that voltages to 15,000 volts can be readily predicted.

Also, Figure 10(b) shows a considerable increase in the magnitude of the current. Although the charge on the distributor gap prior to breakdown remained unchanged, the energy varies with the square of the voltage. Therefore, the energy in the circuit at the time the distributor gap breaks down is noticeably increased.

Finally, an increase in the width of the distributor gap shortens the time between gap breakdowns for the same spark plug firing voltage. This agrees with the observation of Hsu and Schlick [28] mentioned on page 20.



(a) Voltage Waveforms

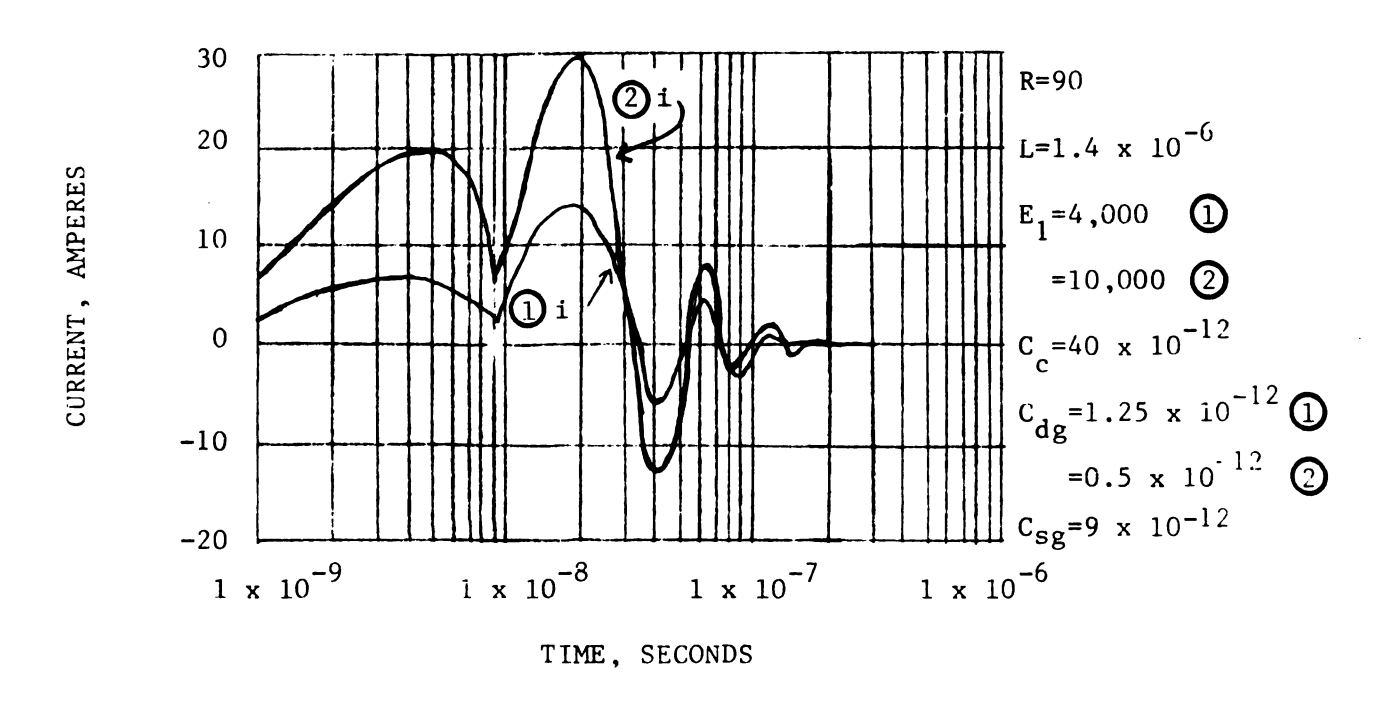


Figure 10 - Theoretical Waveforms for Constant Initial Distributor Gap Charge

(b) Current Waveforms

CHAPTER IV

FREQUENCY SPECTRUM OF SPARK PLUG CURRENT

The preceding development has resulted in closed form expressions of the spark plug current as a function of time. Consideration of the radio frequency interference which results from this current, however, requires knowledge of the frequency variation of the spark plug current.

This chapter develops equations for the amplitude density of the LaPlace transform of the current. Then, tests are performed to imply the correctness of these equations.

The significance of the time between gap breakdowns is investigated, and numerical examples using the amplitude density equations conclude the chapter.

Derivation of Amplitude Density Equations

The amplitude density of the transform of a function expresses the variation of the magnitude of that function in frequency domain. Phase information, while not contained in the amplitude density, is available from intermediate equations.

With the assumption of zero spark plug current for negative values of time, the amplitude density comes from the one-sided LaPlace transform. Substituting $j\omega$ for s and writing the resulting expression in terms of a real and imaginary part, the density is obtained as:

amplitude density =
$$\sqrt{\left[\text{Re }\left\{\text{I}(j\omega)\right\}\right]^2 + \left[\text{Im }\left\{\text{I}(j\omega)\right\}\right]^2}$$
 (4.1)

Calculations of the amplitude density follow for two cases of spark plug current: 1) spectrum of the current arising from breakdown of the spark plug gap only, and 2) spectrum of the total current due to both the distributor and spark plug gap breakdowns.

Amplitude Density - Spark Plug Gap Only. The amplitude density of the current follows from the LaPlace transform of equation (3.2):

$$I(s) = -C_{c} \left[s V_{C}(s) - (initial value of V_{C}) \right]$$
 (4.2)

The initial value of v_C in this case is the coil voltage at a time, t_1 , after the distributor gap breaks down, or $v_C(t_1)$. Also, using the transform of the coil voltage from equation (3.31) and substituting in equation (4.2),

$$I(s) = \frac{\left(\frac{1}{L}\right)\left[v_c(t_1)\right] - (sC_c)\left[\frac{dv_c(t_1)}{dt}\right]}{s^2 + s(\frac{R}{L}) + (\frac{1}{LC_c})}$$
(4.3)

Substituting s = $j\omega$ in the above equation, rationalizing the denominator, and simplifying yields

$$I(j\omega) = \begin{bmatrix} \left(\frac{K_1}{L}\right) \left(\frac{1}{LC_c} - \omega^2\right) - \left(\frac{\omega^2 RC_c K_2}{L}\right) \\ \left(\frac{1}{LC_c} - \omega^2\right)^2 + \left(\frac{\omega R}{L}\right)^2 \end{bmatrix} - j \begin{bmatrix} \left(\omega C_c K_2\right) \left(\frac{1}{LC_c} - \omega^2\right) + \left(\frac{\omega R K_1}{L^2}\right) \\ \left(\frac{1}{LC_c} - \omega^2\right)^2 + \left(\frac{\omega R}{L}\right)^2 \end{bmatrix}$$
where $K_1 = v_c(t_1)$ and $K_2 = \frac{dv_c(t_1)}{dt}$ (4.4)

Finally, applying equation (4.1), the amplitude density of the ignition circuit current due to the spark plug gap breakdown only is:

$$|I(\omega)| = \frac{\sqrt{A_1[\omega^6 + A_5\omega^4 + A_6\omega^2 + A_4]}}{\omega^4 + A_3\omega^2 + A_2}$$
where $A_1 = (C, K_1)^2$ $A_2 = (1/LC_1)^2$ $A_3 = (R/L)^2 - (2/LC_1)$

where
$$A_1 = (C_c K_2)^2$$
 $A_2 = (1/LC_c)^2$ $A_3 = (R/L)^2 - (2/LC_c)$
 $A_4 = (K_1 A_2/K_2)^2$ $A_5 = (A_4/A_2) + A_3$ $A_6 = (A_3 A_4/A_2) + A_2$

Amplitude Density - Distributor and Spark Plug Gaps. The expressions for the spark plug current when the sequential breakdown of both gaps is considered are recalled as:

$$i_0(t) = 0$$
 for $t < 0$ (4.6a)

$$i_{1}(t) = \frac{E}{L\sqrt{X}} \quad e^{-\frac{R}{2L}t} \left(e^{\frac{1}{2}\sqrt{X}^{t}} t - e^{-\frac{1}{2}\sqrt{X}^{t}} t \right) \quad \text{for } 0 < t < t_{1}$$

$$(4.6b)$$
where
$$X = \left(\frac{R}{L} \right)^{2} - \frac{4}{LC_{c}} \left(1 + \frac{C_{c}}{C_{sg}} \right)$$

$$i_{2}(t-t_{1}) = \left[v_{c}(t_{1}) + \left(\frac{RC_{c}}{2} \right) \left(\frac{dv_{c}(t_{1})}{dt} \right) \right] \left[\frac{e^{-\frac{R}{2L}(t-t_{1})}}{L\sqrt{Y}} \right] \left[e^{-\frac{1}{2}\sqrt{Y}} (t-t_{1}) - e^{-\frac{1}{2}\sqrt{Y}} (t-t_{1}) \right] - \left(\frac{C_{c}}{2} \right) \left(\frac{dv_{c}(t_{1})}{dt} \right) \left(e^{-\frac{R}{2L}(t-t_{1})} \right) \left[e^{\frac{1}{2}\sqrt{Y}} (t-t_{1}) + e^{-\frac{1}{2}\sqrt{Y}} (t-t_{1}) \right] \quad \text{for } t > t_{1}$$

$$(4.6c)$$

where
$$Y = \left(\frac{R}{L}\right)^2 - \frac{4}{LC_c}$$

Using Heaviside unit step functions, the above may be written as:

$$i(t) = H(t)i_1(t) - H(t-t_1)i_1(t) + H(t-t_1)i_2(t-t_1)$$
 (4.7)

for $t > t_1$

(4.6c)

The desired transform is then

$$I(s) = \mathcal{L} \left\{ H(t)i_1(t) - H(t-t_1)i_1(t) + H(t-t_1)i_2(t-t_1) \right\}$$
 (4.8)

From the linearity property,

$$I(s) = \mathcal{L}\left\{H(t)i_{1}(t)\right\} - \mathcal{L}\left\{H(t-t_{1})i_{1}(t)\right\} + \mathcal{L}\left\{H(t-t_{1})i_{2}(t-t_{1})\right\}$$
(4.9)

Each of the above will be evaluated separately.

A useful property of transforms concerns real translation in the time domain. This property says that a time-shifted function experiences a phase shift in the frequency domain. Thus,

$$\mathcal{Q}\left\{H(t-t_1)i_2(t-t_1)\right\} = e^{-st_1} I_2(s)$$
 (4.10)

Now, $I_2(s)$ is the transform of the current after the spark plug fires, as given by equation (4.3). Therefore,

$$\mathcal{L}\left\{H(t-t_1)i_2(t-t_1)\right\} = e^{-st_1}\left\{\frac{\left(\frac{1}{L}\right)\left[v_c(t_1)\right] - sC_c\left(\frac{dv_c(t)}{dt}\right]}{s^2 + s\left(\frac{R}{L}\right) + \left(\frac{1}{LC_c}\right)}\right\} \tag{4.11}$$

The next term to be evaluated is $\mathcal{L}\left\{H(t-t_1)i_1(t)\right\}$. First, equation (4.6b) is written as a time-shifted function:

$$i_{1}'(t-t_{1}) = \frac{E}{L\sqrt{X}} e^{\left(-\frac{R}{2L} + \frac{\sqrt{X}}{2}\right)(t-t_{1})} e^{\left(-\frac{R}{2L} + \frac{\sqrt{X}}{2}\right)t_{1}} - \frac{E}{L\sqrt{X}}$$

$$-\left(\frac{R}{2L} + \frac{\sqrt{X}}{2}\right)(t-t_1) - \left(\frac{R}{2L} + \frac{\sqrt{X}}{2}\right) t_1 \tag{4.12}$$

Then

$$\mathcal{J}\left\{H(t-t_1)i_1(t)\right\} = \mathcal{J}\left\{H(t-t_1)i_1'(t-t_1)\right\} = e^{-st_1} I_1(s)$$
 (4.13)

where $I_1(s)$ is the transform of equation (4.12).

By the principle of superposition,

$$I_{1}(s) = \frac{E}{L\sqrt{X}} e^{\left(-\frac{R}{2L} + \frac{\sqrt{X}}{2}\right)t} \left\{ e^{\left(-\frac{R}{2L} + \frac{\sqrt{X}}{2}\right)t} \right\} - \frac{E}{L\sqrt{X}} e^{-\left(\frac{R}{2L} + \frac{\sqrt{X}}{2}\right)t}$$

$$\left\{ e^{-\left(\frac{R}{2L} + \frac{\sqrt{X}}{2}\right)t} \right\}$$

$$\left\{ e^{-\left(\frac{R}{2L} + \frac{\sqrt{X}}{2}\right)t} \right\}$$

$$(4.14)$$

By definition of the one-sided LaPlace transform,

$$\mathcal{Q}\left\{e^{\left(-\frac{R}{2L} + \frac{\sqrt{X}}{2}\right)} t\right\} = \int_{0}^{\infty} e^{-\left[s + \left(\frac{R}{2L} - \frac{\sqrt{X}}{2}\right)\right]} t_{dt} \tag{4.15}$$

The complex variable, s, may be written in terms of a real and imaginary part as

$$s = \sigma + j\omega \tag{4.16}$$

Then, the integral in equation (4.15) is seen to converge when the real part, σ , is greater than -R/2L, so that

$$\mathcal{L}\left\{e^{\left(-\frac{R}{2L} + \frac{\sqrt{X}}{2}\right)t}\right\} = \frac{1}{s + \left(\frac{R}{2L} - \frac{\sqrt{X}}{2}\right)} \quad \text{for } \sigma > -\frac{R}{2L} \tag{4.17}$$

Since the intent is to observe the frequency content of the ignition circuit current, the real part of s is customarily taken as zero, and the restriction required in obtaining the above transform poses no problems.

By a similar integration,

$$\mathcal{Q}\left\{e^{-\left(\frac{R}{2L} + \frac{\sqrt{X}}{2}\right)t}\right\} = \frac{1}{s + \left[\frac{R}{2L} + \frac{\sqrt{X}}{2}\right]} \quad \text{for } \sigma > -\frac{R}{2L}$$
 (4.18)

Substitution of equations (4.14), (4.17), and (4.18) into equation (4.13) yields

$$\mathcal{Q}\left\{H(t-t_1)i_1(t)\right\} = \frac{E}{L\sqrt{X}} e^{-\left(\frac{R}{2L} + s\right)t_1} \underbrace{\begin{cases} \frac{\sqrt{X}}{2}t_1\\ s + \left[\frac{R}{2L} - \frac{\sqrt{X}}{2}\right] \end{cases}}_{s + \left[\frac{R}{2L} + \frac{\sqrt{X}}{2}\right]} - \frac{e^{-\frac{\sqrt{X}}{2}t_1}}{s + \left[\frac{R}{2L} + \frac{\sqrt{X}}{2}\right]} \right\} \tag{4.19}$$

The last term to be evaluated is $\{H(t)i_1(t)\}$. This is easily found to be

$$\mathcal{G}\left\{H(t)i_{1}(t)\right\} = \frac{E}{L\sqrt{X}} \left\{\frac{1}{s + \left[\frac{R}{2L} - \frac{\sqrt{X}}{2}\right]} - \frac{1}{s + \left[\frac{R}{2L} + \frac{\sqrt{X}}{2}\right]}\right\}$$
(4.20)

The desired transform of the ignition circuit current is obtained by substituting equations (4.11), (4.19), and (4.20) into equation (4.9).

$$I(s) = \frac{E}{L\sqrt{X}} \left\{ \frac{1}{s + \left[\frac{R}{2L} - \frac{\sqrt{X}}{2}\right]} - \frac{1}{s + \left[\frac{R}{2L} + \frac{\sqrt{X}}{2}\right]} - \frac{E}{L\sqrt{X}} e^{-\left(\frac{R}{2L} + s\right)t_{1}} \right\}$$

$$\left\{ \frac{\frac{\sqrt{X}}{2}t_{1}}{s + \left[\frac{R}{2L} - \frac{\sqrt{X}}{2}\right]} - \frac{e^{-\frac{\sqrt{X}}{2}t_{1}}}{s + \left[\frac{R}{2L} + \frac{\sqrt{X}}{2}\right]} + e^{-st_{1}} \left\{ \frac{\left(\frac{1}{L}\right)\left[v_{c}(t_{1})\right] - sC_{c}\left[\frac{dv_{c}(t_{1})}{dt}\right]}{s^{2} + s\left(\frac{R}{L}\right) + \left(\frac{1}{LC_{c}}\right)} \right\}$$

$$(4.21)$$

If the radical term in equation (4.21) is real, the circuit may be said to be above resonance. Equation (4.21) may then be simplified using the following definitions and substituting $j\omega$ for s:

$$I(j\omega) = \frac{A_4 \cos \omega t_1}{\left(-\omega^2 + \frac{1}{LC_c}\right) + j\left(\frac{\omega R}{L}\right)} - j\frac{A_4 \sin \omega t_1}{\left(-\omega^2 + \frac{1}{LC_c}\right) + j\left(\frac{\omega R}{L}\right)}$$

$$-j \frac{\omega^{A_5} \cos \omega t_1}{\left(-\omega^2 + \frac{1}{LC_c}\right) + j\left(\frac{\omega R}{2}\right)} - \frac{\omega^{A_5} \sin \omega t_1}{\left(-\omega^2 + \frac{1}{LC_c}\right) + j\left(\frac{\omega R}{L}\right)} - \frac{A_3 e^{-A_1 t_1} \cos \omega t_1}{(j\omega + A_1)}$$

$$+ \mathrm{j} \ \frac{{{\mathrm{A}_3}^{\mathrm{e}}}^{{\mathrm{-A}_1}^{\mathrm{t}}} {\mathrm{1}_{\sin \, \omega \mathrm{t}_1}}}{({{\mathrm{A}_1}} + \mathrm{j} \omega)} + \frac{{{\mathrm{A}_3}^{\mathrm{e}}}^{{\mathrm{-A}_2}^{\mathrm{t}}} {\mathrm{1}_{\cos \, \omega \mathrm{t}_1}}}{({{\mathrm{A}_2}} + \mathrm{j} \omega)} - \mathrm{j} \ \frac{{{\mathrm{A}_3}^{\mathrm{e}}}^{{\mathrm{-A}_2}^{\mathrm{t}}} {\mathrm{1}_{\sin \, \omega \mathrm{t}_1}}}{({{\mathrm{A}_2}} + \mathrm{j} \omega)} + \frac{{{\mathrm{A}_3}}}{({{\mathrm{A}_1}} + \mathrm{j} \omega)}$$

$$-\frac{A_3}{(A_2 + j\omega)} \qquad \text{for}\left(\frac{R}{L}\right)^2 > \frac{4}{LC_c}\left(1 + \frac{C_c}{C_{sg}}\right) \qquad (4.22)$$

where

$$A_{1} = \frac{R}{2L} - \frac{\sqrt{X}}{2}$$

$$A_{2} = \frac{R}{2L} + \frac{\sqrt{X}}{2}$$

$$A_{3} = \frac{E}{L\sqrt{X}}$$

$$A_{4} = \frac{v_{c}(t_{1})}{L}$$

$$A_{5} = C \frac{dv_{c}(t_{1})}{dt}$$

$$e^{-j\omega t_{1}} = \cos(\omega t_{1}) - j \sin(\omega t_{1})$$

Rationalizing the complex denominators and collecting terms,

$$I(j\omega) = \begin{cases} -A_4 \left[\left(\frac{\omega R}{L} \right) \sin \omega t_1 - \left(\frac{1}{LC_c} - \omega^2 \right) \cos \omega t_1 \right] - \omega A_5 \left[\left(\frac{\omega R}{L} \right) \cos \omega t_1 + \left(\frac{1}{LC_c} - \omega^2 \right) \sin \omega t_1 \right] \\ \omega^4 + \omega^2 \left(\frac{R^2}{L^2} - \frac{2}{LC_c} \right) + \left(\frac{1}{L^2 C_c^2} \right) \end{cases}$$

$$+ \frac{A_1 A_3 \left(1 - e^{-A_1 t_1} \cos \omega t_1 \right) + \omega A_3 e^{-A_1 t_1} \sin \omega t_1}{\omega^2 + A_2} - \frac{1}{2} \left(\frac{1}{L^2 C_c^2} \right) \left(\frac{1}{L^2 C_c^2} \right) + \frac{1}{2} \left(\frac{1}{L^2 C_c^2} \right) \left(\frac$$

$$\frac{A_{2}A_{3}\left(1-e^{-A_{2}t_{1}}\cos\omega t_{1}\right) + \omega A_{3}e^{-A_{2}t_{1}}\sin\omega t_{1}}{\omega^{2} + A_{2}^{2}}$$

$$+j\left\{A_{4}\left[\left(\frac{L}{L}\right)\cos\omega t_{1}\right] + \left(\frac{1}{LC_{c}}\cos\omega t_{1}\right) + \left(\frac{1}{LC_{c}}\cos\omega t_{1}\right) + \left(\frac{1}{LC_{c}}\cos\omega t_{1}\right) + \left(\frac{1}{LC_{c}}\cos\omega t_{1}\right) + \left(\frac{1}{L^{2}C_{c}^{2}}\right) + \left(\frac{1}{L^{2}C_{c}^{2}}\right)$$

$$-\frac{\omega A_{3}\left(1-e^{-A_{1}t_{1}}\cos\omega t_{1}\right) - A_{1}A_{3}e^{-A_{1}t_{1}}\sin\omega t_{1}}{\omega^{2} + A_{1}^{2}}$$

$$+\frac{\omega A_{3}\left(1-e^{-A_{2}t_{1}}\cos\omega t_{1}\right) - A_{2}A_{3}e^{-A_{2}t_{1}}\sin\omega t_{1}}{\omega^{2} + A_{1}^{2}}$$

$$+ \frac{\omega A_{3} \left(1 - e^{-A_{2}t} 1_{\cos \omega t_{1}}\right) - A_{2}A_{3}e^{-A_{2}t} 1_{\sin \omega t_{1}}}{\omega^{2} + A_{2}^{2}}$$

$$for \left(\frac{R}{L}\right)^{2} > \frac{4}{LC_{c}} \left(1 + \frac{C_{c}}{C_{sg}}\right)$$
(4.23)

The amplitude density is then obtained as

$$|I(\omega)| = \sqrt{\frac{\text{real part of equation } (4.23)}{\text{for } \left(\frac{R}{L}\right)^2 > \frac{4}{LC_c} \left(1 + \frac{C_c}{C_{sg}}\right)}}$$
 (4.24)

Below resonance, the radical term in equation (4.21) results in an imaginary number. Using the following definitions, substituting $j\omega$ for s, and rearranging, the complex expression for the current as a function of frequency is:

$$I(j\omega) = \frac{A_1 cos\omega t_1}{\left(\frac{1}{LC_c} - \omega^2\right) + j\left(\frac{\omega R}{L}\right)} - j\frac{A_1 sin\omega t_1}{\left(\frac{1}{LC_c} - \omega^2\right) + j\left(\frac{\omega R}{L}\right)} - j\frac{A_2 cos\omega t_1}{\left(\frac{1}{LC_c} - \omega^2\right) + j\left(\frac{\omega R}{L}\right)}$$

$$-\frac{\omega^{A_{2}sin\omega t}_{1}}{\left(\frac{1}{LC_{c}} - \omega^{2}\right) + j\left(\frac{\omega R}{L}\right)} + jA_{3}A_{4}\left\{\frac{e^{-j\left(\omega - \frac{\sqrt{|X|}}{2}\right)}t_{1}}{A_{5} + j\left(\omega - \frac{\sqrt{|X|}}{2}\right)} - \frac{e^{-j\left(\omega + \frac{\sqrt{|X|}}{2}\right)}t_{1}}{A_{5} + j\left(\omega + \frac{\sqrt{|X|}}{2}\right)}\right\}$$

$$-jA_{4}\left\{A_{5} + j\left(\omega - \frac{\sqrt{|X|}}{2}\right) - \frac{1}{A_{5} + j\left(\omega + \frac{\sqrt{|X|}}{2}\right)}\right\}$$

$$for\left(\frac{R}{L}\right)^{2} < \frac{4}{LC_{c}}\left(1 + \frac{C_{c}}{C_{sg}}\right)$$

$$where A_{1} = \frac{v_{c}(t_{1})}{L} \qquad A_{2} = C_{c}\frac{dv_{c}(t_{1})}{dt} \qquad A_{3} = e^{-\left(\frac{R}{2L}\right)}t_{1}$$

where $A_1 = \frac{v_c(t_1)}{L}$ $A_2 = C_c \frac{dv_c(t_1)}{dt}$ $A_3 = e^{-\left(\frac{R}{2L}\right)}t_1$

$$A_4 = \frac{E}{L\sqrt{|X|}}$$
 $A_5 = \frac{R}{2L}$ $e^{-j\omega t_1} = \cos\omega t_1 - j \sin\omega t_1$

Rationalizing the complex denominators, equation (4.25) becomes

$$I(j\omega) = \begin{cases} A_{1}(D_{2}cos\omega t_{1} - D_{1}sin\omega t_{1}) - \omega A_{2}(D_{1}cos\omega t_{1} + D_{2}sin\omega t_{1}) \\ D_{1}^{2} + D_{2}^{2} \end{cases}$$

$$+ \frac{{{A_3}{A_4}}{{D_4}e}^{-j\,{D_4}t}}{{{A_5}^2\,+\,{D_4}^2}} - \frac{{{A_3}{A_4}}{{D_3}e}^{-j\,{D_3}t\,{1}}}{{{A_5}^2\,+\,{D_3}^2}} - \frac{{{A_4}}{{D_4}}}{{{A_5}^2\,+\,{D_4}^2}} + \frac{{{A_4}}{{D_3}}}{{{A_5}^2\,+\,{D_3}^2}} \right\}$$

$$+ j \left\{ \frac{-A_{1}(D_{1}cos\omega t_{1} + D_{2}sin\omega t_{1}) - \omega A_{2}(D_{2}cos\omega t_{1} - D_{1}sin\omega t_{1})}{D_{1}^{2} + D_{2}^{2}} \right.$$

$$+\frac{A_{3}A_{4}A_{5}e^{-jD_{4}t_{1}}}{A_{5}^{2}+D_{4}^{2}}-\frac{A_{3}A_{4}A_{5}e^{-jD_{3}t_{1}}}{A_{5}^{2}+D_{3}^{2}}-\frac{A_{4}A_{5}}{A_{5}^{2}+D_{4}^{2}}+\frac{A_{4}A_{5}}{A_{5}^{2}+D_{3}^{2}}\right\} (4.26)$$

for
$$\left(\frac{R}{L}\right)^2 < \frac{4}{LC} \left(1 + \frac{C}{C_{sg}}\right)$$

where
$$D_1 = \frac{\omega R}{L}$$
 $D_2 = \frac{1}{LC} - \omega^2$ $D_3 = \omega + \sqrt{\frac{|X|}{2}}$ $D_4 = \omega - \frac{\sqrt{|X|}}{2}$

The amplitude density is then obtained as:

$$|I(\omega)| = \sqrt{\text{real part of equation (4.26)}}^2 + \left(\text{imaginary part of equation (4.26)}\right)^2$$
 (4.27)

for
$$\left(\frac{R}{L}\right)^2 < \frac{4}{LC_c} \left(1 + \frac{C_c}{C_{sg}}\right)$$

Check of Equations

As a precaution against mathematical errors, three tests are performed to imply the correctness of the equations in the preceding section.

1. The transform of a real function is Hermitian; i.e., the real part of the transform is even and the imaginary part is odd. Applying this test to equation (4.4), the real part is seen to be even by inspection.

For the imaginary part, the numerator is odd while the denominator is even, yielding an odd imaginary part. Therefore, the transform of the current after the spark plug fires is Hermitian as required.

2. The second test requires equation (4.21) to reduce to equation (4.3) when t_1 =0. This condition occurs when the spark plug gap and the distributor gap breakdown simultaneously.

From equation (4.21),

$$I(s)_{t_{1}=0} = \frac{\left(\frac{1}{L}\right)\left[v_{c}(0)\right] - sC_{c}\left[\frac{dv_{c}(0)}{dt}\right]}{s^{2} + s\left(\frac{R}{L}\right) + \left(\frac{1}{LC_{c}}\right)}$$

$$(4.28)$$

Since the above equation equals equation (4.3) with t_1 set to zero, the test is satisfied.

3. The final test involves setting s equal to zero in equation (4.21). The integration of a function over all time equals the value of that function's transform to the frequency domain at s=0 [35]. Thus,

$$I(0) = \int_{-\infty}^{\infty} i(t) dt$$
 (4.29)

If the spark plug gap and distributor gap break down simultaneously, i.e., if t_1 =0, then the integral of i(t) is simply the summation of the flow of charge in the circuit over all time. But, the total charge in the circuit with both gaps broken down is known to be the charge on the coil capacitor, C_c , when the gaps break down. This is given by the equation:

$$\begin{pmatrix}
\text{total charge on} \\
\text{coil capacitor}
\end{pmatrix} = \begin{pmatrix}
\text{capacitance of} \\
\text{coil capacitor}
\end{pmatrix} \times \begin{pmatrix}
\text{voltage across coil} \\
\text{capacitor when } t_1 = 0
\end{pmatrix} (4.30)$$

From equation (4.21),

$$I(G) = \frac{E \ C_{c}}{\left(1 + \frac{C_{c}}{C_{sg}}\right)} \left\{1 - \left(\frac{e^{-\frac{R}{2L}} t_{1}}{\sqrt{X}}\right) \left[\frac{R}{2L} e^{\frac{\sqrt{X}}{2} t_{1-e}^{-\frac{\sqrt{X}}{2}} t_{1}}\right] + \frac{e^{-\frac{\sqrt{X}}{2}} t_{1}}{e^{-\frac{\sqrt{X}}{2}} t_{1}} + e^{-\frac{\sqrt{X}}{2}} t_{1}\right]\right\} + C_{c} v_{c}(t_{1})$$

$$(4.31)$$

and when t_1 is equal to zero

$$I(0) \Big|_{t_1=0} = C_c v_C(0) \tag{4.32}$$

Satisfaction of the requirements imposed by all three tests supports the amplitude density equations as written.

Significance of Time Between Gap Breakdowns

Because of the length of the equations for the amplitude density, a simplified relationship is sought to explain the significance of the parameter, $\mathbf{t_1}$.

For the following development, the current due to the distributor gap breakdown is viewed as flowing only for $0 < t < t_1$. The current is blocked for time less than zero, and the current which flows after t_1 is due to the spark plug gap breakdown.

The rectangle function, $h \, \mathbb{I}(\frac{t-c}{b})$, accomplishes the desired screening, where h is the height of the function, c is the time at the midpoint of the function, and b is the width of the function [36]. For this development, a rectangle function with unit height, a base of width t_1 , and centered at $t = \frac{1}{2}t_1$ is desired. The function is written as

$$\Pi\left(\frac{t - \frac{t_1}{2}}{t_1}\right) = \Pi\left(\frac{t}{t_1} - \frac{1}{2}\right)$$
(4.33)

From the Fourier series expansion, an infinite number of single frequency components comprises the total current. Thus, observing the effect of t_1 on the amplitude density of a single component lends insight to the overall effect.

Using phasor analysis, a single component of the current may be written as I e $^{j\omega}{}_0{}^t$, where ω_o is the angular frequency of the single component. Thus, the current observed after the distributor gap breaks down is

$$i(t) = \Pi\left(\frac{t}{t_1} - \frac{1}{2}\right) \quad I e^{j\omega_0 t}$$
 (4.34)

Taking the Fourier transform,

$$I(s) = \Im\left\{ \left[\left(\frac{t}{t_1} - \frac{1}{2} \right) \right] * \Im\left\{ I e^{j\omega_0 t} \right\}$$
 (4.35)

where the asterisk indicates convolution.

Using several theorems for Fourier transforms, the above becomes

$$I(s) = e^{-j\pi s} \Im\left\{ \left[\frac{t}{t_1} \right] \right\} * I \Im\left\{ e^{j2\pi f} \circ^{t} \right\}$$

$$= e^{-j\pi s} \frac{1}{\left| \frac{1}{t_1} \right|} \Im\left\{ \left[\frac{1}{t_1} \right] \right] \Big|_{s} = \frac{s}{\left| \frac{1}{t_1} \right|} * I \frac{1}{\left| \frac{1}{2f_0} \right|} \Im\left\{ e^{j\pi t} \right\} \Big|_{s} = \frac{s}{2f_0}$$

$$= t_1 e^{-j\pi s} \left[\frac{\sin(\pi s \ t_1)}{\pi s \ t_1} \right] * \frac{I}{2f_0} \delta(s - f_0)$$

$$(4.36)$$

From the definition of convolution,

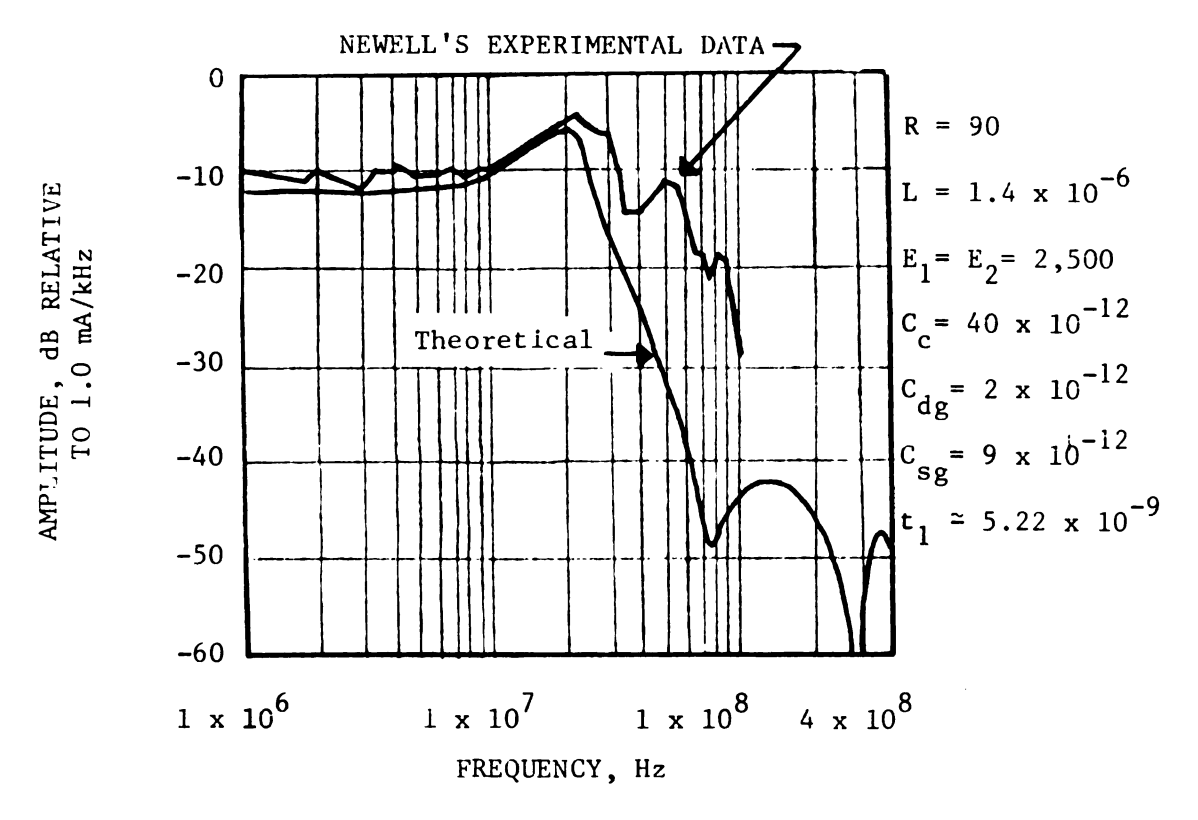
$$I(s) = \int_{-\infty}^{\infty} t_1 e^{-j\pi u} \left[\frac{\sin(\pi u t_1)}{\pi u t_1} \right] \left(\frac{I}{2f_0} \right) \delta(s - u - f_0) du$$

$$= \frac{I}{2f_0} e^{-j\pi(s - f_0)} \left[\frac{\sin(s - f_0) t_1^{\pi}}{\pi(s - f_0) t_1} \right]$$
(4.37)

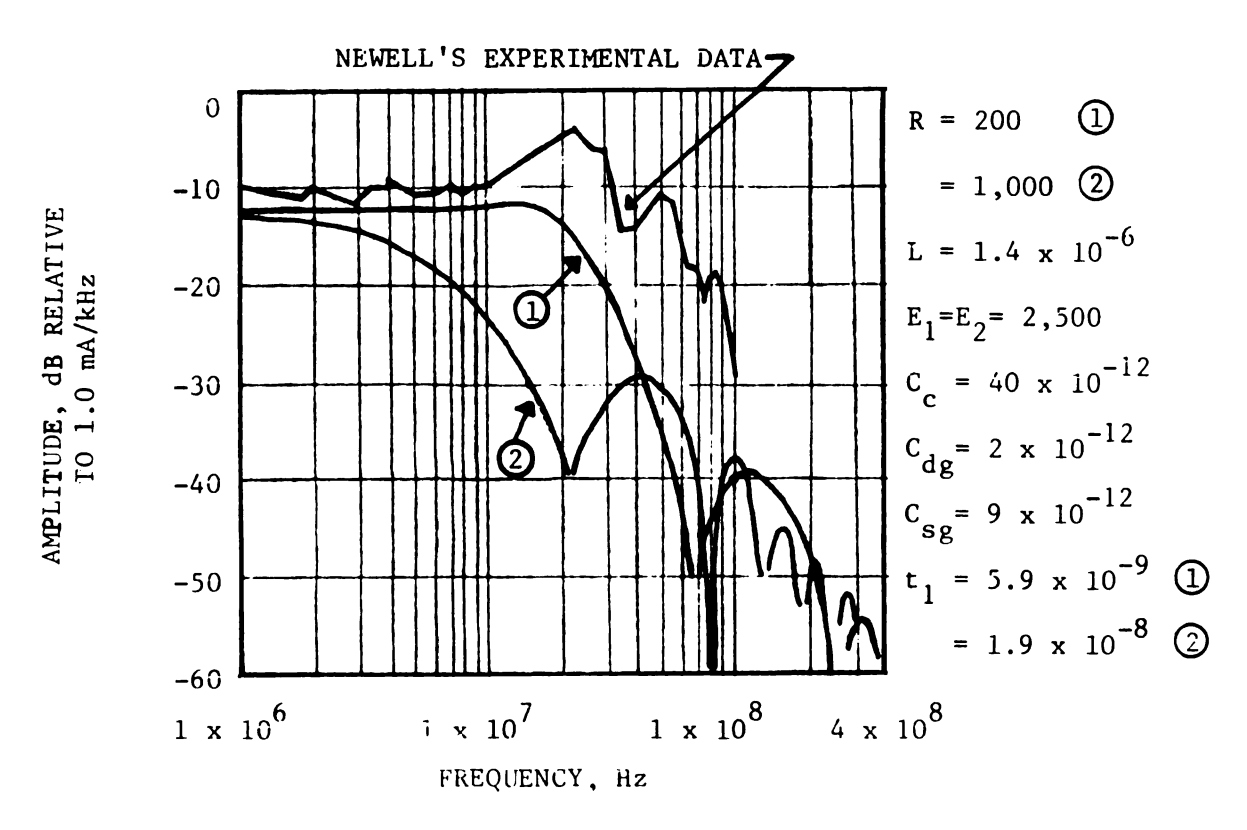
Because of the form of the Fourier transform which was used, set s equal to f, where f is frequency in Hertz. Substituting and rearranging,

$$I(f) = \frac{I t_1}{2\pi f_0 (f - f_0) t_1} \sin [\pi t_1 (f - f_0)] \cos [\pi (f - f_0)]$$

$$- j \frac{I t_1}{2\pi f_0(f - f_0)t_1} \sin[\pi t_1(f - f_0)] \sin[\pi (f - f_0)]$$
 (4.38)



(a) Using Newell's Values



(b) Effect of Change in Resistance

Figure 11 - Theoretical Amplitude Densities of Ignition Circuit Current

Taking the square root of the sum of the squares of the real and imaginary parts, the amplitude density becomes

$$|I(f)| = \begin{cases} \frac{I \sin[\pi t_{1}(f - f_{0})]}{2\pi f_{0}(f - f_{0})} & \text{for } (n - 1)2\pi < \pi t_{1}(f - f_{0}) < (2n - 1)\pi \\ & \text{where } n = 1, 2, \dots \end{cases}$$

$$|I(f)| = \begin{cases} \frac{-I \sin[\pi t_{1}(f - f_{0})]}{2\pi f_{0}(f - f_{0})} & \text{for } (2n - 1)\pi < \pi t_{1}(f - f_{0}) < 2\pi n \\ & \text{where } n = 1, 2, \dots \end{cases}$$

$$(4.39a)$$

$$(4.39b)$$

Maxima are found where the derivative is zero, which leads to the requirement that

$$\left(\frac{I}{2\pi f_{o}}\right) \left[\frac{(f - f_{o})\cos[\pi t_{1}(f - f_{o})](\pi t_{1}) - \sin[\pi t_{1}(f - f_{o})]}{(f - f_{o})^{2}}\right] = 0 \qquad (4.40)$$

or

$$\pi t_1(f - f_0) = tan[\pi t_1(f - f_0)]$$
 (4.41)

Letting a = $\pi t_{\dot{1}}(f - f_{o})$, the above equation becomes

$$tan(a) = a (4.42)$$

which has solutions at $a_0 = 0$, $a_1 = \pm 4.49$, $a_2 = \pm 7.73$, $a_3 = \pm 10.90$, et cetera.

For larger values of a, the maxima repeat approximately every $\boldsymbol{\pi}$ radians, so

$$\pi t_1(f + \Delta f - f_0) = \pi t_1(f - f_0) + \pi$$
 (4.43a)

or

$$\Delta f = \frac{1}{t_1} \tag{4.43b}$$

This simple result predicts that the current which flows after the distributor gap breaks down but before the spark plug fires causes recurring maxima in the frequency domain. These maxima recur at a difference

in frequency which is the inverse of the length of time between the gap breakdowns.

Numerical Examples

This section presents amplitude density plots predicted by equations (4.24) and (4.27) for different component values. The computer program contained in Appendix C was used in solving the equations.

Results using Newell's values. Figure 11a shows Newell's experimental values [8] and the theoretical amplitude density obtained by using Newell's values in equation (4.27). The curves agree below 20 MHz, but discrepancies appear at the higher frequencies.

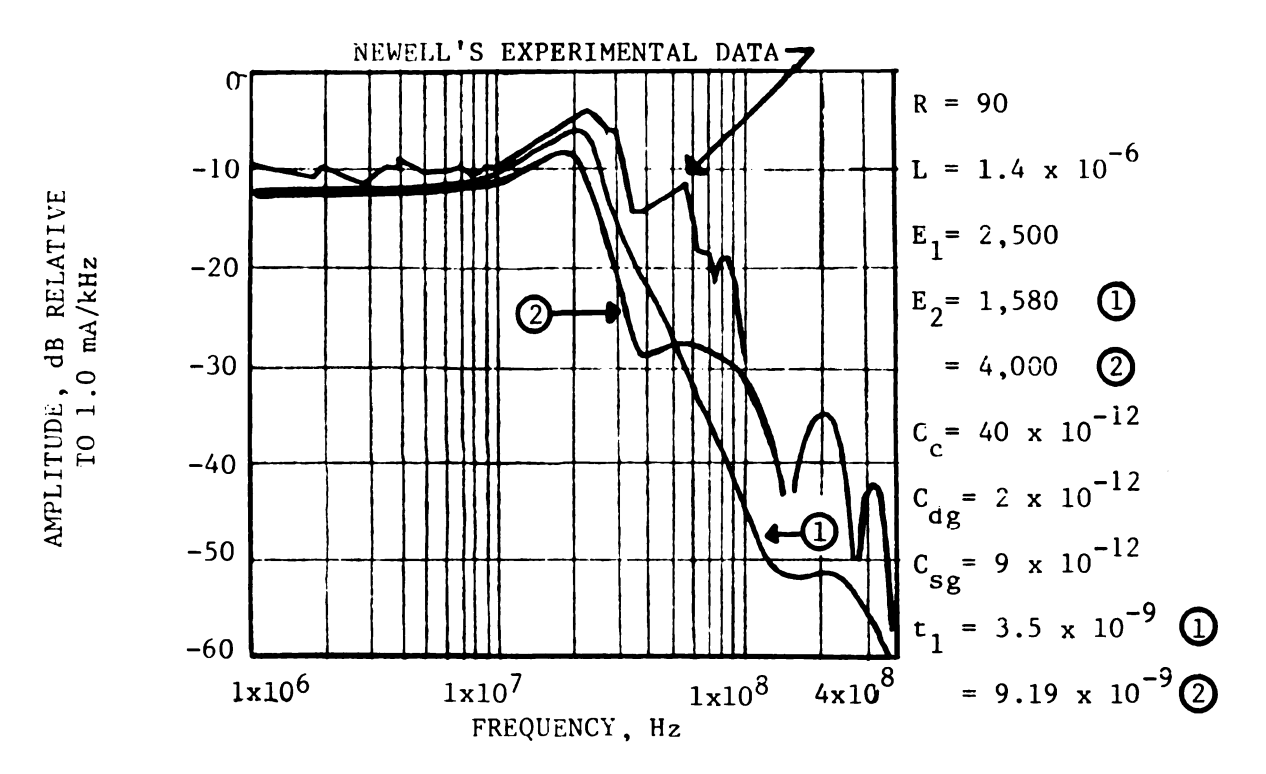
Most noticeably, the last two maxima from Newell's measurements occur about 5.0 x 10^7 Hz and 8.4 x 10^7 Hz, for a Δf of 3.4 x 10^7 Hz. Equation (4.43b) predicts a time between gap breakdowns of 2.94 x 10^{-8} seconds. However, Newell's values give a time, t_1 , of 5.22 x 10^{-9} seconds.

The remaining examples demonstrate the changes in the amplitude density attainable using different component values.

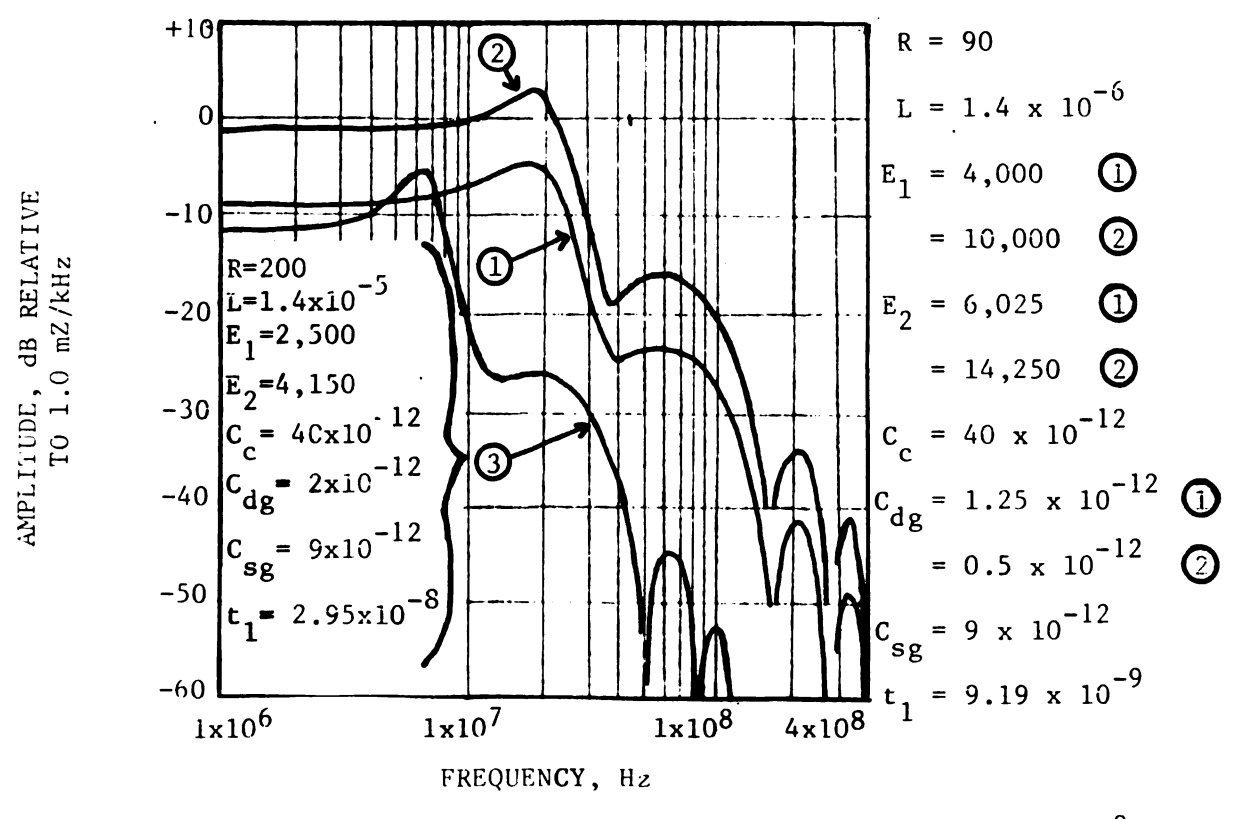
Effect of changing R. As observed in the previous chapter, increasing the resistance, R, effectively increases the time between gap breakdowns for the same breakdown voltages and reduces the amplitude of the current.

Figure 11b shows the effects observed in the amplitude density. The amplitude is reduced, and the lengthened time between gap breakdowns appears as more frequently occurring maxima.

As a check on equation (4.43b), t_1 is 1.9×10^{-6} seconds for the curve with R = 1,000 ohms, so maxima are expected about 5.3×10^{7} Hz apart. Inspection of the results shows this behavior at the higher frequencies.



(a) Effect of Change in Spark Plug Gap Breakdown Voltage



(b) Results for Changes in C_{dg} and E_1 , and for $t_1 = 2.95 \times 10^{-8}$ Figure 12 - Theoretical Amplitude Densitites of Ignition Circuit Current Effect of changing E_2 . Increasing the spark plug gap breakdown voltage directly increases the parameter, t_1 . This is evidenced in Figure 12a by the appearance of additional maxima in the amplitude density.

The effect of the change in amplitude on the electric field is considered in the following chapter.

Effect of changing $C_{\rm dg}$ and $E_{\rm l}$. Figure 12b shows the results of simultaneously changing the distributor gap capacitance and breakdown voltage while keeping their product constant. The increased amplitude for the higher voltage circuit indicates the higher level of energy in that circuit.

Figure 12b also contains a theoretical plot with a time between gap breakdowns of 2.95×10^{-8} seconds. While the maxima recur at the proper intervals to match those of Newell's experimental data, the first maximum appears at too low a frequency, and the amplitude decays too rapidly.

The failure to precisely fit Newell's experimental curve emphasizes the complexity of the equations involved. Obtaining an amplitude density plot with this model requires the following steps:

- 1. Specification of R, L, C_c , C_{dg} , C_{sg} , and E_1 for solution of equations for waveforms after the distributor gap breaks down.
- 2. Selection of time, t_1 , for a specified spark plug gap breakdown voltage using the results from (1) above.
- 3. Calculation of the coil voltage and its slope at $t=t_1$ for use as initial conditions in the amplitude density equations.
 - 4. Solution of the amplitude density equations.

The above procedure requires numerous iterations when attempting to match specific data points. However, the equations provide an effective indication of the consequences of changes in particular component values or operating conditions, as shown by the examples in this section.

CHAPTER V

ELECTRIC FIELD FROM CIRCULAR LOOP ANTENNA MODEL

The final step in modeling the ignition circuit involves the development of a radiation model to predict the level of the interfering electric field.

First, an upper bound on the electric field strength as a function of frequency is found using a circular loop antenna model, and numerical examples are given.

Next, the same model is used to predict the time variation of the electric field. Two approaches to the solution of the equations are given, along with examples.

Discussion of the validity of the ignition circuit model concludes the chapter.

Predicted Field Strength in Frequency Domain

Assuming an $e^{j\omega t}$ time dependence, the electric and magnetic fields can be expressed in terms of a vector potential as

$$\stackrel{\rightarrow}{B} = \nabla \times \stackrel{\rightarrow}{A} \tag{5.1a}$$

$$\dot{\vec{E}} = -j\omega[\vec{A} + \frac{1}{\mu\epsilon} \nabla(\nabla \cdot \vec{A})]$$
 (5.1b)

where the vector potential is a space- and time-varying function which is defined as [37]:

$$\vec{A} (\vec{r},t) = \frac{\mu}{4\pi} \int_{V'} \frac{\vec{J}(\vec{r}')}{R} e^{j\omega(t-\sqrt{\mu\epsilon} R)} dv'$$
 (5.2)

In the above equation, the integration is performed over a volume, V', which contains all sources. The vector, \overrightarrow{r}' , indicates the source location, while the vector, \overrightarrow{r} , describes the field point. The distance between the source and the field point is R, and the volume current density is $\overrightarrow{J}(\overrightarrow{r}')$.

Using the conventions shown in Figure 13, the radiated (far zone) electric and magnetic fields are found using the following assumptions:

- 1. The current in the antenna is independent of ϕ' .
- 2. The antenna's dimensions are small compared with the wavelength; i.e., $a\omega v \mu\epsilon <<1$.
- 3. The current in the antenna is uniform over the wire cross section, and is given by I $e^{j\omega t}$.
- 4. Measurement of the fields occurs far from the antenna so R \simeq r for magnitude calculations.

Johnson [37] gives the equations for the fields as

$$\vec{E} = -j \omega A_{\phi} \hat{\phi}$$
 (5.3a)

and

$$\vec{B} = j\omega\sqrt{\mu\epsilon} \quad A_{\phi} \quad \hat{\theta}$$
 (5.3b)

where
$$A_{\phi} = \frac{j \mu I a}{2r} J_1(\omega a \sqrt{\mu \epsilon} \sin \theta) e^{j\omega(t - \sqrt{\mu \epsilon} r)}$$
 (5.3c)

The vector potential is zero in the $\hat{\theta}$ and \hat{r} directions, and the notation, $J_1($), indicates the first order, first kind Bessel Function of the parenthesized variable.

Substituting equation (5.3c) into equation (5.3a) and simplifying,

$$\vec{E} = \frac{\mu I \omega a}{2r} J_1 \left(\frac{\omega_a \sin \theta}{c} \right) e^{j\omega(t - \frac{r}{c})} \hat{\phi}$$
 (5.4)

where c = $\frac{1}{\sqrt{\mu\epsilon}}$ = propagation velocity in free space = 3 x 10^8 m/second.

The maximum value of the electric field due to a single component of current with angular frequency, ω , occurs when θ is 90° and at time, t=r/c.

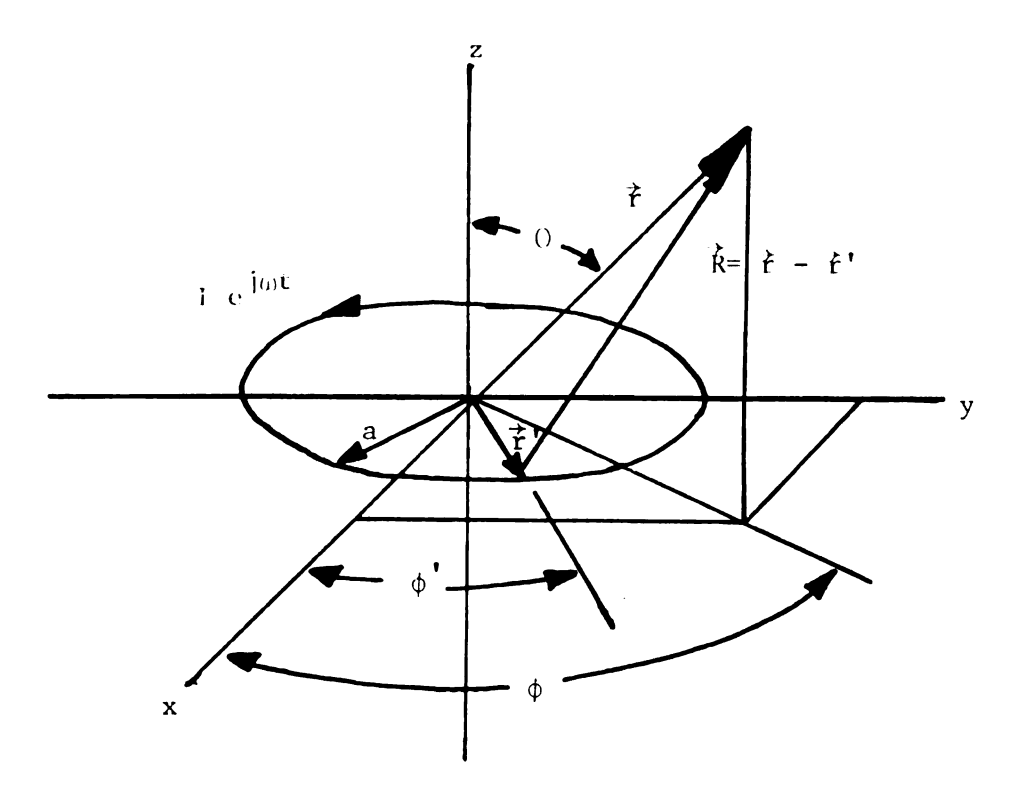


Figure 13 - Coordinate System for Circular Loop Antenna [37].

Thus, an upper bound on the magnitude of the electric field as a function of frequency is given by

$$|\overrightarrow{E}| \le \frac{\mu I \omega a}{2r} \quad J_1(\frac{\omega a}{c})$$
 (5.5)

Writing the Bessel runction as a power series,

$$J_{1}(\frac{\omega a}{c}) = \frac{\omega a}{2c} \left[1 - \frac{1}{2} \left(\frac{(1)a}{2c} \right)^{2} + \frac{1}{12} \left(\frac{\omega a}{2c} \right)^{4} - \frac{1}{144} \left(\frac{\omega a}{2c} \right)^{6} + \dots \right]$$
 (5.6)

Discarding higher order terms (which is consistent with assumption number (2) on the preceding page), equation (5.5) becomes

$$|\vec{E}| \le \frac{\mu I \omega^2 a^2}{4 rc} \tag{5.7}$$

The above equation may also be written as

$$|\vec{E}| \leq \frac{\eta I \omega^2 A}{4\pi D c^2} \tag{5.8}$$

where $\eta = \mu c$, $A = \pi a^2$, and D = r. Equation (5.8) is identical to Newell's equation (2.8) [8].

Numerical Examples - Frequency Domain

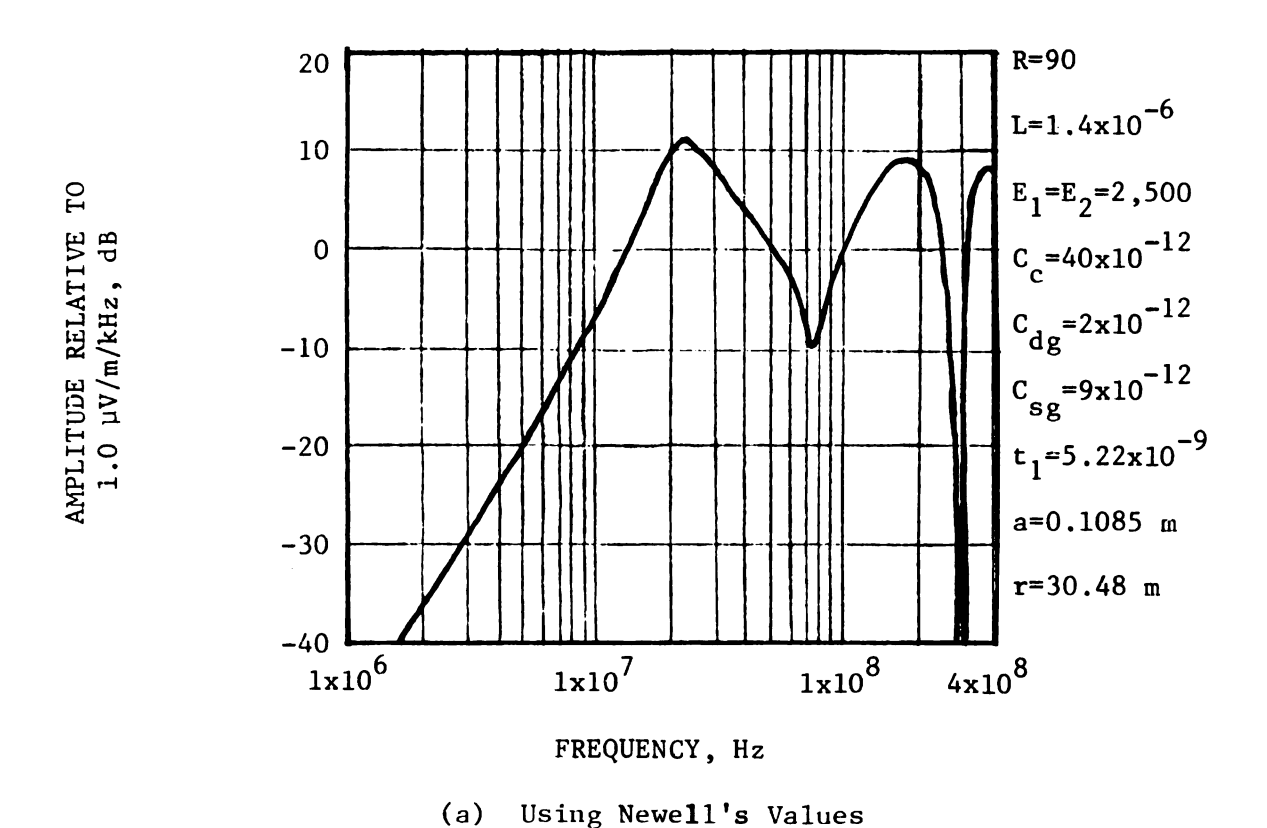
With the availability of Fortran software packages to calculate values of the Bessel function, equation (5.5) was used to obtain the following plots of the upper bound of the electric field versus frequency. The conputer program in Appendix C includes the solution of equation (5.5) in its output.

Results using Newell's values. Figure 14(a) shows the theoretical limit of the radiated electric field strength using Newell's values in equation (5.5). The loop radius of 0.1085 meters and the distance from the antenna of 30.48 meters allow comparison with Newell's theoretical result, shown in Figure 5(b) on page 18.

The approximation for the Bessel function used by Newell is accurate within 3% up to 10 MHz. Therefore, the differences between Figure 5(b) and Figure 14(a) arise from the different current amplitude densities used (see Figure 5(a) and Figure 11(a), respectively).

Assumption number (2) requires $(\frac{\omega a}{c})$ to be much less than unity. For a loop radius of 0.1085 meters, the angular frequency should be much less than 2.765 x 10^9 radians/second (f<<4.4 x 10^8 Hz). Therefore, theoretical results are not shown above this frequency.

From equation (5.7), the limit of the electric field is proportional to ω^2 times the current amplitude density. This accounts for the added significance of the field due to the higher frequency current components.



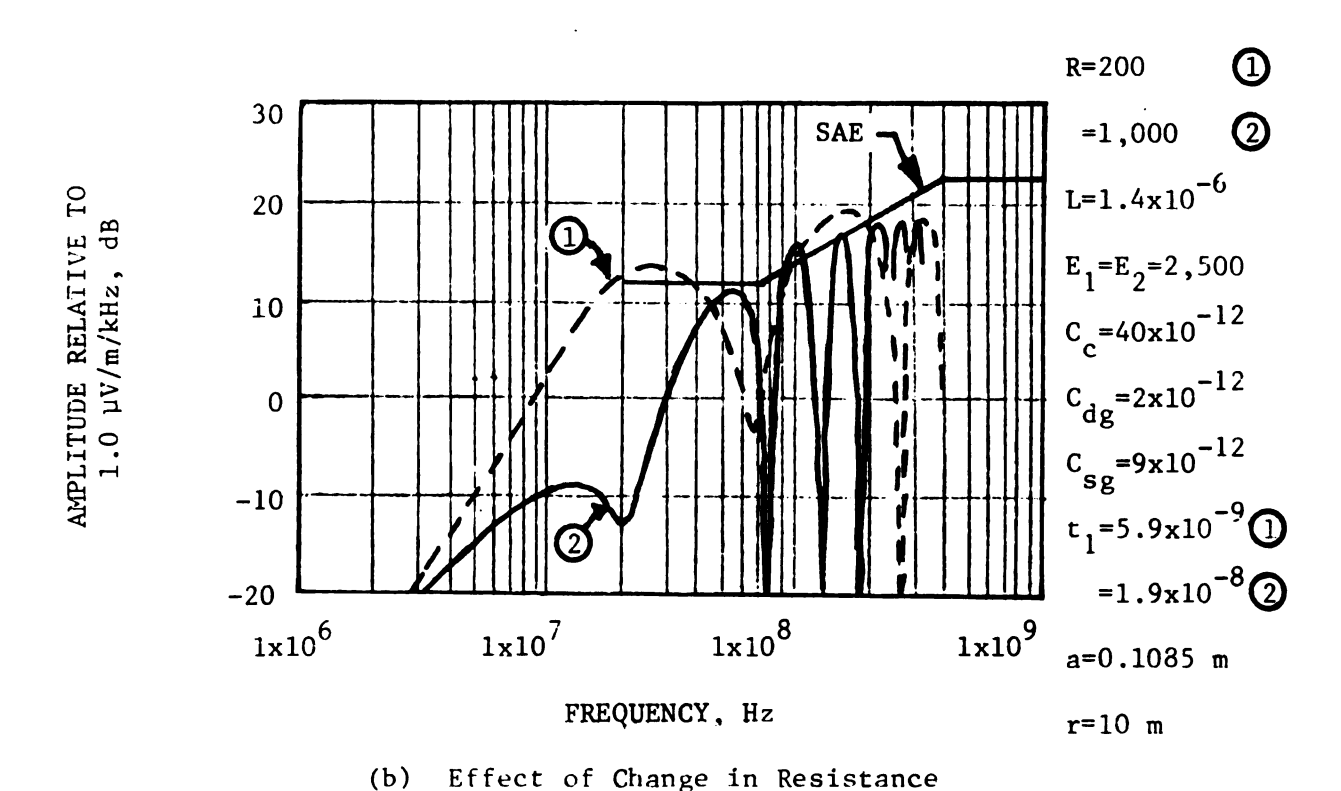


Figure 14 - Theoretical Field Strength Limit in Frequency Domain

Effect of changing R. Adding resistance to the ignition circuit reduces the peak electric field strength, as shown in Figure 4(c) on page 14. Using a radius of 0.1085 meters and a distance of 10 meters, Figure 14(b) shows the theoretical results for two different values of resistance, along with the SAE J551b limit. Significant improvement is predicted below 100 MHz.

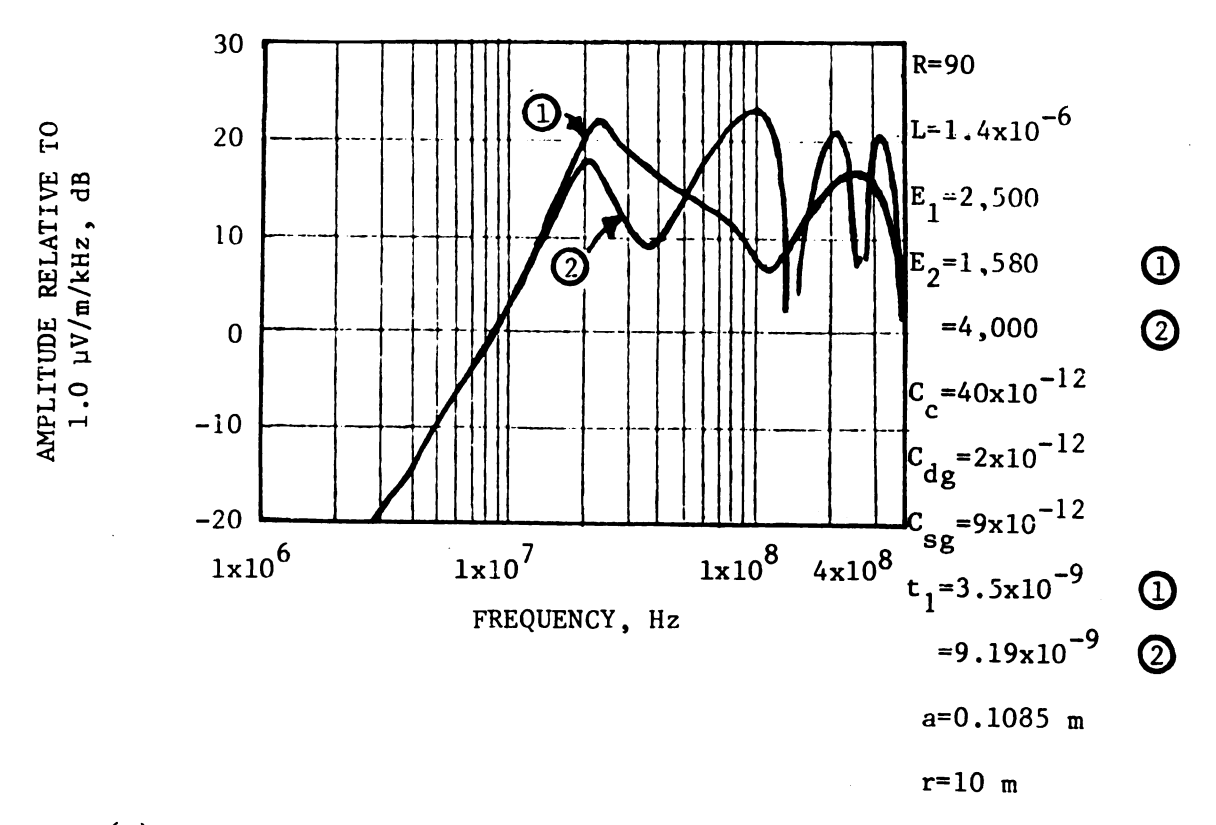
The theoretical results depict an upper bound on the electric field strength from a single spark plug firing, while the SAE standard establishes a limit for the collective peak fields from numerous plug firings. While their relationship was not investigated, the curves should show reasonable agreement.

The preceding statement extends Doty's conclusion [2] that "a number of discretely located random occurrence impulses do not significantly phase-add in space when measured by an instrument having a broadband IF and peak detector. While Doty compared results from a matrix of (21) vehicles against those of a single vehicle, it seems reasonable to expect peak measurements from the repeated firing of several spark plugs to be similar to the model's predicted values.

Effect of changing E_2 . Changes in the spark plug gap breakdown voltage, E_2 , alter the electric field spectrum as shown in Figure 15(a).

Since fuel mixture, cylinder operating conditions, spark plug gap, and other factors determine the spark plug gap breakdown voltage, the time between gap breakdowns is highly random. For the example shown, this random time can cause successive readings to differ by nearly 15 dB at some frequencies.

Effect of changing C_{dg} and E_{1} . Figure 15(b) shows the results of simultaneously changing the distributor gap capacitance and breakdown



(a) Effect of Change in Spark Plug Gap Breakdown Voltage

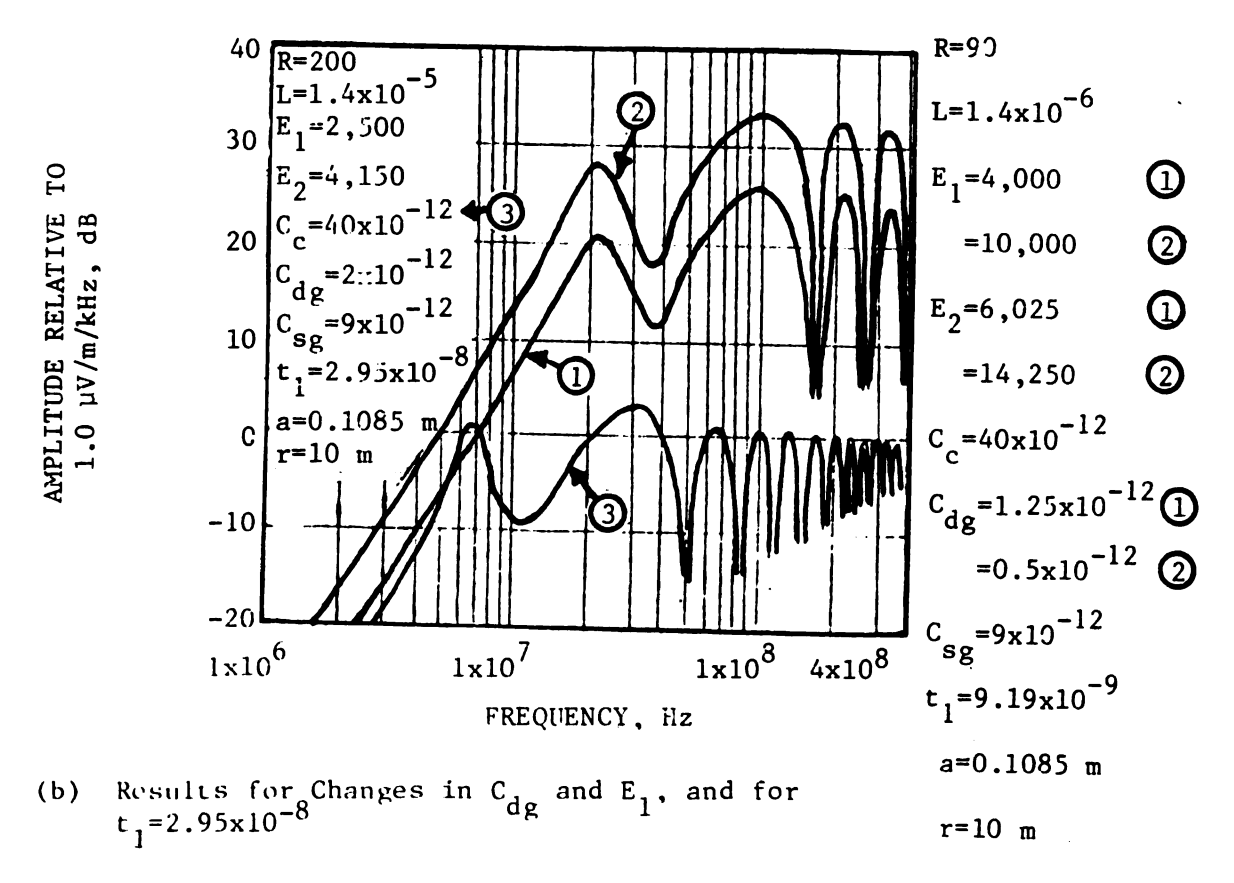


Figure 15 - Theoretical Field Strength Limit in Frequency Domain

voltage while keeping their product constant. As expected, the higher energy circuit produces more interference at all frequencies.

Figure 15(b) also contains a theoretical plot with an inductance of 14.0×10^{-6} henries (10 times Newell's value). The significant reduction in the bound on the electric field suggests that the inductance of the spark plug leads should be increased, an observation which was also made by Newell [8].

The model does not consider the near zone field, and the effect increased lead inductance could have on other circuits in the vehicle.

Also, engine performance would have to be maintained. However, the inference remains that the ignition circuit inductance can be optimized.

Predicted Field Strength in Time Domain

Equation (5.4) contains the time behavior of the electric field strength. This section presents two approaches for predicting the peak measurable electric field, using approximations for the current amplitude density based on previous numerical examples.

For simplicity, let $\theta = 90^{\circ}$, so equation (5.4) becomes

$$\vec{E} = \frac{\mu I \omega a}{2r} \quad J_1(\frac{\omega a}{c}) \quad e \qquad \qquad \phi \qquad (5.9)$$

The measurable electric field is obtained by taking the real part of the above expression, so

$$\operatorname{Re} \left\{ \overrightarrow{E} \right\} = \frac{\mu \omega a}{2r} \quad \operatorname{J}_{1}(\frac{\omega a}{c}) \quad \operatorname{Re} \left\{ I \quad e^{j\omega(t - \frac{r}{c})} \right\} \hat{\phi}$$
 (5.10)

Expressing the comples amplitude of the current, I, by a magnitude and a phase term,

$$\operatorname{Re}\left\{I e^{j\omega(t-\frac{r}{c})}\right\} = \operatorname{Re}\left\{\left|I\right| e^{j\alpha} e^{j\omega(t-\frac{r}{c})}\right\} \hat{\phi}$$

$$= \left|I\right| \cos\left[\omega(t-\frac{r}{c}) + \alpha\right] \hat{\phi}$$
(5.11)

Assuming that the phase term is zero, the measurable electric field becomes

$$\operatorname{Re}\left\{\overrightarrow{E}\right\} \simeq \frac{\mu\omega a}{2r} J_{1}(\frac{\omega a}{c}) \left|I\right| \cos\left[\omega(t-\frac{r}{c})\right] \widehat{\phi} \tag{5.12}$$

The above expressions apply for a uniform current of a single frequency, ω . For a broadband current, i.e., one with a continuous frequency spectrum, the total measured electric field is obtained by integrating over all frequencies, where |I| varies with frequency.

Then

Re
$$\left\{ \stackrel{\leftarrow}{E} \right\}_{\text{total}} \simeq \frac{\mu a}{2r} \int_{-\infty}^{\infty} \omega |I(\omega)| J_1(\frac{\omega a}{c}) \cos[\omega (t - \frac{r}{c})] d\omega \hat{\phi}$$
 (5.13)

Two approaches are used in solving the above equation.

Method #1. This method uses the approximation for the Bessel function from the power series expansion:

$$J_1(\frac{\omega a}{c}) \simeq \frac{\omega a}{2c}$$
 for $\omega \ll \frac{c}{a}$ (5.14)

Then

Re
$$\left\{ \stackrel{\rightarrow}{E} \right\}_{\text{total}} \simeq \frac{\mu a^2}{4 r c} \int_{-\infty}^{\infty} \omega^2 \left| I(\omega) \right| \cos \left[\omega \left(t - \frac{r}{c} \right) \right] d\omega \quad \hat{\phi}$$
 (5.15)

From the examples in Figures 11 and 12 on pages 53 and 56, respectively, the current amplitude density is seen to be approximately constant up to a certain frequency, after which it becomes roughly inversely proportional to frequency. Thus, the amplitude density is assumed as

$$|1(\omega)| = \begin{cases} I_{o} & \text{for } -\omega_{o} < \omega < \omega_{o} \\ \frac{\omega_{o} I_{o}}{\omega} & \text{for } \omega_{o} < |\omega| \end{cases}$$
 (5.16)

Since the integrand is an even function,

Re
$$\left\{\vec{E}\right\}_{\text{total}} \simeq \frac{\mu a^2}{2rc} \int_{-\infty}^{\infty} \omega^2 |I(\omega)| \cos[\omega(t - \frac{r}{c}) d\omega] \hat{\phi}$$

$$\simeq \frac{\mu a^2 I_o}{2rc} \left\{ \int_{0}^{\omega_o} \omega^2 \cos[\omega(t - \frac{r}{c})] d\omega + \omega_o \int_{\omega_o}^{\infty} \omega \cos[\omega(t - \frac{r}{c})] d\omega \right\} \hat{\phi} \quad (5.17)$$

Because of the approximation for the Bessel function, the integration is not actually carried out to infinity. Using an upper value of integration, $\boldsymbol{\omega}_m$, and performing the integrations,

Re
$$\left\{\vec{E}\right\}_{\text{total}} \simeq \frac{\mu a^2 \omega_o I_o}{2rc(t - \frac{r}{c})} \left\{ \cos\left[\omega_o(t - \frac{r}{c})\right] + \cos\left[\omega_m(t - \frac{r}{c})\right] \right\}$$

$$+ \omega_{m}(t - \frac{r}{c}) \sin\left[\omega_{m}(t - \frac{r}{c})\right] - \frac{2 \sin\left[\omega_{o}(t - \frac{r}{c})\right]}{\omega_{o}(t - \frac{r}{c})} \hat{\phi}$$
 (5.18)

The above equation satisfies six essential tests:

- 1. The predicted electric field strength is proportional to the magnitude of the current, $\omega_0 I_0$.
- 2. The field is radiated and, therefore, varies as the inverse of the distance.
 - 3. The field is proportional to the area of the loop antenna.
- 4. The field is a maximum at the time, $t = \frac{r}{c}$. This is expected, since the current is nearly an impulse, and the maximum field from an impulse is delayed only by the time it takes to travel from the antenna to the field point.

- 5. The field asymptotically goes to zero with time because of the $(t-\frac{r}{c})^2$ term in the denominator.
 - 6. The units are correct.

Using L'Hopital's rule, the numerator and denominator of equation (5.18) can be successively differentiated to obtain an expression for the largest predicted value of the electric field, which occurs at $t = \frac{r}{c}$. The resulting expression is

Re
$$\left\{\vec{E}\right\}_{\text{total}}\Big|_{t=\frac{r}{C}} \simeq \frac{\mu a^2 \omega_o^{\text{I}} o}{12 \text{rc}} \left(3 \omega_m^2 - \omega_o^2\right) \hat{\phi}$$
 (5.19)

An obvious difficulty with equations (5.18) and (5.19) are their dependence on the limit of integration, ω_m . This difficulty is circumvented with the second approach.

Method #2. This approach uses a continuous function similar to that in equation (5.16) to represent the current amplitude density:

$$|I(\omega)| \simeq \frac{\omega_0 I_0}{\sqrt{\omega^2 + \omega_0^2}}$$
 (5.20)

Thus, equation (5.13) becomes

Re
$$\left\{\vec{E}\right\}_{\text{total}} \simeq \frac{\mu_{a\omega} I_{o}}{r} \int_{o}^{\infty} \frac{\omega}{\sqrt{\omega^{2} + \omega^{2}}} J_{1}(\frac{\omega a}{c}) \cos[\omega(t - \frac{r}{c})] d\omega \hat{\phi}$$
 (5.21)

Using a piece-wise continuous linear approximation for the function

$$\frac{\omega}{\sqrt{\omega^2 + \omega_o^2}},$$

$$\operatorname{Re} \left\{ \overrightarrow{E} \right\}_{\text{total}} \lesssim \frac{\mu a \omega_o I_o}{r} \qquad \left\{ \int_o^{\omega_o} (\frac{\omega}{\omega_o}) J_1(\frac{\omega a}{c}) \cos[\omega(t - \frac{r}{c})] d\omega \right\}$$

$$+ \int_{\omega_{o}}^{\infty} J_{1}(\frac{\omega_{i1}}{c}) \cos[\omega(t-\frac{r}{c})]d\omega \right\} \hat{\phi} \lesssim \frac{\mu a \omega_{o} I_{o}}{r} \left\{ \int_{o}^{\infty} J_{1}(\frac{\omega a}{c}) \cos[\omega(t-\frac{r}{c})]d\omega \right\}$$

$$-\int_{0}^{\omega_{0}} \left(1 - \frac{\omega}{\omega_{0}}\right) J_{1}(\frac{\omega a}{c}) \cos\left[\omega(t - \frac{r}{c})\right] d\omega$$
 (5.22)

Setting the second integral equal to zero (this assumption is verified later),

Re
$$\left\{ \stackrel{\rightarrow}{E} \right\}_{\text{total}} \lesssim \frac{\mu a \omega_o^{\text{I}}_{\text{o}}}{r} \int_{0}^{\infty} J_1(\frac{\omega a}{c}) \cos[\omega(t - \frac{r}{c})] d\omega \qquad \hat{\phi}$$
 (5.23)

Using the solution to the above integral as given by Abramowitz and Stegun [38], equation (5.23) becomes

$$\operatorname{Re} \left\{ \stackrel{\neq}{E} \right\}_{\text{total}} \leq \begin{cases} \frac{\mu c \omega_{o} I_{o}}{r} & \text{for } \frac{r}{c} < t < \frac{a+r}{c} \\ \frac{-\mu a^{2} \omega_{o} I_{o}}{r c \sqrt{\left(t - \frac{r}{c}\right)^{2} - \left(\frac{a}{c}\right)^{2}}} & \left(t - \frac{r}{c}\right) + \sqrt{\left(t - \frac{r}{c}\right)^{2} - \left(\frac{a}{c}\right)^{2}} \\ & \text{for } t > \frac{a+r}{c} & (5.24b) \end{cases}$$

The peak value of the electric field is predicted to occur in the time interval $\frac{r}{c}$ < t < $\frac{a+r}{c}$, and is given by the simple relationship

$$\operatorname{Re} \left\{ \overrightarrow{E} \right\}_{\text{total}} \leq \frac{\eta \omega_{\text{o}}^{\text{I}}}{r} \tag{5.25}$$

where ω_0 = cutoff frequency of current in radians/second

I = low-frequency amplitude of current in frequency domain,
 amperes per radians/second

r = distance, meters

 η = characteristic impedance of free space (=120 π ohms)

Now, the assumptions in going from equation (5.22) to (5.23) is reviewed. First, the peak value of the field occurs when $t \simeq \frac{r}{c}$, which means that the cosine term is nearly unity. Using the approximation for

the Bessel function, the second integral of equation (5.22) is approximately

$$\int_{0}^{\omega_{O}} \left(1 - \frac{\omega}{\omega_{O}}\right) J_{1}(\frac{\omega a}{c}) \cos \left[\omega(t - \frac{r}{c})\right] d\omega \simeq \int_{0}^{\omega_{O}} \left(1 - \frac{\omega}{\omega_{O}}\right) \left(\frac{\omega a}{2c}\right) d\omega$$

$$\simeq \frac{a\omega_{O}}{12c} \tag{5.26}$$

Thus, the contribution due to this integral (for $t \approx \frac{r}{c}$) is

$$\frac{\mu^{2}\omega_{0}^{3}I_{0}}{12 rc}$$
 (5.27)

Comparing equation (5.24a) with equation (5.27),

$$\frac{\text{equation } (5.24a)}{\text{equation } (5.27)} = \frac{12}{\left(\frac{\omega_0 a}{c}\right)^2}$$
 (5.28)

However, in using the approximation for the Bessel function (and in developing the circular loop antenna equations), the assumption was already made that $\left(\frac{\omega}{c}\right)$ is much less than unity. Thus, the contribution of the second integral in equation (5.22) is insignificant in determining the peak value of the electric field, and was justifiably discarded.

Numerical Examples - Time Domain

Figure 16 compares the maximum electric field strength predicted by the two methods described in the preceding section. The computer programs contained in Appendix D and Appendix E facilitate the calculations required by equation (5.18) and (5.24), respectively.

Method #1 relies heavily on the value selected for the upper limit of integration, ω_{m} . Conversely, Method #2 allows a concise prediction of the peak electric field and its subsequent decay.

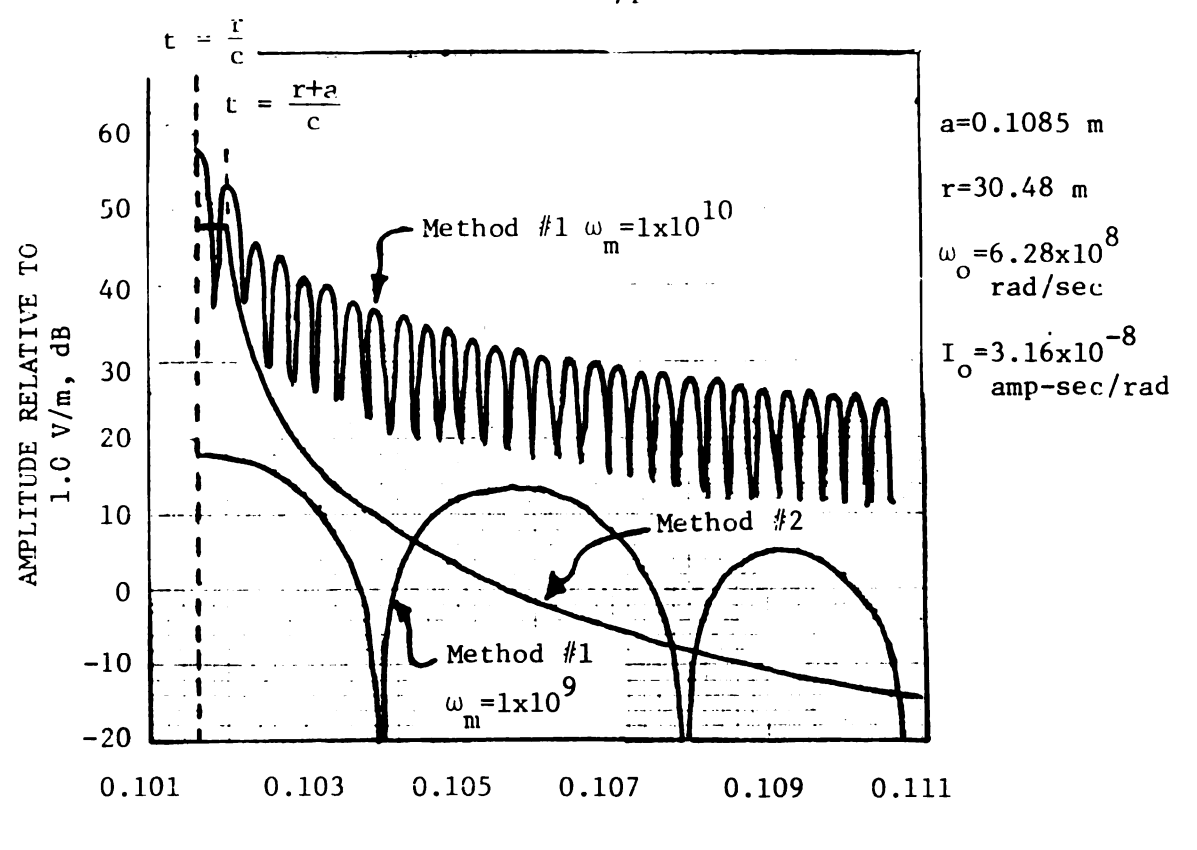
rc |

-20 L

The

two key a

secendary



TIME, MICROSECONDS

Figure 16 - Theoretical Field Strength Limit in Time Domain

The assumption for the current amplitude density used in Method #2 might result in an abnormally high predicted peak field strength (Figure 16 shows a peak electric field of about 250 V/m). However, equation (2.25) does indicate the well-documented fact that objectionable levels of interference arise from operation of an unsuppressed ignition circuit.

Discussion and Recommendations

While the preceding development emphasizes the sufficiency of the model, this section suggests possible areas of improvement.

In determining the time variation of the ignition circuit current, two key assumptions appear questionable. First, the assumption that the secondary circuit charges instantaneously with the opening of the contact

breaker ignores any energy transfer through the coil after the distributor and spark plug gap breakdowns.

Second, the spark plug gap maintains a finite voltage across it after breakdown, as shown in Figure 2 on page 8.

In spite of the above assumptions (which considerably simplify the model), the current waveform shows a similarity to that measured by Hsu and Schlick [28] and approximated in Figure 6 on page 21. Therefore, while further improvements to the model may improve the amplitudes predicted by selected component values, the general shape of the solution should not change drastically.

The amplitude density of the transform of the current requires no additional assumptions over those made in time domain. Since this density instrumentally determines the electric field strength, the field is limited by the assumptions for the current in time domain.

Additionally, the assumption of a uniformly distributed current in a circular loop antenna limits the equations for the field strength to frequencies such that $\omega << \frac{c}{a}$. An antenna model with a non-uniform current distribution would improve the treatment.

An apparently arbitrary assumption for the time varying electric fields was the zero phase angle assumption in going from equation (5.11) to (5.12). Figure 17 plots this angle for Newell's values.

Obviously, the phase angle varies with frequency, and inaccuracies result from the assumption. However, for this development, the simplicity resulting from the assumption was considered of greater benefit than the potential gain in accuracy.

Finally, while the model incorporates some improvements over previous models, the limited availability of supporting data suggests the need for additional measurements of the predicted quantities.

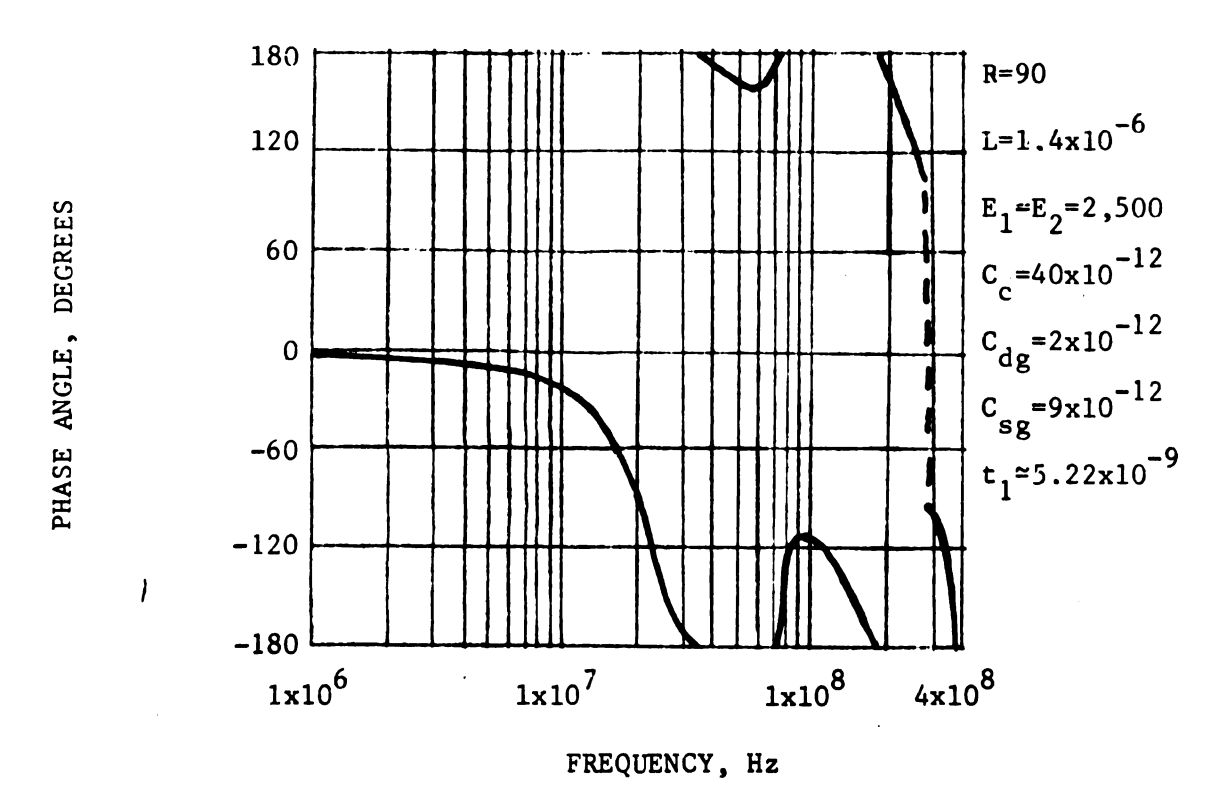


Figure 17 - Theoretical Phase Angle of Transform of Current Using Newell's Values

The ates the

downs.

જા≎del:

tinuing

1.

2.

satisfac 3.

form of

agrees w

4.

gap brea

the abov

٥. peak am;

sity of

Predicte

6. over 10.

[8].

CHAPTER VI

CONCLUSIONS

The model presented in the preceding chapters successfully incorporates the sequential nature of the distributor and spark plug gap breakdowns. The following conclusions are drawn from the development of this model:

- 1. The general problem of radio frequency interference requires continuing attention, as documented in the literature.
- 2. Prediction of the time variation of the ignition circuit current satisfactorily approaches known behavior using this model.
- 3. The equations developed for the amplitude density of the transform of the current predict recurring maxima in frequency domain, which agrees with the experimental data of Newell [8].
- 4. The inverse of the time between the distributor and spark plug gap breakdowns predicts the approximate separation in frequency between the above-mentioned maxima.
- 5. Increasing the resistance in the ignition circuit decreases the peak amplitude of the current in time domain, reduces the amplitude density of the current in frequency domain, and significantly reduces the predicted electric field strength.
- 6. The model can predict spark plug gap breakdown voltages of well over 10,000 volts, which constitutes an improvement over Newell's model [8].

- 7. The circular loop antenna model provides reasonable prediction of the maximum electric field strength for frequencies to about 100 MHz.
- 8. The maximum measureable value of the electric field strength as a function of time is predicted to be less than

where ω_0 = cutoff frequency of current in frequency domain, radians/second

I = low-frequency amplitude of current in frequency domain, amperes
 per radian/second

r = distance from the antenna in meters

 η = characteristic impedance of free space (=120 ohms)

9. The electric field at the observation point is predicted to reach its maximum value a propagation delay time, t $\simeq \frac{r}{c}$, after the peak ignition circuit current occurs.

LIST OF REFERENCES

[1]

[2]

[3]

[4]

[5]

[6]

[7]

[8]

[9]

[10]

[11]

[12]

LIST OF REFERENCES

- [1] H. E. Dinger, "RFI Measurements and Standards", <u>Proceedings of</u> the IRE (Institute of Radio Engineers) May, 1962 pp. 1313.
- [2] A. C. Doty, "A Progress Report on the Detroit Electromagnetic Survey", 1971 SAE Transactions No. 710031 pp. 107-119.
- [3] F. Bauer, "Controlling Radio Spectrum Pollution from Automotive Engines Ignition Suppression Updated", 1967 SAE Transactions No. 670103 pp. 681-691.
- [4] Edward F. Weller, "Radio Frequency Ignition Interference Suppression - 1969", <u>CM Research Publication</u> GMR-878, General Motors Research Laboratories, General Motors Corporation, Warren, Michigan.
- [5] Richard A. Shepherd, James C. Gaddie, and Donald L. Nielson, "Emission Impossible: New Techniques for Suppression of Automobile Ignition Noise", Stanford Research Institute, Menlo Park, California under contract FCC-072 with the Federal Communications Commission January, 1975.
- [6] C. C. Eaglesfield, "Motor-Car Ignition Interference", Wireless Engineer October, 1946 pp. 265-272.
- [7] C. C. Eaglesfield, "Car-Ignition Radiation", <u>Wireless Engineer</u>
 January, 1951 pp. 17-22.
- [8] G. F. Newell, "Ignition Interference at Frequencies Below 100 Mc/s: The Mechanism of Its Production", <u>British Broad-casting Corporation (BBC) Quarterly</u> Autumn, 1954, Vol. 9, No. 3, pp. 175-184.
- [9] W. Nethercot, "Car-Ignition Interference", <u>Wireless Engineer</u>, August, 1949 pp. 352-357.
- [10] Cleon C. McLaughlin, "Suppression of Automotive Radio Frequency Interference", Master's Thesis at Texas A & M, 1969. Copy available at General Motors Institute, Flint, Michigan.
- [11] Walter B. Larew, <u>Ignition Systems</u> (Philadelphia: Chilton Book Company, 1968), p. 131.
- [12] Ibid, p. 127.

[[:]

[14]

[15]

[16]

[15]

[19]

[20] [21]

[22]

[23]

[24]

[25]

[26]

[27]

[28]

,

- [13] A. P. Young and L. Griffiths, <u>Automobile Electrical Equipment</u> (Philadelphia: Chilton Company, Inc., 1956), p. 225.
- [14] R. F. Graf and G. J. Whalen, <u>Automotive Electronics</u> (Indianapolis: Howard W. Sams and Company, Inc., 1971) p. 79.
- [15] Chilton's Repair and Tune-up Guide: Chevrolet/CMC Vans (Radnor, Pennsylvania: Chilton Book Company, 1974), p. 184.
- [16] Ibid, p. 42.
- [17] Walter B. Larew, op. cit., p. 120.
- [18] A. P. Young and L. Griffiths, op. cit., p. 343.
- [19] Richard R. Burgett, Richard E. Massoll, and Donald R. Van Uum,
 "Relationship Between Spark Plugs and Engine-Radiated
 Electromagnetic Interference", IEEE Transactions on Electromagnetic Compatibility, Volume EMC-16, No. 3, August, 1974
 p. 160-172
- [20] A. P. Young and L. Griffiths, op. cit., p. 375.
- [21] Walter B. Larew, op. cit., p. 133.
- [22] R. F. Graf and G. J. Whalen, op. cit., p. 69
- [23] R. W. George, "Field Strength of Motorcar Ignition Between 40 and 450 Megacycles", Proceedings of the I.R.E., September, 1940 pp. 409-412.
- [24] B. G. Pressey and G. E. Ashwell, "Radiation from Car Ignition Systems", Wireless Engineer, January, 1949 p. 31-34.
- [25] "Measurement of Electromagnetic Radiation from Motor Vehicles (20-1,000 MHz)", SAE J551b, Society of Automotive Engineers, Two Pennsylvania Plaza, New York, New York 10001 (1973).
- [26] International Electrotechnical Commission, International Special Committee on Radio Interference (CISPR), "Recommendation No. 18/2, Interference from Ignition Systems", (1970). Available from the American National Standards Institute, care of the National Electrical Manufacturers Association, 155 East 44th Street, New York, New York, 10017.
- [27] H. Dean McKay and Kenneth W. Bach, "Basic Electromagnetic Interference Measurements on Automobiles", 1971 SAE Transactions No. 710027.
- [28] H. P. Hsu and D. C. Schlick, "Effect of Distributor Gap on Radiated Ignition Interference", 1969 IEEE Electromagnetic Compatibility Symposium Record Asbury Park, New Jersey June 17-19, 1969, Published by the Institute of Electrical and Electronic Engineers, Inc., New York, New York 1969, pp. 319-324.

[29]

[30]

[31]

[32]

[33]

[34]

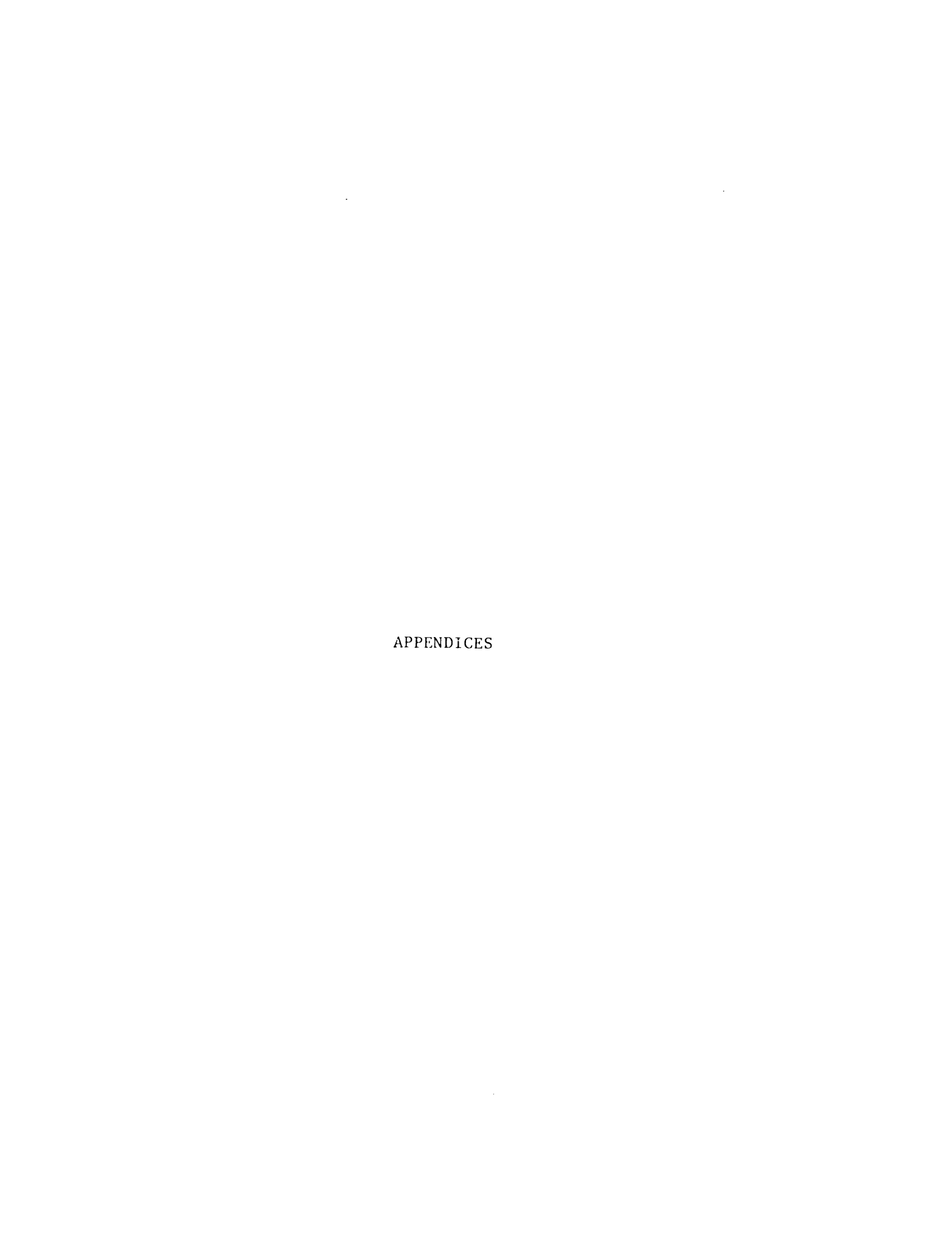
[36]

[35]

[37]

[38]

- [29] R. M. Storwick, D. C. Schlick, and H. P. Hsu, "Measured Statistical Characteristics of Automotive Ignition Noise", 1973 SAE Transactions No. 730133.
- [30] R. A. Shepherd, "Measurements of Amplitude Probability Distributions and Power of Automobile Ignition Noise at HF", <u>IEEE Transactions on Vehicular Technology</u> Volume VT-23, No. 3, August, 1974.
- [31] Fumio Minozuma, "Radio Noise Interference for Frequency Management-Automobile Radio Noise and Its Suppression Methods", Received through private communications.
- [32] Robert H. Cannon, Jr., <u>Dynamics of Physical Systems</u> (McGraw-Hill Book Company, 1967), p. 202.
- [33] R. Saucedo and E. Schiring, "Introduction to Continuous and Digital Control Systems", McMillan Company, 1968 pp. 31-33.
- [34] N. N. Rao, <u>Basic Electromagnetics with Applications</u>, (Englewood Cliffs, <u>New Jersey</u>) 1972 Prentice-Hall, Inc., pp. 373-376).
- [35] Ron Bracewell, <u>The Fourier Transform and Its Applications</u>, McGraw-Hill, Inc. 1965, p. 136.
- [36] Ibid, p. 52.
- [37] C. C. Johnson, <u>Field and Wave Electrodynamics</u>, McGraw-Hill, Inc., 1965 pp. 22-23.
- [38] M. Abramowitz and I. A. Stegun, "Handbook of Mathematical Functions with Formulas, Graphs, and Mathematical Tables", U. S. Department of Commerce National Bureau of Standards, Applied Mathematical Series 53, June, 1964, p. 487.



APPENDIX A
PROGRAM IGNITI

Descri

Input

C

CD

CS

С

T.

T

Out put

T(I)

,C(I)

CUR(I)

APPENDIX A

Description: The computer program, IGNITI, solves equations (3.10), (3.20), (3.21), and (3.22).

Input variables:

CC = coil capacitance, farads

CDG = distributor gap capacitance, farads

CSG = spark plug gap capacitance, farads

R = resistance, ohms

CL = inductance, henries

V = distributor gap breakdown voltage, volts

TA = starting value of time, seconds

TB = maximum value of time, seconds

TM = multiplier, so that $(t_{n+1}) = (TM)x(t_n)$

Output variables:

T(I) = time, seconds

VSG(I) = spark plug gap voltage, volts

VC(I) = coil voltage, volts

CUR(I) = current, amperes

```
PROGRAM IGNITI (INPUT, OUTPUT)
      DIMENSION 1(200).v56(200).vC(200).CUR(200)
B1=B2=D1=D2=D3=X=D4=D5=D6=D7=Y=D9=0.0
      I = I
      ŘEÁD 100.CC.CDU.CSG,R.CL.V
READ 101.TA.TH.TM
       CX=1.0/((1.0/CC)+(1.0/CDG)+(1.0/CSG))
      H1=(K/CL)**2
      H2=(4.0/(CL#CC))#(1.0+(CC/CSG))
D1=(V*CC)/(CSG+CC)
      D2=CD6/CX
D3=CS6/(CS6+CC)
D9=-CC/CS6
IF(B1-B2) 30,90,10
  10 X=SGR+ (B1-82)
      T(1) = fA
      D4=(R/(CL*X))+1.0
D5=U4-2.0
  11 CONTINUE
      D5=EXP(-((R/CL)-X)*0.5*T(I))
      D7=EXP(-((R/CL)+X)*0.54((1))
      CUR(1) = (V/(CL4X)) (06-07)
      VC([)=(D1*D2)+(0.5*D3*CUR([)*R)+(0.5*V*D3*(D6+U7))
VS([)=D9*(VC([)+(V*U2))
      Y = I(I)
      I = I + \tilde{I}
      T(I) = (TM) \stackrel{\circ}{\sim} (Y)
      IF (1(1).61.18) GO TO 50
          10 11
  30 X=SURT(B2-81)
      T(I) = IA
 D4=R/(CL*X)
31 CONTINUE
      DS=EXP(-(R*((1))/(2.U*CL))
D6=51N(0.5*x*((1))
      D7=CO5(0.54x4T(I))
      CUR(1) = (2.04 V4 U54 U6) / (CL4X)
      ŸČ(Ĭ)=(ĎĪ*ĎZ)+(Ŏ+Š#Ŕ*Ď3#CÜŔ(I))+(V#Ŋ3#Ŋ5#Ŋ7)
      VSG(I) = 0.94 (VC(I) - (V402))
      Y = I(I)
      \underline{I} = I + 1
      T(I)=TM#Y
      IF (1(1).6(.TH) GO TO 50
      GO TU 31
 PRINT 105
PRINT 100.CC.CDG.CSG.R.CL.V
PRINT 102
     N=1+(ALOG(TH/TA)/ALOG(TM))
     DO 51 I=1.N
 51 PRINI
             103,T(I),VSG(I),VC(I),CUR(I)
     60 10 110
90 PRINT 104
100 FORMAT (6610.3)
101 FORMAT (2610.3.F10.7)
102 FORMAT (#U++5X++TIME++11X++VSG++1UX++VC++11X++I++/)
103 FORMAT (2X+E12+5+3X+F10+3+3X+F10+3+3X+F12+8)
104 FORMAT (#0#+2X+#RESONANCE#)
105 FORMAT (#0#+5X+#CC#+8X+#CDG#+7X+#CSG#+8X+#R#+8X+#CL#+8X+#V#)
110
     CONTINUE
     STUP
     END
```

APPENDIX B
PROGRAM IGNITII

Desc

Inpu

Out pu

RT(VC(

CUR()

r.C.

DVCZ

APPENDIX B

Description: The computer program, IGNITII, solves equations (3.32) and (3.33)

Input variables:

CC = coil capacitance, farads

CDG = distributor gap capacitance, farads

CSG = spark plug gap capacitance, farads

R = resistance, ohms

CL = inductance, henries

V = distributor gap breakdown voltage, volts

TA = time when spark plug fires (t_1) , seconds

TB = maximum value of time, seconds

TM = multiplier, so that $(t_{n+1}) = (TM)x(t_n)$

Output variables:

RT(I) = time after distributor gap breaks down, seconds

VC(I) = coil voltage, volts

CUR(I) = current, amperes

VCT1 = coil voltage when spark plug fires, volts

DVCT1 = slope of coil voltage when spark plug fires, volts/second

```
PROGRAM IGNITII (INPUT, OUTPUT)
    DIMENSION I (100) . VC (100) . CUR (100) . RT (100)
    DIMENSION DUMI (100) . DUM2 (100) . DUM3 (100)
    A1=A2=A3=A4=A5=A6=A7=A8=AA1=AA2=AA3=AA4=AA5=AA6=AB1=AB2=0.0
    AC1=AC2=AC3=B1=B2=B3=CX=CURT1=D1=D2=D3=D7=D8=D9=D14=DVC11=0.0
VCA=VCB=VC11=X=XA=Y=YA=Z=ZY=ZZ=0.0
   M = 0
    I = 1
    RFAD 100+CC+CDG+CSG+R+CL+V
    READ 101 • [A • TB • TM (A=1.0/(1.0/C5G))
    H1=(K/CL) **2
   H2=(4.0/(CL*CC))*(1.0+(CC/CSG))
    D1 = (V+CC) / (C5G+CC)
   D3=C56/(C56+CC)
    IF(B1-B2) 30.90.10
10 X=50KT(B1-B2)
    D7=(V*R)/(2.0*A*CL)
D9=-(R/(2.0*CL)-(A/2.0))
    D9=-(R/(2.04CL)+(X/2.0))
    A1=0.54V*U3
A2=U1*D2
    A3=V/(CL*X)
    VCA=EXP (UBATA)
    VCB=EXP(D9+TA)
VCT1=A2+D/+D3+(VCA-VCB)+A1+(VCA+VCB)
    CURTI=(V*(VÜĀ-VČB))/(ČĹ*X)
   DVCTI = - CURTI/CC
    60 10 40
30 XA=5URT (H2-H1)
A4=-R/(2.0 °CL)
    A5=XA/2.0
    A6=((V#R)/(CL#XA))#D3
    A7=U1*D2
    AB=V4D3
   D14=(2.0*V)/(CL*XA)
VCT1=A7+A6*EXP(TA*A4)*SIN(TA*A5)+A8*EXP(TA*A4)*CUS(TA*A5)
    CURTI=D1+4EXP((-R4TA)/(2.0*CL))*SIN((XA4TA)/2.0)
    DVCT1=-CURTI/CC
40 B3=4.0/(CL*CC)
IF (B1-R3)60,95,50
50 Y=50KT(B1-B3)
    ZY=TA+(1300.0/Y)
   IF (TB.GT.2Y) TB=2Y

AA1=((R/CL)+Y)*VCT1

AA2=(AA1+(2.0*DVCT1))/(2.0*Y)
    AA3=((R/CL)-Y) "VCTI
    AA4=(AA3+(2.04UVCT1))/(2.04Y)
    AA6=-((R/(2.0°CL))-(Y/2.0))
AA6=-((R/(2.0°CL))+(Y/2.0))
AB1=(VCT1+((R°CC°DVCT1)/2.0))/(CL*Y)
    AHZ=(CCMOVCT1)/2.0
```

```
RT(I) = IA
 51
     CONT INUE
     T(1) = \kappa T(1) - T\Lambda
     VC(1) = (AA24EXP(AA54I(1))) - (AA44EXP(AA64I(1)))
     DUM3(1)=EXP(-(R*I(I))/(2.0*CL))
     DUM1(I) = DUM3(I) * (EXP((Y*I(I))/2.0) + EXP(-(Y*I(I))/2.0))

DUM2(I) = DUM3(I) * (EXP((Y*I(I))/2.0) + EXP(-(Y*I(I))/2.0))

CUR(I) = (Ad1*DUM1(I)) - (AB2*DUM2(I))
     Z=K1(1)
     I = i + i
     RI(I)=IMBZ
     IF (RT(T) . G [ . TB) GO TO 80
     GO TO 51
 60 YA=SURT (H3-H1)
     77=TA+((1300.0°CL)/R)
IF([B.GT.ZZ) TB=Z/
ACl=(((R*VCT1)/CL)+(2.0°DVCT1))/YA
     AČ2=((2.0*VCT1)+(R*CC*DVCT1))/(CL*YA)
     AC3=CC#DVCII
     RT(I) = TA
 61 CONTINUE
     T(I) = RT(I) - IA
     DUM1(1) = (AC1451N((YA47(1))/2.0)) + (VCT) + CUS((YA41(1))/2.0))
     VC(I) = (FXP(-(R*T(I))/(2.0*CE)))*(UUM1(I))
     DUM2(1) = (EXP(-(K*T(1)))/(2.0*(L)))*(51N((YA*T(1)))/2.0))
     DUM3(1) = (EXP(-(R*f(1))/(2.0*CL))) * (CUS((YA*f(1))/2.0))
     CUR(T) = (ACZ^{\alpha}UUM2(T)) - (ACZ^{\alpha}UUM3(T))
     Z=RT(1)
     I = 1 + 1
     PT(I)=IM#Z
     IF (RT (I) . GT . TB) GU TU 80
     60 10 61
 101H9 08
             107
     PRINT
              100,CC,CDG,C56,R,CL,V
     PRIMI
             102
     N=1+(AEOG(IB/TA)/ALOG(TM))
     DO 81 1=1.N
 81 PRINT
              103, KT(1), VC(1), CUK(1)
              106, VC11, DVC11
     PRINI
             110
     60 10
 90 PRINT
             104
95 PRINT 105
100 FORMAT(6L10.3)
 95
101 FORMAT (2E10.3.F10.7)
102 FORMAT (#U#+2X+4TIME4+11X+4VC4+11X+4T4+/)
103 FORMAT (20.12.5.3%.F10.3.3%.F12.8./)
104 FORMAT (20.2.2.4.4.12.5.14)
105 FORMAT (40.2.2.4.4.12.50)
105 FORMAT (40.4.2.4.4.12.50)
107 FORMAT (40.4.2.4.4.12.50)
106 FORMAT (#U#+2X+*VCT1=#+2X+E14.7+5X++DVCT1=#+2X+E14.7)
     FORMAT (404,5X,4CC4,8X,4CDG4,7X,4C5,4,8X,4R4,8X,4CL4,8X,4V4)
107
110
     CONTINUE
     STUP
     END
```

APPENDIX C

PROGRAM ADP

Des

Inp

Out_P

W(I

ANS

A%S

APPENDIX C

Description: The computer program, ADP, solves equations (4.24), (4.27), and (5.5).

Input variables:

RADIUS = radius of loop antenna, meters

DIST = distance from antenna, meters

CC = coil capacitance, farads

CDG = distributor gap capacitance, farads

CSG = spark plug gap capacitance, farads

R = resistance, ohms

CL = inductance, henries

V = distributor gap breakdown voltage, volts

VT1 = coil voltage when spark plug fires, volts

DVT1 = slope of soil voltage when spark plug fires, volts/second

T1 = time when spark plug fires, seconds

ZA = starting value of angular frequency, radians/second

ZB = maximum value of angular frequency, radians/second

ZM = multiplier, so that $(\omega_{n+1}) = (ZM)x(\omega_n)$

Output variables:

W(I) = angular frequency, radians/second

ANS(I) = current, amperes/Hertz

 $ANSDB(I) = 20 \log_{10} [ANS(I)]$

F = frequency, Hertz

PHASER(I) = phase angle, radians

Fl = phase angle, degrees

EMAX(I) = maximum electric field, Volts/meter

 $EMAXDB(I) = 20 \log_{10} [EMAX(I)]$

 $ANDB(I) = 20 \log_{10} [2 \times ANS(I)]$

```
PROGRAM ADP (INPUT.OUTPUT)
    DIMENSION W(200), ANS (200), ANSDB(200), PHASER(200), EMAX(200),
   *EMAXUB(200) *AMDb(200)
    X1=A1=A2=A3=A4=A5=A6=A7=A8=0.0
    D1=02=03=04=05=06=07=08=09=0.0
    Y1=Y2=T1=12=13=[4=15=16=17=2=0.0
    R1=R2=R3=R4=R5=R6=B1=82=0.0
    KAU1U5=D15T=U.U
    N = 0
    I = 1
    L = 1
    READ 99. RADIUS. DIST
    READ INU . CC . CDG . CSG . R . CL . V
    REAU 101, VT1, DVT1, T1
    KEAU 102+ZA+ZH+ZM
    CON= (RAD LUS 46. 283185E-7) /DIST
CONS=RAD LUS / 3.0E8
    B] = (R/CL) 462
B2=(1.0+(CC/CSG)) (4.0/(CL CC))
IF(B1-H2) 30.80.10
10 X1=SURT(B1-H2)
    Ai = (R/(2 \cdot 0 + CL)) - (X1/2 \cdot 0)
    AZ=(R/(Z.U*CL))+(X1/2.U)
AZ=V/(CL*X1)
    A4=VII/CL
    AS=CC#DVT1
    A6=81-(2.0/(CL4CC))
    A7=EXP(-A1411)
    AH=EXP (-AZ+(I)
    W(1) = ZA
20 CONTINUE
    D) = (1.0\(CF,CC)) - (M(1) & 45)
D) = (M(1) & K) \CF
    D3 = (W(T)^{44}4) + (A6)^{4}(W(T)^{42}) + ((T.0)(CL4CC))^{44}2)
    1)4=A3+(1.0-(A7+CUS(W(I)+T1)))

\begin{array}{ll}
D_{2} = A_{3} \circ (1 \circ 0 - (A_{3} \circ COS(W(1) \circ T1))) \\
D_{2} = A_{3} \circ A_{3} \circ (SIN(W(1) \circ T1))
\end{array}

    D7=A34A84 (51N(W(1) 411))
    DA=(A1002) + (W(I)002)
D9=(A2002) + (W(I)002)
Y1=(D105IN(W(I)002)
Y1=(D105IN(W(I)002)
    YŽ=(ŪĪ*CUS(W(Ī)*T1))+(ĎŽ*ŠIN(W(Ī)*ŤĪ))
    R1 = ((-A4^{4}Y1) - (w(1)^{4}A5^{4}Y2))/D3
    R2=((A1404)+(W(I)406))/08
    R3 = ((A2405) + (W(I)407))709
    R4 = ((w(1) * 04) - (A1 * 06)) / 08
    P5=((W(I)*D5)-(A2*D7))/D9
    RG=((-A4472)+(W(1)4A5471))/03
    T7=K1+R2-K3
    T2=-(R4-R5-R6)
ANS(I)=SURI((T7982)+(T2882))
    PHASER(I) = ATANZ ([2.17)
    ANSUB([] = (20.0) "ALOG10(ANS(I))
    ANDB(1) = (20.0) #ALOGIO(2.0#ANS(1))
    X=W(1) #CUN5
    CALL HESU(X+L+BI+LER)
    EMAX (1) = CUN ANS (1) & W (1) & B1
    EMAXDB(I) = 20.0 \text{ } ALOGIO(EMAX(I))
    Z=W(1)
    I = I + I
    W(I)=2462
    IF (W(I).61.28) GO TO 50
    60 TU 20
30 X1=50RT (82-81)
    A1=V[1/CL
A2=CC*nV[1
    A4=V/(CL^6\times L)
    AS=R/(2.0°CL)
    A3=EXP(-A5*11)
    W(I) = \angle \Delta
40 CONTINUE
```

51

Ŀ

```
\begin{array}{l} D1 = (W(1) + R) / CL \\ D2 = (1 \cdot 0) / (CL + CC)) - (W(1) + R2) \\ D3 = W(1) + (X1/2 \cdot 0) \end{array}
     D4=W(I)-(X1/2.0)
D5=(D1092)+(D2402)
     D6=(A44A5)/((A5442)+(D4442))
     D7=(A4+U4)/((A5+42)+(U4+42))
     DA=(A44A5)/((A544Z)+(U344Z))
Dy=(A44U3)/((A544Z)+(U344Z))
     Y1=(D2*CU5(W(1)*T1))-(D1*SIN(W(I)*T1))
     YZ=(D1*CUS(W(1)*T1))+(DZ*SIN(W(1)*T1))
     R1 = ((\Lambda 1 + Y 1) - (W(1) + \Lambda 2 + Y 2)) / U5
     R2=((A1*Y2)+(W(1)*A2*Y1))/D5
     ((Îκ40)NIZ) «EA=ÊH
     P4=A3*(CU5(D4*T1))
     R5=A3*(SIN(D3*T1))
     R6=A34 (CUS (1)3411))
     T7=RI+(R3+O5)+(R4+O7)+O9
     T2=(K5408) + (R6409) +07
     T3=(R4406)+(R5409)+D8
     14=K2+(K3*D7)+(K6*D8)+D6
     15=11-12
     16=13-14
     ANS(1)=SURT((T5442)+(T6442))
     PHASER (1) = ATAN2 (16.TS)
ANSUB(1) = (20.0) #ALUGIO(ANS(I))
     ANDU(1)=(20.0)*ALUG10(2.0*ANS(1))
X=w(1) >CONS
     CALL BESU(X+L+BI+IER)
     EMAX (1) = CUN+AN5 (1) +W (1) +BI
     EMAXUB(I)=20.0%ALUGIU(EMAX(I))
     Z=w(1)
     I = I + I
     W(I)=ZMªZ
     IF (W(I). of. ZB) GO TO 50
     60 10 40
 50 CONFINUE
     PRINT 103
     PRINT
             100 . CC . CD6 . CS6 . R . CL . V
     PRINT
             104,VT1,UVT1,T1,CON
     PRINT 105
     N=1+(ALOU(ZB/ZA)/ALOU(ZM))
     DO 60 I=1.N
     F=W(1)/6.283185308
     F1=(360.08PHASLR([))/6.283185308
 60 PRINT 106.W(1), ANS(1), ANSOB(1), F, PHASER(1), F1, EMAX(1), EMAXO
    + B ( I ) + AN DH ( I )
 80 PRIOT 107
 99 FORMAT (2110.4)
100 FORMAT (6L10.3)
101
     FURMAT (3E14.7)
102 FORMAT (2E20.7.F20.7)
103 FORMAT (404.5X.4CC4.8X.4CD64.7X.4C5G4.8X.4R4.8X.4CL4.8X.4V4)
104 FORMAT (404.2X.4VC1)=4.E15.7.5X.4DVCT1=4.E15.7.5X.4T1=4.E15.
    +/•5X•4CON=4•E15•7•/)
105 FORMALLOUGO BX . "ANG FREQ . WO . 6X . 4 I (W) + . 6X . 4 I (W) IN DH4 . 8X . 4 FR
    +EQ+F++2x++PHASE (HAD)++2X++PHASE (DEG)++5X++E IN V/M++9X++E IN
    *DB4+4X+42I(W) IN DB4+/)
106 FORMAT (2X+112.5+2X+12.5+2X+10.5+2X+E12.5+6X+16.3+4X+F8.3+
+2X+E12.5+4X+10.5+4X+10.5)
107 FORMAT (*O*+5X+4RESONANCE+)
120
     CONTINUE
     STOP
     END
```

APPENDIX D

PROGRAM EMAX

Des

In

AA

AR

W.F

C! T.

T

T

N

(

}

APPENDIX D

Description: The computer program, EMAX, solves equation (5.18).

Input variables:

J = data set number (first set, N=1,; second set, N=2; . . .; N=0 terminates program and prints output)

AA(J) = radius of loop antenna, meters

AR(J) = distance from antenna, meters

WB(J) = angular frequency (ω_0) , radians/second

CURB(J) = current amplitude in frequency domain, amperes/Hertz

TA = starting value of time, seconds

TB = maximum value of time, seconds

TM = multiplier, so that $(t_{n+1}) = (TM)x(t_n)$

WM(J) = cutoff value of angular frequency (ω_m) , radians/second

Output variables:

T(J,I) = time, seconds

EMAXT(J,I) = maximum electric field strength, Volts/meter/Hertz

 $EMAXTDB(J,I) = 20 \log_{10} [EMAXT(J,I)]$

50 19

```
PROGRAM LMAX (INPUL, OUTPUT)
     DIMENSION AA(5) . AK(5) . WB(5) . CURB(5) . WM(5) . T(5, 100) . EMAXT
    + (5,100), EMAXIDE (5,100), N(5), BLUE (5,100)
     M = 0
  5 I = 1
     RFAD 100+J
     IF (J.EQ. U) GU TU 30
     RFAD 101 • AA(J) • AR(J) • WB(J) • CURH(J) RFAD 102 • IA • IB • IM • WH(J)
     M = M + 1
     CON=(2.094395E-15*(AA(J)**2)*CURB(J)*WB(J))/AR(J)
T(J:1)=]A
 10 AI=T(J.I) - (AR(J)/3.0E8)
IF(AI.EQ.0)60 TO 19
     LA*(U) BW=SA
     A3=WM (J) *A1
     A4=A1482
     B1=CUN/A4
     H2=CU5 (AZ)
     H3=CUS (A3)
     B4=A3+SIN(A3)
     H5=(2.04214(A2))/A2
     EMAXI(J.1)=014(02+83+84-85)
     Y1 = ABS(EMAXT(J,I))
     EMAXIUB(J.I) = 20.0 ALUG10(Y1)
     Z=I(J,I)
     I = I + I
     T(J \bullet I) = IM \bullet Z
     IF (1(J.I).6[.[B)60 IO 20
     GO TO 10
 19 PŘINT TÖS
     GO TO S
 20 N(J) = I + (ALUG(TB/IA)/ALUG(TM))
     GO TU 5
 30 DO 35 J=1.M
PRINT 103.AA(J).AK(J).WB(J).CURB(J).WM(J)
     PRINT 104
     1=11(リ)
 00 35 I=1+1.
35 PMINT 105+1 (U+1) +EMAXT (U+1) +EMAXIDB (U+1)
100 FORMAT (9X,11)
101 FORMAT (4610.4)
102 FORMAT(2E10.4.F10.4.E10.4)
103 FORMAT(#14.IX, "A=", E12.4.2X.*R=", E12.4.2X, "wo=", E12.4.2X
    + , 410=4 , E12 . 4 . 2x . 0 WM=4 . E12 . 4 . /)
104 FURMAT (*04,9X, *TIME IN SEC+,9X, *E(T) IN V/M*, 10X, *E(T)
+IN DB#+/)
105 FORMAT(9X+E11.5+1UX+L10.4+1UX+F1U.4+)
106 FORMAT (1x, "DENUMINATUR WAS ZERU", Z)
     STOP
     END
```

APPENDIX E

PROGRAM EMTBES

APPENDIX E

Description: The computer program, EMTBES, solves equation (5.24).

Input variables:

J = data set number (first set, N=1; second set, N=2; . . .; N=0 terminates program and prints output)

AA(J) = radius of loop antenna, meters

AK(J) = maximum value of current in time domain $(\omega_{0}I_{0})$, amperes

AR(J) = distance from antenna, meters

TB = maximum value of time, seconds

TM = multiplier, such that $(t_{n+1}) = (TM)x(t_n)$

Output variables:

T(J,I) = time, seconds

EMAXT(J,I) = maximum electric field strength, Volts/meter/Hertz

 $EMAXTDB(J,I) = 20 \log_{10}[EMAXT(J,I)]$

POST THE SEFECT A CRAIN AND THE SECTION OF COMMINING THE SECTION OF COM

```
PROGRAM EMTBES (INPUT, OUTPUT)
     DIMENSION AA(5) + AK(5) + AR(5) + FA(5) + F(5, 100) + ANS(5) + EMAXT(5
    +,100),EMAXIDB(5,100),N(5)
     M = ()
  5
     I = 1
     READ 100+J
IF (J.EQ. 0) GO TO 30
     READ 101.AA(J).AK(J).AR(J)
READ 102.IB.TM
     M = M + 1
     CON=376.991119
     CONS=-4.188/90E-15
     TA(J) = (AA(J) + AR(J))/3.0E8
     T(J) A T^{\oplus}MT = (I \cdot U) T
     ANS(J) = (CUN^{\alpha}AK(J))/AR(J)
 A2=AA(J)/3.0E8
10 A1=T(J.I)-(AR(J)/3.0E8)
     A3=SURT (A1**2-A2**2)
IF (A3.E0.0) GO TO 18
     A4=A3+(A1+A3)
     A5=(CONS*(AA(J) ++2) +AK(J))/AK(J)
     EMAXT (J.I) = A5/A4
 17 Y_1 = ABS(EMAXI(J \cdot I))
     EMAXIDA (J.I) = 20.0 "ALUG10 (Y1)
     Z=「(J.])
     I = I + I
     \tilde{T}(\tilde{J}) = TM4Z
     IF (1(J.1).G1.TB)G0 TO 20 G0 10 10
 18 EMAXT (1.1) = ANS (J)
GO TU 17
 19 PRINT 106
 20
    N(J)=1+(ALOG(TB/TA(J))/ALOG(TM))
         10 5
    DO 35 J=1.M
     PRINT 103, AA (J), AK (J), AR (J), ANS (J), TA (J)
     PRINT 104
    DO 35 1=1+F
PHINT 102+1(7+1) +FWAX1(7+1) +EWAX1DB(7+1)
 35 PRINT
100 FORMAT (9X.11)
101 FURMAT (3E10.4)
    FURMAT (Elu.4, F10.4)
102
103 FURMAT (*14.1X.4A=4.E12.4.2X.4K=4.E12.4.2X.4R=4.E12.4.5X.4
   +E(T) IN V/M=++F12.4+2X+4FOR T LESS THAN++E12.4./)
104 FORMAT (#U#+9X+#TIME IN SEC#+9X+#E(T) IN V/M#+1UX+#E(T)
   + IN UB4 ,/)
105 FURMAT (10x . E10 . 4 . 10X . E10 . 4 . 10X . F10 . 4)
106 FORMAT (1A. "DENOMINATOR WAS ZERO" . )
     5T()P
     END)
```

MICHIGAN STATE UNIVERSITY LIBRARIES
3 1293 03169 3926